Development and evaluation of real-time PCR techniques for the early detection of three airborne fungal pathogens of wheat

by

Ilakkiya Thirugnanasambandam

A thesis submitted in partial fulfillment of the requirements for the degree of

Master of Science

in

Plant Science

Department of Agricultural, Food and Nutritional Science
University of Alberta

ABSTRACT

Wheat is a staple food crop with 760 million tonnes consumed globally in 2020 with Canada being a major producer. Airborne fungal pathogens pose a severe threat to wheat growers all over Canada. New isolates of pathogens evolve through mutations which may become resistant to control measures and can cause significant yield losses. To minimize these losses, early detection of these pathogens is needed. This research aims to develop highly specific and sensitive real-time immuno-PCR (RT-iPCR) assays for the detection of three different pathogenic fungi infecting wheat: *Pyrenophora tritici-repentis* (*Ptr*), *Fusarium graminearum* (*Fg*), and *Puccinia striiformis f.sp.tritici* (*Pst*) causing tan spot, Fusarium head blight, and stripe rust of wheat, respectively. RT-iPCR resulted in a limit of detection of 1, 188, and 938 spores for *Ptr, Pst,* and *Fg*, respectively without requiring DNA extraction as this method measures spores directly. RT-iPCR sensitivity was improved 5-, 12-, and 30-fold for *Fg, Pst,* and *Ptr*, respectively compared to its corresponding enzyme-linked immunosorbent assays (ELISA). However, specificity remained a challenge for the RT-iPCR assay when assessed through cross-reactivity tests. All three antibodies evaluated reacted strongly with non-target antigens suggesting high cross-reactivity. An alternative and more established quantitative PCR (qPCR) technique was investigated to further evaluate the accuracy of the more novel RT-iPCR technique developed here. Additionally, an approach was developed to determine spore DNA extraction efficiency for qPCR which represents a methodological gap in most qPCR spore measurements. Using fungal reproductive biology a formula was derived to calculate spore numbers from the DNA quantified by the qPCR. The calculated spore

numbers were compared to pure spore cultures counted under a microscope to determine DNA extraction efficiency. Ultimately, this approach will help plant pathologists quantify pathogens more accurately. DNA extraction efficiency determined for *Fg, Pst* and *Ptr* spores are 5 ± 0.1%, 14 ± 0.7% and 290 ± 36%, respectively. qPCR resulted in a limit of detection of 3, 400, and 800 spores for *Ptr, Pst,* and *Fg* respectively after being corrected to DNA extraction efficiency. Finally, air samples were collected over the 2022 field season from two research fields located at the Agriculture and Agri-Food Canada – Lethbridge Research and Development Centre. The two fields were inoculated with *Pst* and samples were evaluated and compared using three detection techniques; RT-iPCR, qPCR and microscopy. Overall, the three techniques showed similar trends in *Pst* spore numbers over time. Microscopy and RT-iPCR showed higher measurement variability compared to qPCR, likely due to the challenges associated with spore identification at the species level using microscopy and known cross-reactivity associated with RT-iPCR. The established technique of qPCR appears to be the most accurate technique for fungal spore detection if extraction efficiencies are considered and used to correct reported spore numbers. While more research is needed to refine the RT-iPCR technique to improve specificity, this research is an important step forward and will help in efforts to prevent the spread of plant diseases through the early detection of fungal spores.

PREFACE

This thesis is an original work done by me Ilakkiya Thirugnanasambandam. I conducted all the experiments, collected and analyzed the data for this thesis. I wrote the first draft of the thesis, Dr. Jonathan Challis and Dr. André Laroche (Agriculture and Agri-Food Canada – Lethbridge) intensively reviewed and provided additional suggestions for the improvement of each chapter.

My thesis research work was conducted at the Agriculture and Agri-Food Canada – Lethbridge under the guidance of Dr. Jonathan Challis and Dr. André Laroche. Financial support was provided by grants to Dr. Jonathan Challis from Agriculture and Agri-Food Canada.

ACKNOWLEDGEMENTS

I'm very grateful to all the individuals who have assisted me along the way in my master's journey, and I consider myself extremely fortunate to have been given this opportunity.

First of all, I would like to express my sincere gratitude to my supervisors at the Agriculture and Agri-Food Canada, Dr. Jonathan Challis and Dr. André Laroche. It has been such a privilege to work for both of you. Thank you for your extraordinary support, advice, and encouragement. My degree would not have been possible without your guidance. I would also like to extend my gratitude to my supervisor at the University of Alberta Dr. Nat Kav for your continued support. I would like to express my sincere thanks to my former supervisor Dr. Claudia Sheedy (Late) for providing me with this amazing opportunity and for believing in me. You'll be missed forever, Claudia.

I had the great fortune to get outstanding funding and awards during my master's including awards from the University of Alberta – Altalink Master's Scholarship, Guelph Food Technology Legacy Fund, and notably the Western Grains Research Foundation award and Alberta Graduate Excellence Scholarship. Thanks to the monetary support from the Agriculture Wheat Consortium (Alberta Wheat Commission and Sask Wheat Development Commission) for my master's stipend throughout the program.

Special thanks to my lab technicians Tara Vucurevich, and Tara Shelton for teaching me the techniques and sharing your knowledge, and Carl Holland for all your efforts. You, people, are the best lab mates one could ask for. My sincere thanks to Dr. André Laroche's team – Gabriela Araujo, Chelsi Harvey, and Michelle Cradduck for providing

me with stripe rust spores, for collecting air samples for this project, and for always being there. I would like to thank Dr. Reem Aboukhaddour and her team for providing me with tan spot spores and teaching me to culture them. I would also like to thank Dr. Nora Foroud and her team for providing me with Fusarium inoculum and for teaching me to culture them. My sincere thanks to Dr. Shimaila Ali for her help with my calculations, and Dr. Timothy Schwinghamer for his moral support and help with statistical analysis.

I would like to thank my mom Premalatha, sister Preethi, and my brother-in-law Santhosh for their unconditional love and support throughout my journey. My dear friends Jesse and Musthafa, thank you for all the fun memories and chit-chat.

Finally, I would like to thank and dedicate this thesis to my dad in heaven Thirugnanasambandam. Thank you for everything and I miss you terribly. I would also like to dedicate this thesis to Manoj, the love of my life, and my beloved nephew Sai Mahizhan.

Table of Contents

List of Tables

List of Figures

List of abbreviations

ABTS	2,2'-azino-bis (3-ethylbenzothiazoline-6-sulphonic acid)
Ct	Cycle threshold
CV	Co-efficient of variability
℃	Degree Celsius
DNA	Deoxyribonucleic acid
dPCR	Digital PCR
ELISA	Enzyme linked immunosorbent assay
fg	Femtogram
Fg	*Fusarium graminearum*
FWD	Forward
g	Gram
× g	Gravity
GAR	Goat anti-rabbit
HRP	Horseradish peroxidase
h	Hour
iPCR	Immuno-PCR
LCB	Low Cross-Buffer
LOD	Limit of detection
Log_{10}	Logarithmic base 10
µL	Microlitre
µm	Micrometer
Min	Minute
mL	Millilitre
ng	Nanogram
OVA	Ovalbumin
PBS	Phosphate buffered saline
PBS-T	Phosphate buffered saline + Tween 20 (0.05%)
PCR	Polymerase chain reaction
PDA	Potato dextrose agar

Pst	*Puccinia striiformis* f. sp. *tritici*
Ptr	*Pyrenophora tritici-repentis*
qPCR	Quantitative PCR
Rev	Reverse
RT-PCR	Reverse transcription PCR
RT-iPCR	Real time immuno-PCR
rpm	Rotations per minute
s	Seconds
SD	Standard deviation
SEM	Standard error of mean

Chapter 1 Introduction

Increasing food production by 50% is needed to satisfy the global population's estimated demand by 2050 (Chakraborty and Newton 2011; Chapagain and Good 2015). Various crop diseases in agricultural fields can pose a serious threat to crop yield and national food security. By reducing food production losses, a balance between escalating food demand and global agricultural productivity can be achieved (Shin et al. 2019). Rice, wheat, barley, and maize contribute more than 50% of all human calories consumed from plants and accounted for 2.82 billion tonnes, nearly 95% of global cereal production in 2017 (Dinh et al. 2020). Wheat is a staple food crop across the world (Figueroa et al. 2018), with 761.5 million tonnes of wheat produced annually across the globe in 2019-2020 (FAO 2020). There is a heavy reliance on wheat production globally and within Canada for food security. Improving wheat yield is critical to meet the growing food demand driven by the predicted increase in the global population (Chakraborty and Newton 2011; Chapagain and Good 2015). Canadian wheat production rose to 35.2 million tonnes in 2020, with the Prairie Provinces of Alberta, Manitoba, and Saskatchewan being the major producers (Statistics Canada 2020). However, there are certain challenges worldwide that can limit both the quality and yield of wheat, including, rising temperatures and drought (Asseng et al. 2014), varied rainfall patterns (Feng et al. 2018), and plant pathogens (Figueroa et al. 2018).

Improved pest and disease control has played a part in the doubling of food output in the last 40 years, but pathogens still account for 10–16 percent of global harvest losses (Chakraborty and Newton 2011). Among plant pathogens such as bacteria, fungi, and

viruses, the fungal pathogens have the greatest potential to impact wheat crops and can reduce yields by up to 65% (Tewari and Sharma 2019). The geographical distribution of fungal pathogens is influenced by cultivation practices, environmental factors, and host distribution (Borer et al. 2016; Dietzel et al. 2019). Fungal spores are dispersed thousands of kilometers through air, water, insects, and other animal and human activities (Golan and Pringle 2017; Dietzel et al. 2019; Jain et al. 2019). The adhesion of fungal spores on the plant surface is necessary for infecting plants (Braun and Howard 1994). Adhesion of most fungal spores to the host surface is mediated by a glue-like secretion extending from the fungi to the adjacent surface (Epstein and Nicholson 2016). They may remain dormant as resting spores until the conditions are conducive to causing an infection.

For any pathogen to cause an infection there are three important factors: a virulent pathogen, a susceptible host, and favorable environmental conditions (Figure 1.1). Virulence and inoculum abundance are the major factors of a pathogen in causing a disease (Scholthof 2007). A susceptible host is important for a pathogen to live on and obtain nutrients from, ultimately resulting in symptoms and signs of a disease in the host and causing harm (Schumann and D'Arcy 2006). The third vertex of the disease triangle is the environmental factors such as temperature, rainfall, and light intensity which favors the pathogen's ability to infect the host plant and cause disease (Schumann and D'Arcy 2006). The combination of all three conditions results in plant disease, however modifying any one of the above-mentioned factors alters the plant susceptibility.

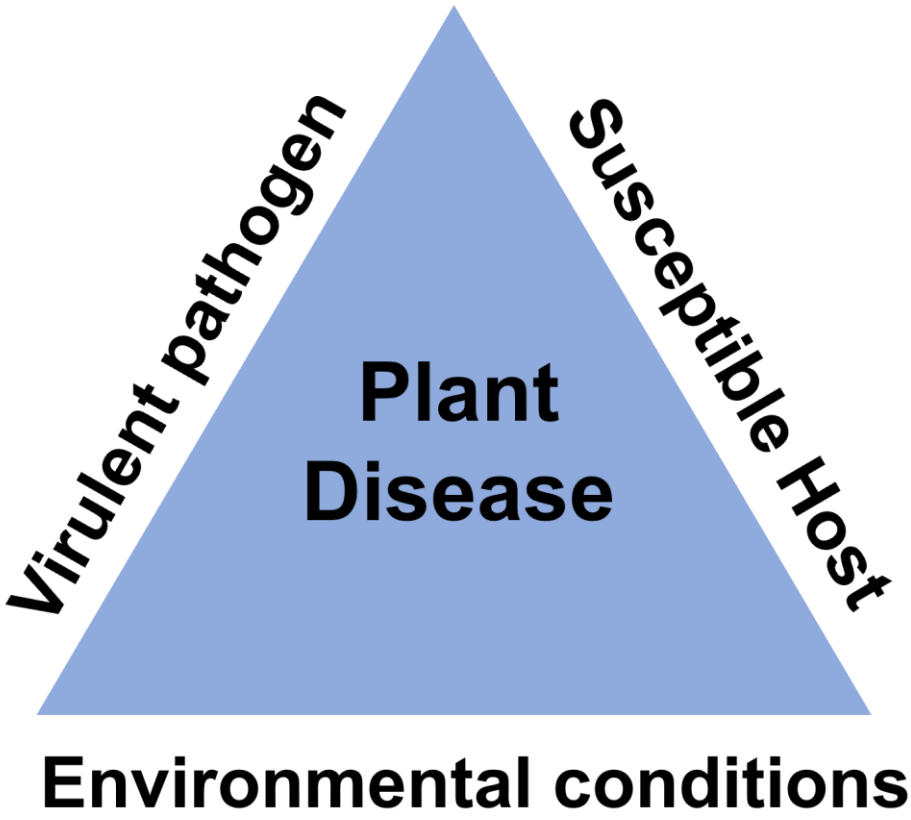

Figure 1.1: A pictorial representation of the ‘Disease triangle’ explaining the factors required by a pathogen to cause an infection. Adapted from Muhammad (2018).

If the percentage of inoculum and host susceptibility are high with favorable environmental conditions, the percentage of disease and its impact would be higher (Scholthof 2007). For example, developing a resistant cultivar, cultural methods of management, and fungicide application reduces the virulence of a pathogen which results in a lower impact of a pathogen causing an infection. In addition to the three factors mentioned in the disease triangle (Figure 1.1) (Muhammad 2018), time also plays an important role in causing a disease as the pathogen takes time to develop infection until environmental conditions become suitable for an infection to proceed (Muhammad 2018). Therefore, time should be considered in crop protection and measures to control pathogens must be implemented at the earliest possible signs of infection to minimize yield losses.

Most of the global wheat production is affected and threatened by fungal diseases: Fusarium head blight, wheat rusts (stripe, leaf, and stem), powdery mildew, leaf spot complex (tan spot), and wheat blast (Brazil & Bangladesh) (Cruz and Valent 2017; Aboukhaddour et al. 2020). In Western Canada, there are more than 20 different fungal pathogen species affecting wheat production. Nevertheless, these five diseases are considered to be the most important "Priority 1" diseases of wheat, which could potentially result in an epidemic resulting in considerable yield losses (Aboukhaddour et al. 2020). As a result, understanding and managing plant pathogens in wheat crops are critical for food security (Enghiad et al. 2017).

Detection methods on plant disease monitoring rely on visual symptoms and microscopic methods which often take time and are only possible once infection has reached a point where yield losses may be inevitable (Araujo et al. 2020). Fungicide application is

considered to be one of the most effective ways of controlling plant diseases. However environmental degradation of the ecosystem associated with fungicide application is a major concern, and emergence of new isolates of pathogens resistant to applied fungicides remain a constant threat. This has triggered plant pathologists to explore modern detection techniques that provide quicker, cost-effective, sensitive, and accurate analyses for earlier identification of fungal spores and ultimately facilitate more timely interventions (Figueroa et al. 2018; Araujo et al. 2020).

Although environmentally friendly methods such as resistant cultivars have been developed for different wheat diseases, multiple disease resistance still remains a challenge. Recent improvements in molecular approaches, including real-time quantitative PCR (qPCR) and multiplex PCR assays provide more efficient tools to detect fungal spores in real time and are rapid and cost-effective.

To perform molecular analysis such as PCR, DNA must be extracted and purified from target samples. Commercially available DNA extraction kits for fungi and other organisms include the Power Soil® DNA Isolation kit, the Soil Master™ DNA Extraction kit, and the Fast DNA® SPIN kit. Following extraction and purification, DNA can be amplified and quantified using qPCR. The quantified DNA using a highly specific primer set cannot be used directly to interpret the quantification of pathogens. This is because the efficacy of PCR or qPCR diagnosis is affected not only by the primer and PCR reaction but also by the efficiency of DNA extraction from the sample, which many researchers have neglected (Yang et al. 2021).

DNA extraction gets difficult when it has to be performed with environmental samples such as air, soil, and water. Various inhibitors exist naturally in environmental matrices

and can be extracted alongside DNA. Co-extractants like humic and fulvic acids, pesticides, and organics may interact with the template DNA, causing incorrect gene amplification, decreased accuracy, false-negative results, and decreased sensitivity (Schrader et al. 2012).

Given the challenges with DNA extraction and its tedious procedures, a simple yet sensitive monitoring tool is necessary to quantify plant pathogens in real-time without needing to perform DNA extraction to detect and quantify the pathogens directly. This research aims to adapt a novel technique, real-time immuno-PCR (RT-iPCR), to detect and quantify three important fungal pathogens of wheat. This technique has been employed previously for the detection of environmental contaminants, bacterial enterotoxins, and cancer-causing antigens (Fischer et al. 2007; Mondal et al. 2020), but there are limited applications describing the quantification of airborne fungal pathogens. This study also describes a potential solution to the above stated research gap that exists within the molecular analysis to calculate DNA extraction efficiency based on the fungal reproductive biology and the factors involved in DNA extraction. Finally, the developed methods are used in this thesis to quantify fungal spores in real-air samples and the advantages and limitations of each method are compared and discussed.

1.1 Literature review on wheat diseases

1.1.1 Tan spot

Tan spot is one of the most devastating foliar diseases of wheat caused by the ascomycete homothallic fungus *Pyrenophora tritici-repentis* (Died.) Drechs. (*Ptr*) (Figure 1.2)

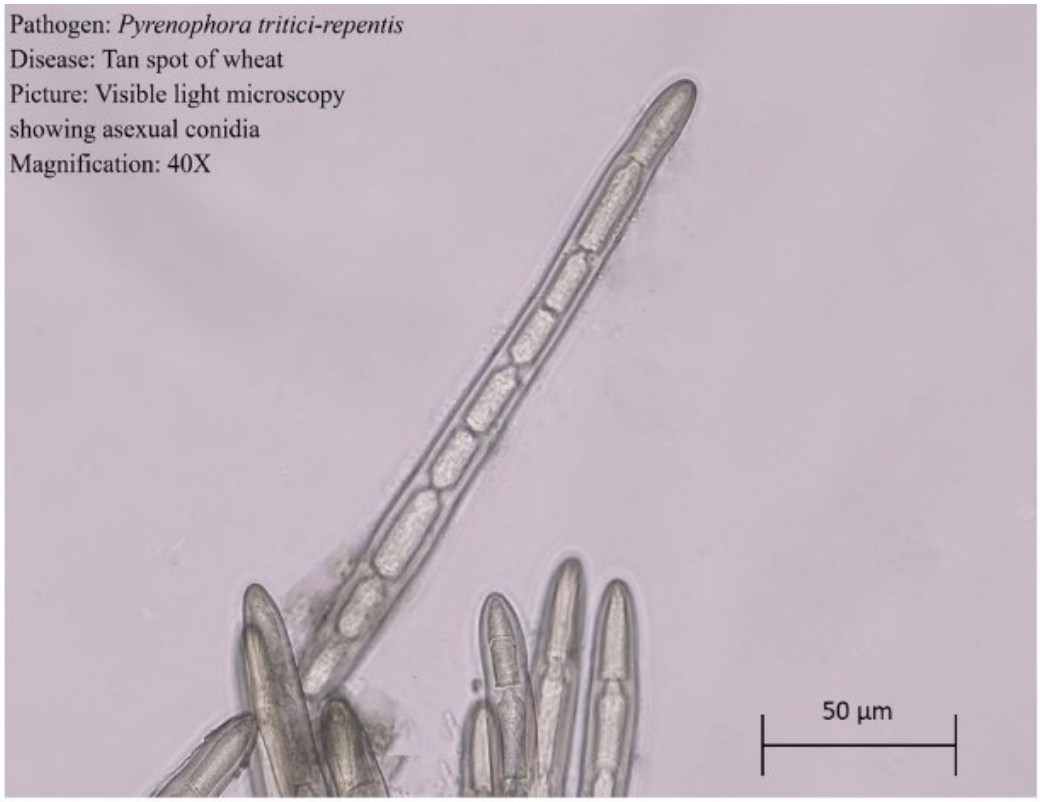

Figure 1.2: Light microscopy image of *Pyrenophora tritici-repentis*

which damages leaves by producing necrotrophic lesions (Lamari and Bernier 1991; Wei et al. 2021).

Symptoms and biology: During initial stages of infection, the visible symptoms are black spots with a white centre. Chlorotic and necrotic areas develop around the spots. The lesions coalesce and form large areas of dead tissue during disease development (Bankina and Priekule 2011). The primary infection of wheat is initiated by sexual ascospores (Bankina and Priekule 2011) and many cycles of secondary infection are caused when asexual conidia develop on the necrotic leaf lesions and plant debris (Figure 1.3) (Bankina and Priekule 2011). Ascospores are dark brown, oval to globose, measuring usually 47-65 µm × 20-26 µm whereas the asexual conidia are cylindrical in shape ranging from 117-217 µm × 15-18 µm (Figures 1.2 and 1.3) (Figueroa et al. 2018; Araujo et al. 2020).

This air-borne fungal pathogen was first identified in the United States in the 1940s, which caused significant crop losses of up to 20-70% in the subsequent years (Bankina and Priekule 2011; Moreno et al. 2012). *Ptr* was found to be one of the important wheat pathogens across the world (Bankina and Priekule 2011) and the most prevalent pathogen among leaf spot pathogens identified in a 12-year survey (2001- 2012) conducted across commercial fields of Canadian Prairies (Fernandez et al. 2016). Of the eight races (R1 to R8) of *Ptr* that have been identified and characterized worldwide, only R1 and R2 are prevalent in Alberta, Canada (Aboukhaddour et al. 2013).

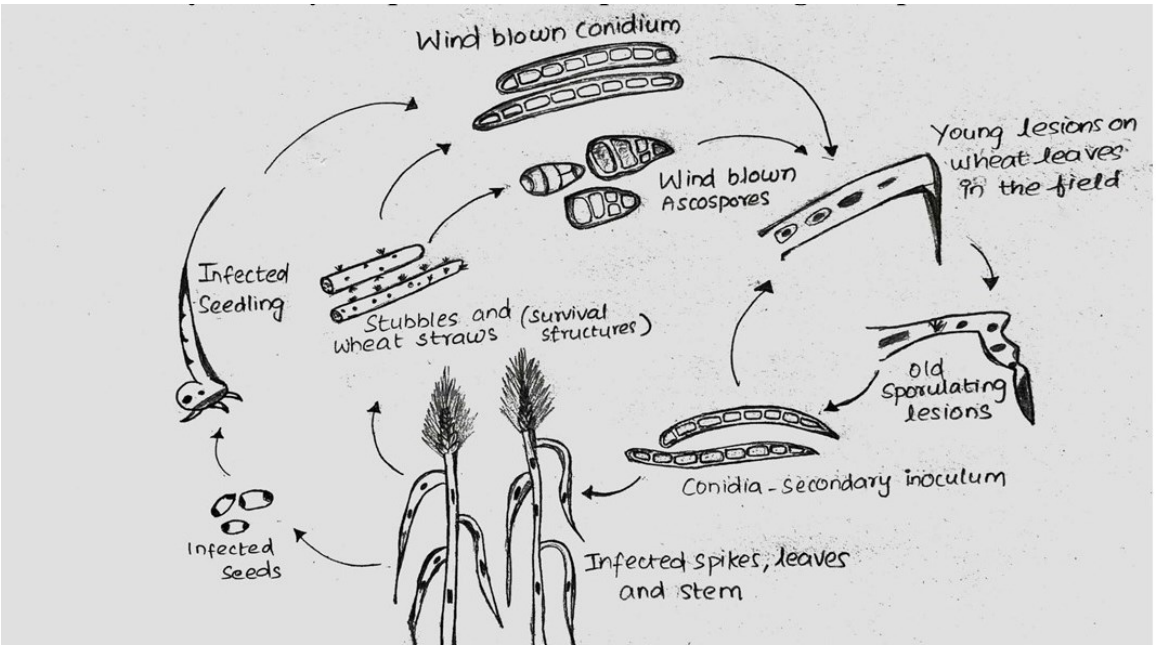

Figure 1.3: Life cycle of *Pyrenophora tritici-repentis*; Modified from Santana and Friesen (2008) and Ciufetti et al. (2014).

Tan spot and septoria nodorum blotch caused by *Ptr*, and *Parastagonospora nodorum,* respectively are the two most important foliar diseases of wheat sharing common symptoms, including damage in the leaf area which makes the identification difficult and often results in misdiagnosis (Abdullah et al. 2018). Therefore, a more sensitive, reliable, and specific detection tool is needed to manage and minimize the disease spread.

1.1.2 Fusarium head blight

Fusarium head blight is one of the important diseases of wheat globally, caused by the air-borne fungal pathogen *Fusarium graminearum* (Schwein) Petch (*Fg*) (Figure 1.4) which was identified in 1839 (Walter et al. 2010; Aboukhaddour et al. 2020; Araujo et al. 2020) and caused a major epidemic in Canada in 1980 (Gilbert and Tekauz 2000).

Symptoms and biology*: Fg* infection on the spike head can reduce kernel set and kernel weight causing yield reductions. It also destroys starch granules and storage proteins, resulting in poor grain quality (Walter et al. 2010). Degradation of epidermal cuticle on the flowering spikelet takes place during the disease development and fungus spreads from one spikelet to the other through the vascular tissue (Walter et al. 2010; Yang et al. 2013). This disease can also produce an extremely harmful mycotoxin affecting animal and human health, called tricothecene deoxynivalenol (DON) that degrades and affects the market quality of grains (Walter et al. 2010).

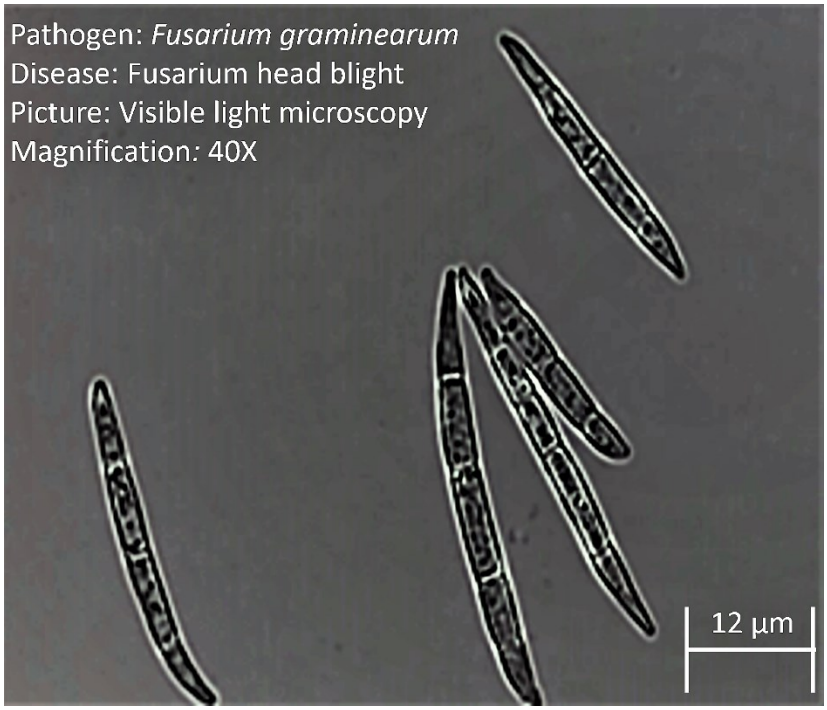

Figure 1.4: Light microscopy image of *Fusarium graminearum*

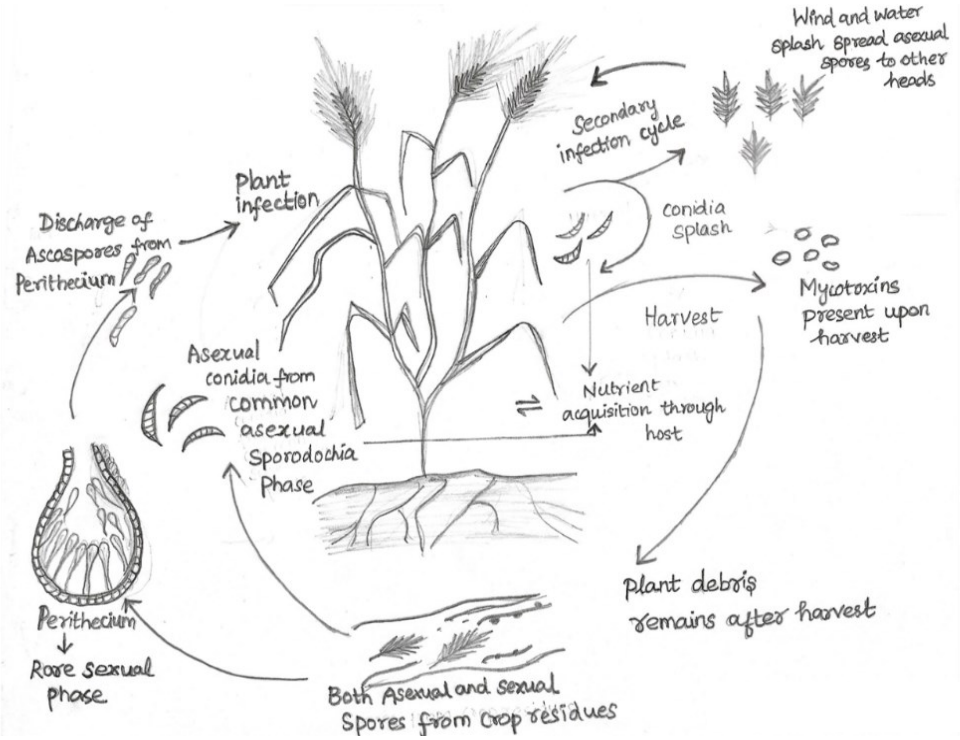

Figure 1.5: Life cycle of *Fusarium graminearum*; Adapted from Trail (2009).

This disease is disseminated by airborne fungal spores including both sexual ascospores and asexual conidia (Figure 1.5) (Osborne and Stein 2007) serving as a primary source of inoculum disseminated mainly through wind (Araujo et al. 2020). Ascospores are usually translucent to light brown in colour with curved ends and the size ranges from 19-24 µm × 3-4 µm and macro conidia are also translucent canoe with a foot-shaped basal cell ranging from 25-50 µm × 3-4 µm (Figures 1.4 and 1.5) (Keller et al. 2013).

This disease led to losses of more than $3 billion to agriculture in the U.S and Canada during the 1990s alone (Ward et al. 2008). Western Canada faced a severe epidemic due to this disease in 1993 (Aboukhaddour et al. 2020). The number of counties reporting the presence of *Fg* has increased from 9 to 26 in Alberta between 2001 and 2016 (Alberta Agriculture and Forestry 2020). In 2016, Canada faced a loss of $1 billion CAD due to this disease affecting wheat production (Dawson 2016).

1.1.3 Stripe rust

The causal agent of stripe rust (also known as yellow rust in other parts of the world) is an air-borne fungal pathogen, *Puccinia striiformis* Westend. f. sp. *tritici* Erikss., (*Pst*) (Figure 1.6) which was first identified in Europe in 1827 and was reported in Canada (Alberta) in 1918 (Line 2002; Araujo et al. 2020).

Symptoms and biology: When infected with stripe rust, plant leaves show yellow powdery pustules arranged in narrow stripes (usually along the veins of a leaf) (Zhao et al. 2014). Both seedling and adult stages of wheat plants are susceptible to this disease where rust is formed by clusters of yellow-orange coloured urediniospores (Figure 1.7) (Figueroa et al. 2018; Araujo et al. 2020).

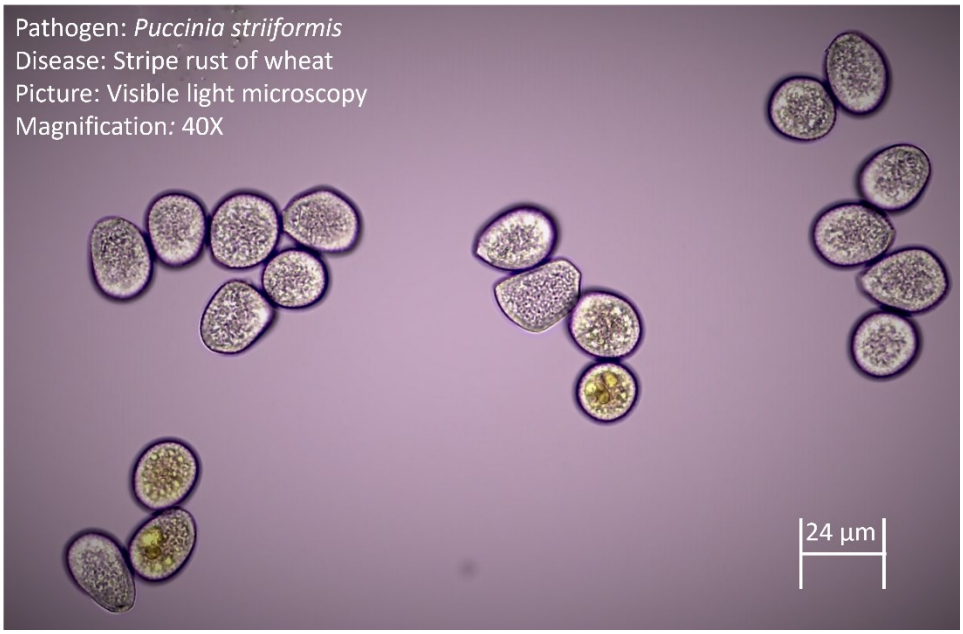

Figure 1.6: Light microscopy image of *Puccinia striiformis* f. sp. *tritici*

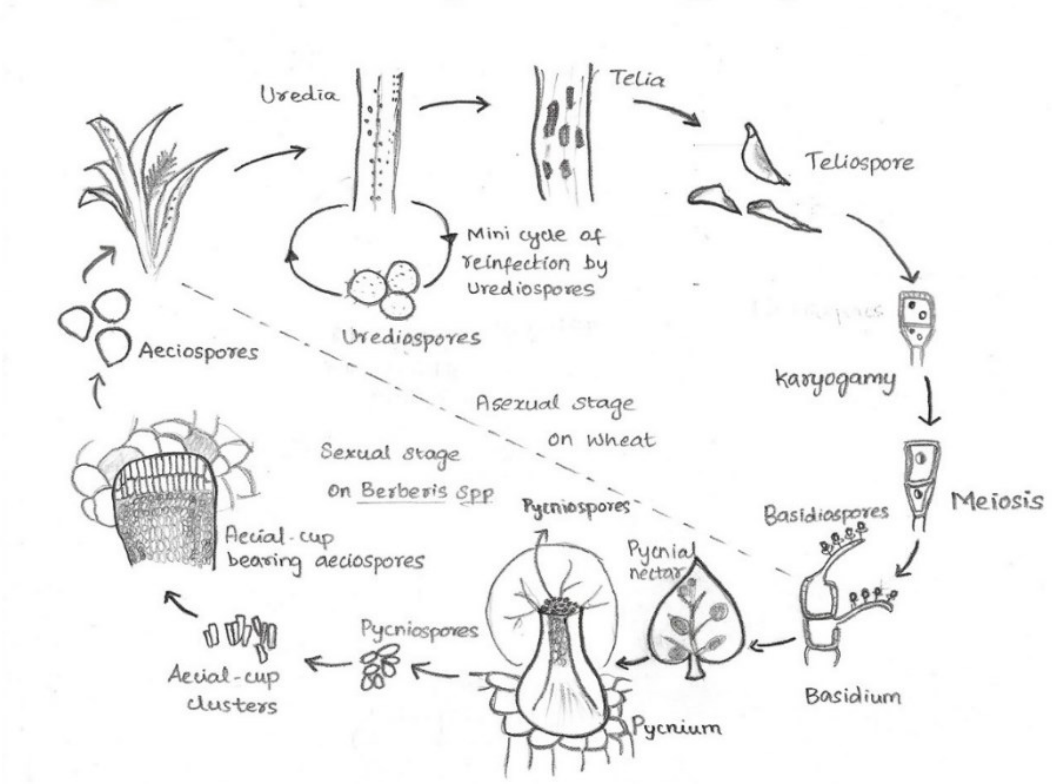

Figure 1.7: Life cycle of *Puccinia striiformis* f. sp. *tritici* causing stripe rust of wheat. Adapted from Ali et al. (2014) and Zheng et al. (2014).

In most cases, urediniospores are the primary source of inoculum produced in asexual stages of reproduction in wheat plants (Zheng et al. 2014). Sexual reproduction takes place in alternate host *Berberis* spp (Figure 1.7) (Zheng et al. 2014). Urediniospores are asexual spores with several cycles of secondary infection causing stripe rust in all the stages of the wheat plant and the spores usually appear in various shapes from round to obovoid, ranging from 18-29 µm × 20-27 µm (Figures 1.6 and 1.7) (Liu and Hambleton 2010; Araujo et al. 2020).

Today, 88% of wheat varieties in the world are susceptible to this disease, and losses of $1 billion / year are estimated (Beddow et al. 2015; Aboukhaddour et al. 2020). Growers spend at least 1 billion USD every year to control this disease (Chen 2020). An average loss of 0.29 to 7.2 tonnes / hectare has been recorded for the susceptible cultivars of stripe rust in Western Canada (Kumar et al. 2019). This disease is considered an important disease world wide as stripe rust has caused a considerable yield loss in 60 countries in Central, East, and West Asia, Europe, East and South Africa, and South America (Chen et al. 2010; Chen 2020).

The airborne fungal spores from the U.S. are the main source of primary inoculum for the infection in Alberta. There are two major pathways for the spores to enter Canada; Pacific Northwest and US Great Plains pathways, the former leading the inoculum to settle in British Columbia, Alberta, and western Saskatchewan and the latter delivering the inoculum to Eastern Saskatchewan, Manitoba, and Ontario (Brar and Kutcher 2016). Between the years 2000 and 2007, the total number of *Pst* races characterized in the US was 115 (Chen et al. 2010). Fifty-nine *Pst* isolates, the majority of which were obtained from Saskatchewan and Southern Alberta between the years 2011 and 2013, were

analyzed for virulence frequency and race diversity (Brar and Kutcher 2016; Ghanbarnia et al. 2021).

Virulence frequency was compared between the isolates from Saskatchewan and southern Alberta with isolates from the Great Plains and Pacific Northwest of the United States and the results established a strong correlation between the two, suggesting the US is the major source of airborne fungal pathogens in Canada. For the race diversity analyses, 33 races were distinguished from the 59 isolates, of which, one race, C-PST-1, accounted for 31 % of the isolates (Brar and Kutcher 2016). Understanding race structure and classification of pathogenic isolates is crucial for determining effective control measures.

1.1.4 Arms race strategy

Understanding the arms race strategy is crucial for implementing effective pathogen management strategies and reducing plant disease impacts. It underlines the importance of integrated approaches that consider the complex connections between hosts and pathogens, as well as the evolutionary dynamics of these interactions (Hu et al. 2022). In host-pathogen interactions, an arms race can result in the evolution of novel pathogen strains that are more virulent and resistant to host defenses. This process has the potential to result in the emergence of new diseases as well as resistance to existing treatments.

Host-pathogen interactions are complex processes that involve a number of molecular, cellular, and physiological events that influence whether or not a pathogen can infect a plant. A disease-causing pathogen must first overcome physical barriers such as the cell wall and cuticle before it can infect a plant (Schumann and D'Arcy 2006; Hu et al. 2022). To ensure its multiplication and reproduction, the pathogen must elude detection by the

immune system and modify plant processes once inside the plant. Plants have both natural and induced defensive mechanisms that help them recognize and respond to pathogen threats. Pre-existing protections include physical barriers such as the cuticle and cell wall, as well as chemical defenses such as antimicrobial compounds. Inducible defenses include the activation of various signaling pathways (Hu et al. 2022).

Pathogens, on the other hand, have devised numerous strategies for evading plant defenses. These strategies comprise producing effectors that can manipulate plant processes in order to boost pathogen growth and survival. Pathogens overcome plant defenses in the following ways, breaking the physical barriers including cell wall and cuticle, synthesis of cellulases and lipases to damage plant membranes and cell walls, and suppression of plant defense mechanisms by triggering reactive oxygen species production (Hu et al. 2022). These pathogens can then target plant systems and cause major crop losses. As a result, it is vital to create effective methods to protect plants from these threats. One of the most effective plant protection strategies is plant breeding with resistance genes (Schumann and D'Arcy 2006; Hu et al. 2022). These genes let plants sense and respond to pathogen attacks, as well as activate a number of defense mechanisms that limit disease development and spread.

1.2 Detection and control methods for wheat diseases

The first step in diagnosing a plant disease is to find out whether the symptoms are caused by a pathogen (disease) or an environmental factor (physiological disorder). Usually, if the disease and the symptoms are caused by a pathogen then a detailed evaluation of the characteristics of a causal agent is required beyond the obvious

symptoms for a correct diagnosis (Schumann and D'Arcy 2006). Early disease monitoring methods relied on visual symptoms and microscopic identification which were often time consuming and the symptoms can be recognized only after the diseases are persistent in the field (Araujo et al. 2020). This leads to an increased disease spread which lowers the possibility of controlling the infection. In phytopathology, early detection of pathogens helps facilitate their control and prevent disease (Atkins and Clark 2004).

Some of the airborne spores belonging to different genera can lead to serious crop losses. When genetic resistance is not available, then it is important to treat the fungal diseases early in infection by applying necessary treatments. Plant disease identification and evaluation is a costly procedure that requires important efforts to achieve reduction in yield loss. Accordingly, accurate methods and affordable techniques for diagnosing plant pathogens are needed. Numerous attempts have been made to detect and manage plant diseases effectively using preventive techniques and best management practices (Tewari and Sharma 2019; Araujo et al. 2020), however, no single method or approach is universally used.

There are three components to preventing disease spread, namely, avoidance, exclusion, and eradication (Schumann and D'Arcy 2006; Snehi et al. 2015; Narayan et al. 2022). In avoidance, the ultimate goal is to avoid exposure to the pathogen. It mainly focusses on the environmental factor of the disease triangle by changing the planting site or planting season (Snehi et al. 2015; Narayan et al. 2022). But in temperate countries like Canada, it is difficult to change the planting time as field production is mostly seasonal. Exclusion is the method of preventing the entry of pathogens into agricultural fields through

quarantine and legal restrictions (Schumann and D'Arcy 2006). However, it is not possible to restrict the entry of airborne fungal spores through these methods. Eradication refers to removing or destroying pathogens through cultural practices and chemical and biological controls (Schumann and D'Arcy 2006; Snehi et al. 2015; Narayan et al. 2022).

Cultural practices, including management of plant debris by removing stubble through burning can effectively reduce the inoculum but poses a severe risk of soil erosion. Also, it does not work for the spores carried away by the wind from the other fields (Moffat and Santana 2018) as most of the *Ptr, Pst,* and *Fg* spores get on to the leaves mainly via wind dispersal (Moreno et al. 2012; Brar and Kutcher 2016; Araujo et al. 2020). Crop rotational practice was also found to be an effective strategy to manage these diseases as monocultures added an increased risk of infection. However, economic considerations can make growers restrict crop rotational practices (Moffat and Santana 2018).

Significant methods for controlling *Ptr* are fungicide applications, removing infected plant debris, and use of resistant genes. Stripe rust can be controlled by developing resistant cultivars, fungicide treatments, and suitable cultural practices (Chen 2020). Reduction of wheat growing areas is one of the strategies followed in North Western China to limit the spread of the disease, but this approach would not be effective in areas where wheat is grown as a staple food crop (Chen 2020). A few decades ago, fungicide treatments were commonly applied worldwide to treat this disease as there were only limited resistant cultivars (Chen and Zhou 2009).

For *Fg* resistance, it is important to mention that new isolates of *Fg* caused by mutations in China have led to resistance to commonly used fungicides such as carbendazim (Chen and Zhou 2009). Although fungicide applications and resistant cultivars are developed

against these diseases, new isolates of pathogens evolve through mutations that are resistant to control measures taken and can cause significant yield losses.

While some diseases can be diagnosed by examining pathogens in infected plant tissues, the majority of diseases involve laboratory culturing. This is typically performed for common bacterial and fungal infections but can take weeks to complete and requires considerable diagnostic skills to detect and interpret the findings. Furthermore, many pathogens are obligate parasites including stripe rust spores, which are impossible to culture in a laboratory without host tissues (Schumann and D'Arcy 2006). Therefore, immunoassays and polymerase chain reactions (PCR) are two popular methods for identifying pathogens in plant tissues that can be performed easily within a short time and do not require any culturing (Schumann and D'Arcy 2006).

1.2.1. Molecular detection methods

Current molecular techniques for real-time detection and quantification of crop pathogens are fast and sensitive. These methods can detect spore numbers at very low levels, much smaller than inoculum thresholds for diseases (Araujo et al. 2020). In phytopathology, early detection of pathogens is key to help in control and suppression of the disease. Therefore, the ability to detect very few spores of these diseases is needed to minimize yield losses. Although the methods of molecular diagnostics have improved over the last few decades, there is still a long way to go in the routine utilization of molecular techniques to support diagnostics of plant diseases. Molecular testing procedures used for detecting plant pathogens need to be robust, sensitive, accurate, rapid reliable, and inexpensive (Sanoubar et al. 2015).

The technique of polymerase chain reaction (PCR) has contributed significantly towards disease identification (Aslam et al. 2017). Initially, PCR was effectively utilized to identify bacterial and virus-causing infections in humans due to its specificity. Now, it is widely used for the detection of plant viral, bacterial, and fungal pathogens as well. There are numerous PCR-based assays developed for identifying numerous cereal pathogenic fungi such as *Fusarium* sp., *Puccinia* sp., *Zymoseptoria tritici, Blumeria graminis* f.sp. *tritici*, and *Pyrenophora tritici-repentis* (Kuzdralinski et al. 2017).

RT-PCR technique combines the reverse transcription of RNA into complementary DNA (cDNA) by oligo deoxythymidine primers, sequence-specific primers, and random primers and then its amplification by a regular PCR-based method. It's often used to measure the amount of specific RNAs (Schumann and D'Arcy 2006). However, this technique is qualitative, the major remaining limitation of RT-PCR techniques. The development of real-time quantitative PCR (qPCR) has overcome this limitation by combining quantification with PCR-based amplification (McCartney et al. 2003).

When a qPCR reaction is carried out, the accumulation of PCR products is measured using a fluorimeter after each cycle in an automated condition (McCartney et al. 2003). This direct measurement of PCR products allows the reactions to be monitored. 'Cycle threshold' (Ct), is defined as the cycle number at which a significant increase in fluorescence is observed (McCartney et al. 2003). Monitoring of responses during this amplification process requires the use of fluorescent dyes such as SYBR Green I or sequence-specific fluorescent-labeled probes like the TaqMan probe (Aslam et al. 2017). These probes are used for their high specificity and sensitivity. In a previous study, qPCR assays were developed to detect the spores of rust species, *Pst* and *Puccinia graminis*

causing stripe rust and stem rust, respectively (Liu et al. 2015). While qPCR assays are quantitative and have a better sensitivity and specificity than regular PCR assays, there are increased costs, are generally more complex due to simultaneous thermal cycling and fluorescence detection (Aslam et al. 2017), and are specific to a single pathogen and lack multiple detections.

Rapid, accurate, and cost-effective multiplex PCR (multiple DNA targets) methods have been successfully used to diagnose a number of pathogens in a single assay concurrently (Aslam et al. 2017). Whereas uniplex qPCR can be costly and resource-intensive (requiring time and money to screen independently for each pathogen), multiplex qPCR contains numerous sets of target specific primers for one or more targets in a single reaction tube and enables simultaneous amplification of multiple target nucleic acids (Aslam et al. 2017). In previous research, four viruses with the same symptoms in wheat were simultaneously detected using a multiplex RT-qPCR method. They were wheat dwarf virus, barley yellow striate mosaic virus, rice black-streaked dwarf virus, and northern cereal mosaic virus (Zhang et al. 2017).

A series of advancements in PCR techniques have led to a novel technique called digital PCR (dPCR) for the quantification of target nucleic acids (Quan et al. 2018), which has certain advantages over qPCR, including increased sensitivity (Salipante and Jerome 2020). In real-time PCR, the reaction is tracked during the amplification step and at the exponential level based on the fluorescent signal, and the DNA concentration is quantified using a standard curve whereas dPCR gathers fluorescent signals through end-point calculation, and the PCR reaction is partitioned to many individual droplets that are counted as positive or negative and evaluated; dPCR does not require a standard curve as

this method directly quantify a sequence (Quan et al. 2018). In a recent study reported, digital PCR (dPCR) assays were developed to quantify *Fg, F. culmorum, F. sporotrichioides, F. poae,* and *F. avenaceum* in Italy where a detection limit of 13 copies / µL was achieved for *Fg* (Morcia et al. 2020).

1.2.2 Antibody based detection assays

Immunology deals with the research of the immune response against microbial infection (Murphy and Weaver 2017). The defense mechanism produced against a pathogen is termed an immune response. It originated in the 18th century from Edward Jenner through the development of vaccines for small pox (Murphy and Weaver 2017). In addition to the vaccinations against pathogenic infections, this approach can also be used to generate antibodies against different proteins (Tang et al. 1992). Antibodies are produced by an immunization process where antigens are injected into the test animal such as rabbits, mice, goats, and sheep to produce antiserum specific to the antigen (Kim et al. 2012). The serum fluids obtained from an immunized animal are called antiserum since it includes specific antibodies bound to the antigens and certain soluble serum proteins (Murphy and Weaver 2017). The use of an antibody specific to a given antigen to detect or quantify a target substance is termed an immunoassay.

1.2.2.1 Enzyme-linked immuno sorbent assay

The enzyme-linked immunosorbent assay (ELISA) is the most commonly used immunoassay for the diagnosis of plant diseases which is usually performed in 96-well microtiter plates (Schumann and D'Arcy 2006). Sandwich ELISA and indirect ELISA are the commonly used ELISA method in the detection of pathogens. According to

Schumann and D'Arcy (2006), in the sandwich ELISA method, wells are first coated with antibodies produced against pathogens (antigens) that are responsible for the disease (Figure 1.8 A). Then, in each well, a plant tissue containing the pathogen is added and incubated to allow the pathogen to bind to the antibodies already present in the well. After each phase, the wells are washed to eliminate any unbound reagents. To each well, a solution containing the conjugate antibodies that can bind to antigen binding sites is added. These antibodies are conjugated to an enzyme. When the antigen has been bound to the originally coated antibodies, the conjugated antibodies can bind to available antigen sites, forming a "sandwich" (Figure 1.8 A). Following washing, an enzyme substrate is added, resulting in color formation only if the conjugate has bound to the antigen (Figure 1.8 A). For example, a yellow color forms in wells where the pathogen is present, and can be quantified with a spectrophotometer. The absorbance measurement obtained is proportional to the concentration of pathogens. Whereas in indirect ELISA, the target antigen is coated first, followed by the addition of a primary antibody and then a secondary antibody that has an enzyme (Figure 1.8 B). Following washing, an enzyme substrate is added, resulting in color formation (Figure 1.8 B) (Schumann and D'Arcy 2006).

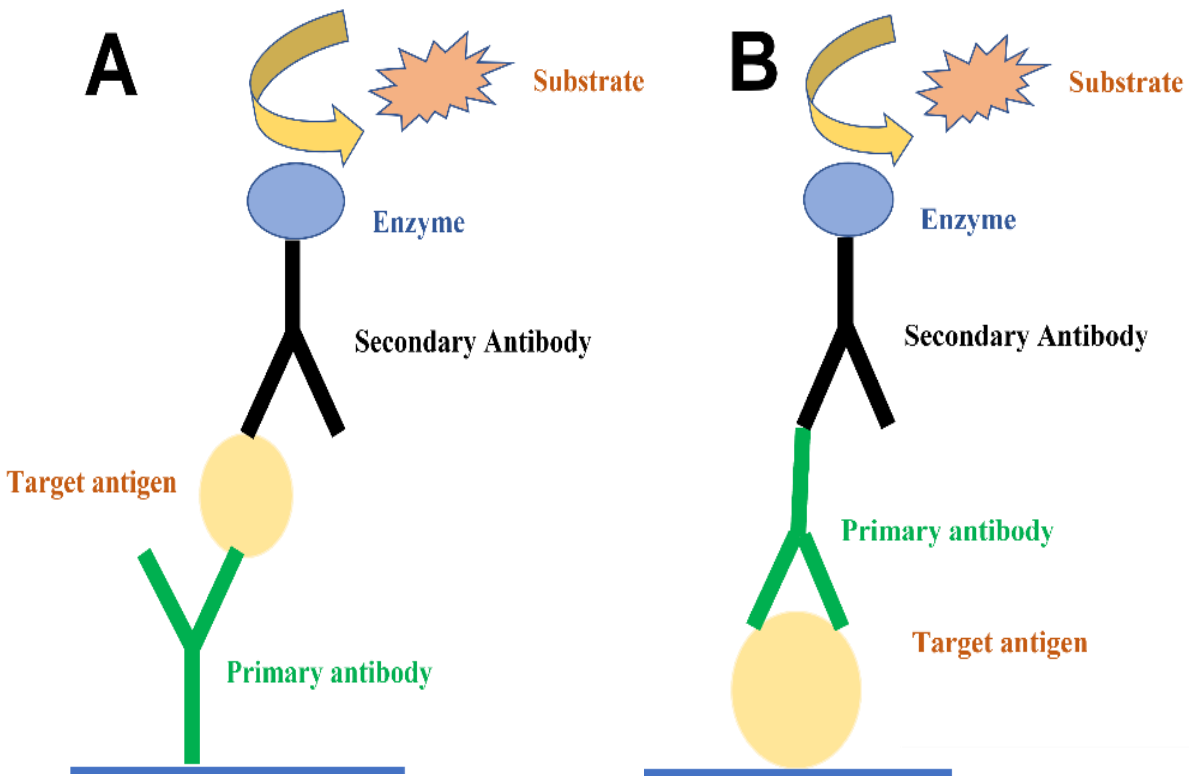

Figure 1.8: The steps followed in sandwich ELISA (A) and an indirect ELISA (B). In sandwich ELISA, the capture antibody is first added followed by coating of the target antigen, then a secondary antibody and a substrate at the end to measure color developed during the process; whereas in indirect ELISA, the surface antigen is coated followed by the addition of primary antibody, then secondary antibody and a colorimetric reagent is added. The color developed is then quantified by spectrophotometry. Adapted from Murphy and Weaver (2017).

Indirect ELISA is preferred over sandwich ELISA for a variety of reasons. Indirect ELISA has a higher sensitivity than direct ELISA since more than one labelled secondary antibody can bind to the primary antibody; it is also less expensive because fewer labelled antibodies are required. Because many primary antibodies can be used with a single labeled secondary antibody, indirect ELISA is more versatile (Schumann and D'Arcy 2006). Sandwich ELISA is a type of ELISA that uses two antibodies to detect and quantify an antigen. When the antigen concentration is low and no suitable pairs of antibodies are available for use in an indirect ELISA, sandwich ELISA is used. In this study, indirect ELISA is employed to quantify fungal pathogens.

Higher specificity, rapidity, and sensitivity are the main advantages of ELISA. When pathogen populations in the host tissue are limited and signs of the disease are not yet visible, this method can still detect the pathogen with lower concentration causing a color reaction (Schumann and D'Arcy 2006). Furthermore, if the required antibodies are present, a diagnostic laboratory can perform several immunoassays to test a large number of samples in a short period of time. This method could also be automated for large-scale testing, which is needed to certify pathogen-free seed or vegetative propagules (Schumann and D'Arcy 2006).

1.2.2.2 Real-time immunoPCR assay

The use of antibody immunoassays emerged in the 1960s whereas the real-time immunoPCR (RT-iPCR) is a modern technique used to detect and quantify target antigens with high specificity and sensitivity (Malou and Raoult 2011). RT-iPCR is the combination of immunology and PCR amplification that has the efficiency of a specific antibody and amplifying power of real-time PCR (Gaudet et al. 2015). The technique was

first introduced by Sano et al. (1992). The surface antigen is coated with the primary antibody, followed by a secondary antibody conjugated to template DNA, and the template DNA is amplified by PCR (Figure 1.9). More specifically, the RT-iPCR assay is carried out by adding the fungal spores (antigen) in a 96-well microtiter plate, then coating the spores with rabbit sera specific to the fungal spore (primary antibody), followed by secondary antibody conjugated to a DNA oligonucleotide via direct conjugation method and finally amplified in the qPCR instrument (Figure 1.9).

In RT-iPCR, the advantages of both ELISA and qPCR are combined providing highly sensitive and specific detection, with an improved limit of detection (LOD) up to 10,000-fold compared to that of corresponding ELISA LODs (Niemeyer et al. 2005). RT-iPCR has played an important role in the detection of several disease-causing organisms like bacteria, viruses, fungal mycotoxins, human immuno-deficiency virus (HIV), and cancer-causing antigens (Barletta et al. 2004; Adler et al. 2005; He et al. 2011; He et al. 2012; Bonot et al. 2014). In a previous study, an environmental contaminant 17β-estradiol was quantified using a RT-iPCR assay (Gaudet et al. 2015).

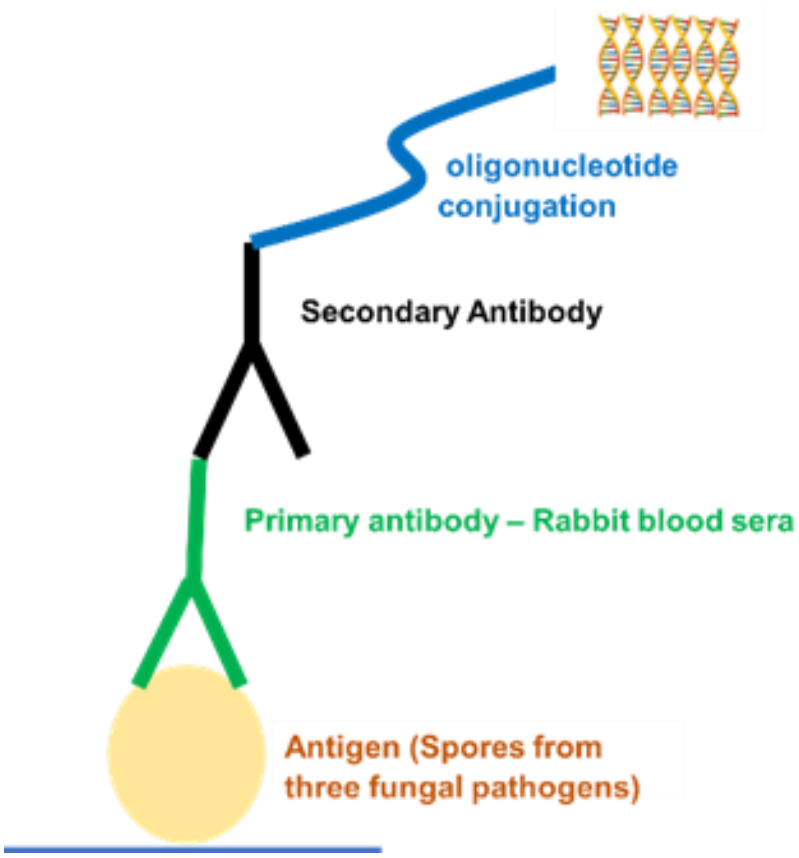

Figure 1.9: Antigen – antibody complex and DNA conjugation. The surface antigen is coated with the primary antibody followed by a secondary antibody conjugated to template DNA which is amplified by qPCR. Adapted from Murphy and Weaver (2017).

1.3 Objectives

This research aims to develop an early detection method for three airborne fungal pathogens infecting wheat by an RT-iPCR assay. The objectives of this research are as follows:

1. Validate the polyclonal antibodies raised against *Ptr, Fg,* and *Pst* through indirect ELISA and develop a highly specific and sensitive RT-iPCR assays
2. Quantification of *Ptr, Fg,* and *Pst* spores using an optimized qPCR method
3. Compare microscope counting, RT-iPCR, and qPCR for quantifying *Pst* spores in real air samples

1.4 Thesis organization

The rest of this thesis is structured as follows:

- Chapter 2 describes the development of an RT-iPCR assay against *Ptr, Fg,* and *Pst* through polyclonal antibodies and the challenges involved in developing these assays.
- Chapter 3 describes the quantification of *Ptr, Fg,* and *Pst* spores using an optimized qPCR method. An important research gap related to DNA extraction techniques used in qPCR is highlighted and a potential solution is proposed.
- Chapter 4 presents the data on the quantification of *Pst* spores in real air samples using microscope counting, RT-iPCR, and qPCR techniques.
- Chapter 5 provides a summary and future directions of this work.

Chapter 2 Development of an RT-iPCR assay for the detection of three airborne fungal pathogens of wheat

2.1 Introduction

Wheat is a cereal crop in the family Poaceae, subfamily Pooideae, and tribe Triticeae. Common or bread wheat (*Triticum aestivum* L) and durum or pasta wheat (*Triticum durum* Desf) are the most commonly produced wheat varieties (Figueroa et al. 2018). Wheat is consumed by humans and animals across the world for its high nutritional value and the crop's adaptability to different environments (Dinh et al. 2020).

The production and yield of the wheat crop are affected by both biotic and abiotic stresses; plant scientists and food agencies work together to minimize the losses and increase wheat production. The three important wheat diseases studied in this research are tan spot, Fusarium head blight, and stripe rust.

Tan spot is an important foliar disease of wheat caused by *Pyrenophora tritici-repentis* (*Ptr*). The tan spot spores overwinter on crop residues and causes infection (Wei et al. 2021). The pathogen first penetrates through the epidermal layer as the fungi multiply and infection spreads, chlorotic and necrotic lesions develop on the wheat leaves which eventually coalesce to form large dead tissues (Wei et al. 2021). The taxonomy of *Ptr* and other spores can be found on the web Mycobank (https://www.mycobank.org/) as follows (Figures 2.1).

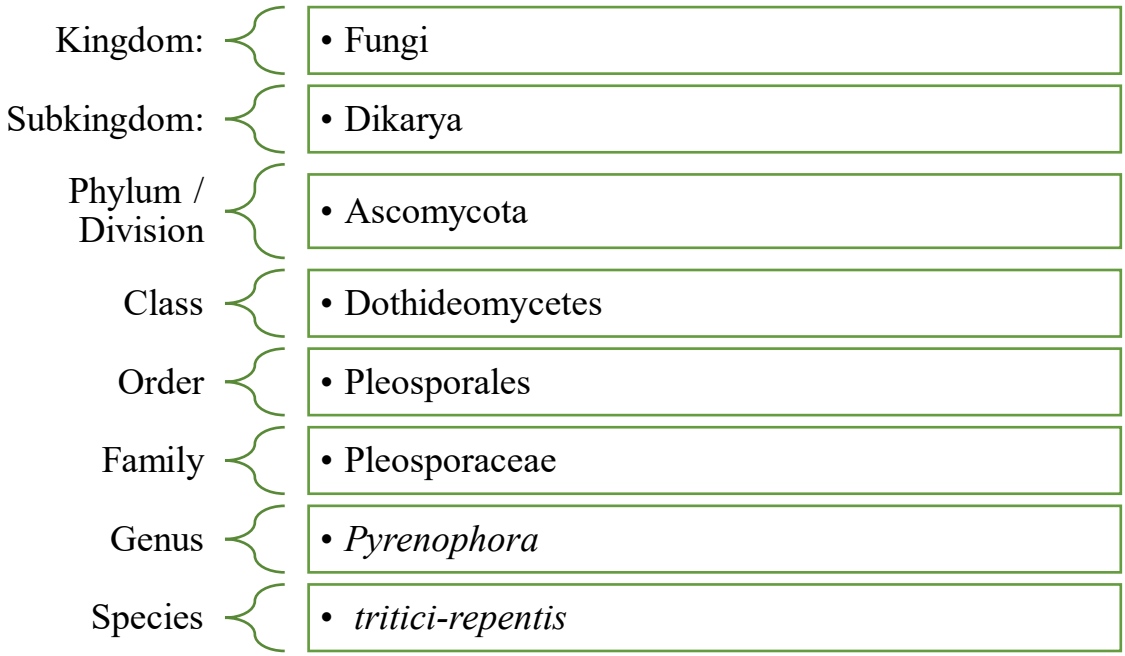

Figure 2.1: The taxonomy of *Pyrenophora tritici-repentis* species including kingdom, subkingdom, phylum, class, order, family, genus, and species. Redrawn from https://www.mycobank.org/

The most commonly available control and detection methods are cultural practices like burning wheat stubbles and crop residues, crop rotational practices, fungicides treatment, and resistant cultivars (Brar and Kutcher 2016; Chen 2020). Molecular detection approaches such as quantitative PCR (qPCR) are employed to detect and quantify *Ptr* spores.

Fusarium graminearum (*Fg*) causes another devastating disease Fusarium head blight of wheat. This pathogen can infect wheat plants at any stage from anthesis until the phase where kernels are fully filled in which the anthesis stage is the most susceptible (Aboukhaddour et al. 2020; Araujo et al. 2020). As a result of Fusarium infection, pinkish colour appears on the spikelets which is a genus specific symptom, grains are not filled and storage proteins are destroyed leading to the damage of overall grain quality. The taxonomy of *Fg* is as follows (Figure 2.2). The control methods include fungicide application, seed treatments, and resistant cultivars (Chen and Zhou 2009). Previously published research has used molecular detection methods such as PCR, qPCR, and dPCR to quantify *Fg* spores (Morcia et al. 2020).

Another important foliar wheat disease stripe rust or yellow rust is caused by an air-borne fungal pathogen *Puccinia striiformis* Westend. f. sp. *tritici* (*Pst*). Stripe rust can impact wheat plants at any stage of development affecting the wheat leaves (Line 2002; Araujo et al. 2020). The seedlings show yellow blotches and adult plants show a sign of yellow-orange narrow stripes. The stripes are formed by yellow-orange colored urediniospores. Under conducive environmental conditions, this pathogen can multiply and become destructive causing 100% yield loss (Araujo et al. 2020). The taxonomy of *Pst* is as follows (Figure 2.3):

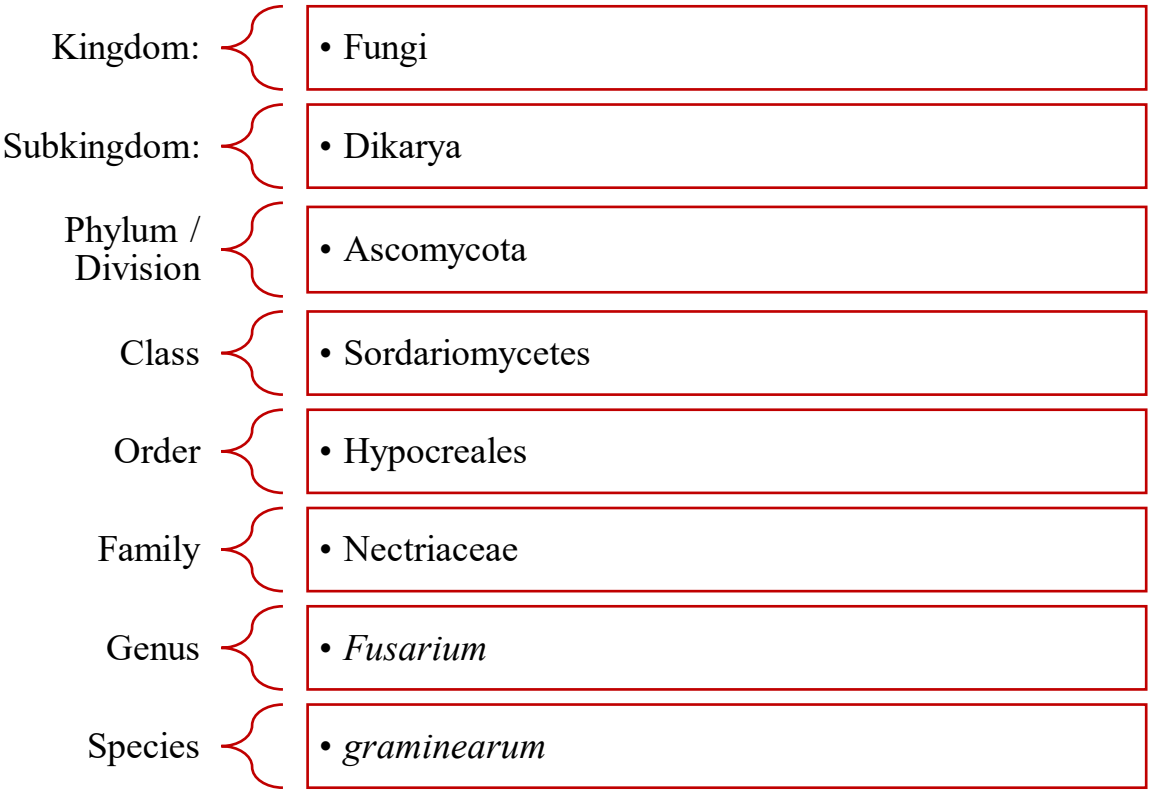

Figure 2.2: The taxonomy of *Fusarium graminearum* species including kingdom, subkingdom, phylum, class, order, family, genus, and species. Redrawn from https://www.mycobank.org/

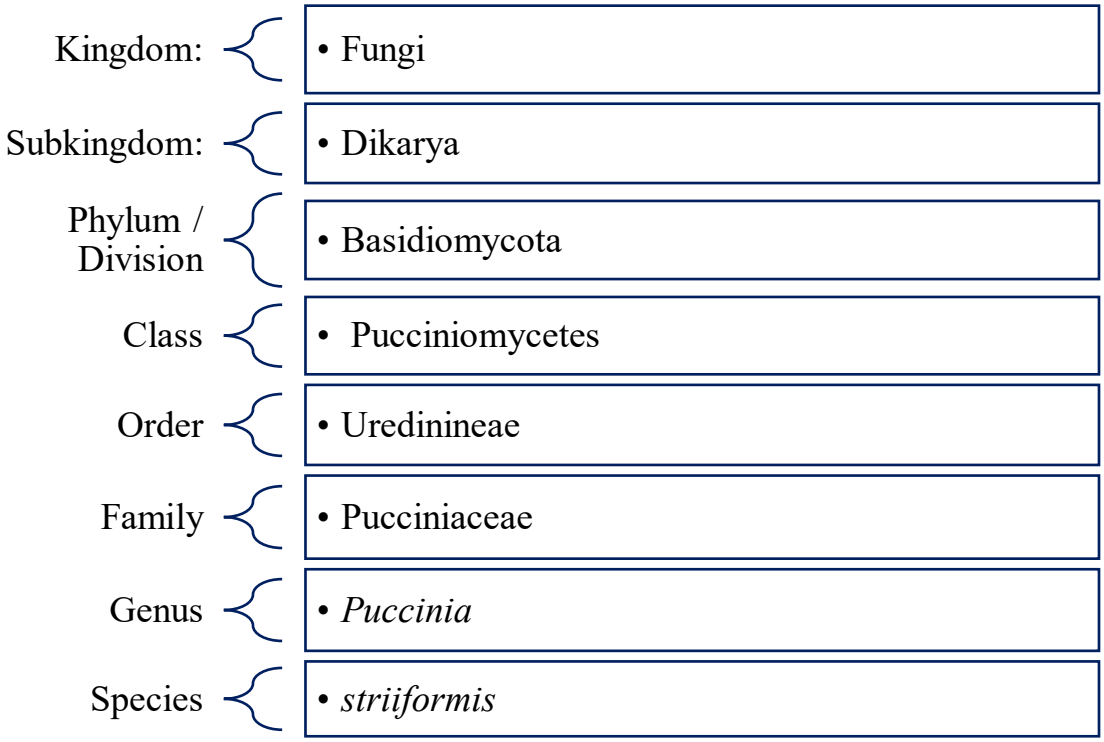

Figure 2.3: The taxonomy of *Puccinia striiformis* species including kingdom, subkingdom, phylum, class, order, family, genus, and species. Redrawn from https://www.mycobank.org/

The management practices include fungicide application, crop rotation and the most effective method is usage of resistant varieties. The commonly used detection methods are PCR and qPCR techniques to quantify this pathogen (Araujo et al. 2020).

This chapter describes the development of a real-time immunoPCR (RT-iPCR) assays for the detection of the airborne fungal spores of *Ptr, Fg, and Pst.* The goal of this development is to achieve a detection assay with improved sensitivity and ease-of-use compared to established techniques (e.g., qPCR) in order to facilitate the earliest possible detection to prevent the spread of these diseases leading to severe yield losses. An indirect ELISA method is used to quantify these fungal spores and a RT-iPCR assay is developed for each of these pathogens. Limits of detections are compared to investigate the sensitivity of both the methods. Finally, in order to determine the specificity, cross-reactivity assays are evaluated and the challenges involved are discussed.

2.2 Materials and methods

2.2.1 Reagents

Phosphate buffered saline (PBS) was diluted in Milli-Q water and it had 0.755 g of $K_2HPO_4.3H_2O$ / Litre (L), 0.25 g of KH_2PO_4 / L, and 8.2 g of NaCl / L. Non – fat dry milk powder was purchased from Bio-Rad (Hercules, CA). Tween 20 was from Sigma – Aldrich (St. Louis, MO). Horseradish peroxidase (HRPO) – conjugated goat anti-rabbit antibody was obtained from Cedarlane Laboratories (Hornby, ON), and 2,2$^{'}$ – azino-bis (3-ethylbenzothiazoline-6-sulphonic acid) (ABTS) was purchased from Kirkegaard and Perry Laboratories (Gaithersburg, MD). The Bright-Line Hemacytometer and Fuchs-

Rosenthal chamber used to count spores were purchased from Hausser Scientific (Horsham, PA, USA)

For this study, ovalbumin (OVA, Mr = 45,000 Daltons) and Tween 20 were purchased from Sigma-Aldrich (St. Louis, MO). 2x QuantiTect Master Mix was obtained from QIAGEN (Mississauga, ON), Probes, forward, and reverse primers (FWD 5' TGATATCGCAGTATATCGCAGAG 3'), (REV 5' CATGCTAGTTGACTGTGACTGTG 3'), and probe (5'-[6FAM] ACTCTCTCCCCGAGAGATCG [BHQ1]-3' where, 6FAM is the reporter dye and BHQ1 is the quencher dye) were from Integrated DNA Technologies, Inc. LowCross-Buffer (LCB) was from CANDOR Bioscience GmbH, (Wagen, Germany). Thunder-Link® Plus Oligo Conjugation Kit was purchased from Abcam (Oligonucleotide Conjugation Kit from product # ab218260). Thunder-Link® Plus Oligo Conjugation Kit was used with AffiniPure Goat Anti-Rabbit IgG (H+L) purchased from Jackson Immuno Research (West Grove, USA). Amicon Ultra-0.5 mL Centrifugal Filters (Ultracel-100) were purchased from Millipore (product # UFC510024). Sterile Optima Water (W7-4) was from Fisher Scientific, Canada.

2.2.2 Spore production

Fungal spores were collected from different laboratories at the Lethbridge Research and Development Centre (RDC). The isolates used were AB-88 for *Ptr* spores, GZ3639 for *Fg* spores, and SWS 484 for *Pst* spores. The spore production techniques for each pathogen are described below.

2.2.2.1 Tan spot

The *Ptr* fungal plugs of strain AB-88 (from Dr. Reem Aboukhaddour's lab, Lethbridge RDC) were placed with the mycelia side facing down on V8 Potato dextrose agar (PDA) media plates containing PDA – 10g, Agar – 10g, CaCO3 – 3g, V8 juice – 150 mL and Milli-Q water – 850 mL / L of media. The plates were kept in the dark at room temperature (RT) for 5 days until growth measured approximately 5 cm in diameter. After 5 days, the mycelia grown in the plates were disrupted by pouring 1-2 mL of autoclaved water with the flame sterilized end of a test tube, and the plates were put under fluorescent lights at RT. After 19 h of incubation, plates were moved from under fluorescent lights to a dark incubator at 15°C. After 24 h, the conidia formed on the outer surface were gently scraped using flame sterilized metal inoculation loops and suspended in 10 mL PBS.

2.2.2.2 Fusarium head blight

In a 2L flask,100 mL of carboxymethyl cellulose (CMC) media containing 15.0 g of CMC, 1.0 g NH_4NO_3, 1.0 g KH_2PO_4 (monobasic), 0.5 g $MgSO_4 \cdot 7H2O$, 1.0 g yeast extract was added along with 100 µL of streptomycin-sulfate (50 µg / mL) to the CMC media to avoid bacterial contamination. Inoculated 100 µL of a previous *Fg* inoculum, strain GZ3639 (from Dr. Nora Foroud's lab, Lethbridge RDC) in the CMC media and added 700 mL water to make up the total volume of 1L. The suspension was split equally into six 250 mL flasks (approximately 167 mL / flask). The flasks containing *Fg* inoculum were agitated at 170-190 rpm at RT for 4-7 days until the culture was cloudy with mycelial growth. Then, each culture flask was vigorously agitated to release macro-

conidia from mycelia and filtered through one layer of autoclaved lab towel into another 250 mL flask. The spore suspension was collected in 50 mL Falcon tubes and centrifuged at 3220 × g in a swinging bucket rotor centrifuge (Eppendorf Centrifuge 5810 R, A-4-62) for 10 min. The supernatant was discarded and the pellet was washed three times with sterile water. Finally, the spores were re-suspended in 20 mL PBS.

2.2.2.3 Stripe rust

Pst spores cannot be grown under lab conditions as it is an obligate biotroph. So, a susceptible wheat cultivar grown in a growth chamber was inoculated with *Pst* spores of strain SWS 484 and spores were collected after two weeks of inoculation (Araujo et al. 2020) by Dr. André Laroche and his team (Lethbridge RDC) and were used to carry out the experiments.

2.2.3 Determination of spore concentration

The *Ptr, Fg, and Pst* spores were counted to generate standard curve working solutions for the detection assays. For each spore, 1 mg of freeze-dried spores were weighed and suspended in 1 mL of PBS. Spore concentrations were determined using a Bright-Line hemacytometer for *Fg* and *Pst* spores, whereas a Fuchs-Rosenthal counting chamber was used to determine the spore concentration of *Ptr* spores under a compound microscope (Olympus CX43). *Fg* spores were diluted 4× prior to counting due to the presence of innumerable spores in 1 mg. For each count, 10 µL of the spore suspension was pipetted into the counting chamber, covered with a cover glass and spores were counted under the microscope. The number of grids counted under the microscope was four (4 corner grids out of 9) / count for *Fg* and *Pst* spores whereas two grids / count were counted for *Ptr*

spores due to a different counting chamber. Each spore sample was counted in 12 replicate counts. Therefore, the total grids counted were (n = 12 × 2) 24 for *Ptr,* and (n = 12 × 4) 48 for *Fg* and *Pst*.

2.2.4 Production of polyclonal antibodies

Polyclonal antibodies against *Ptr* (AB-88) and *Fg* (GZ3639) were purchased from MÉDIMABS, Montreal (Quebec), Canada. Two rabbits were immunized for each spore species through their "classic" protocol and the test bleeds were evaluated by ELISA in MÉDIMABS research laboratory. Final bleeds of approximately 50 mL / rabbit were sent to our lab (Immuno-chemistry lab, Lethbridge RDC) to carry out our research using these antibodies.

Polyclonal antibodies against *Pst* spores were previously produced by the Immuno-chemistry lab at Lethbridge RDC for a different project. Three New Zealand white rabbits were immunized with *Pst* spores containing 2×10^5 spores in Freund's complete adjuvant and two booster injections in Freund's incomplete adjuvant were given with the same spore count; two weeks after each booster, the bleed sera was collected and placed at 37°C for 1 h prior to 4°C overnight incubation. The final term bleed sera were collected 4 days after final immunization and stored at -20°C (previously conducted unpublished work at the Lethbridge RDC). The serum from each rabbit was evaluated by checkerboard ELISA.

2.2.5 ELISA

An indirect ELISA involves a series of additions that bind sequentially to one another: 1) antigen / spore coated onto a plate; 2) primary antibodies; 3) secondary antibodies

conjugated to enzymes; and 4) colorimetric reagent that is measured by spectrophotometry (Figure 2.4) (Gaudet et al. 2015). An indirect checkerboard ELISA was used to determine the effective specificity of polyclonal antibodies against fungal spores by using different concentrations of both antigens and antibodies.

The three pathogenic spores were dissolved in 10 mL phosphate-buffered saline (PBS) with a concentration of 1×10^4 spores / mL for *Ptr*, 1.15×10^6 spores / mL for *Fg*, and 3.5×10^5 spores / mL for *Pst* spores. Additionally, *Pst* spores were dissolved in PBS, frozen in liquid nitrogen, and thawed at room temperature four times to obtain a homogeneous spore suspension. These spore suspensions were coated on Microtiter Nunc plates (cat # 269620) in a two-fold dilution starting from 1000 spores / well (100 µL / well) for *Ptr,* 115×10^3 for *Fg,* and 35×10^3 for *Pst* spores and incubated overnight at 37°C. After overnight incubation, the wells were gently washed thrice with 200 µL of PBS-Tween (0.05%) (PBS-T) through manual washing using a multi-channel pipettor. The plate was blocked with 3% milk in PBS (200 µL / well) and incubated in the dark for 1 h at room temperature (Figure 2.4). After 1 h incubation, the wells were gently washed thrice with 200 µL of PBS-T by manual wash. Primary antibody (100 µL / well) was added in two-fold dilutions staring from 1:1000 in PBS and incubated in the dark for 1 h at RT.

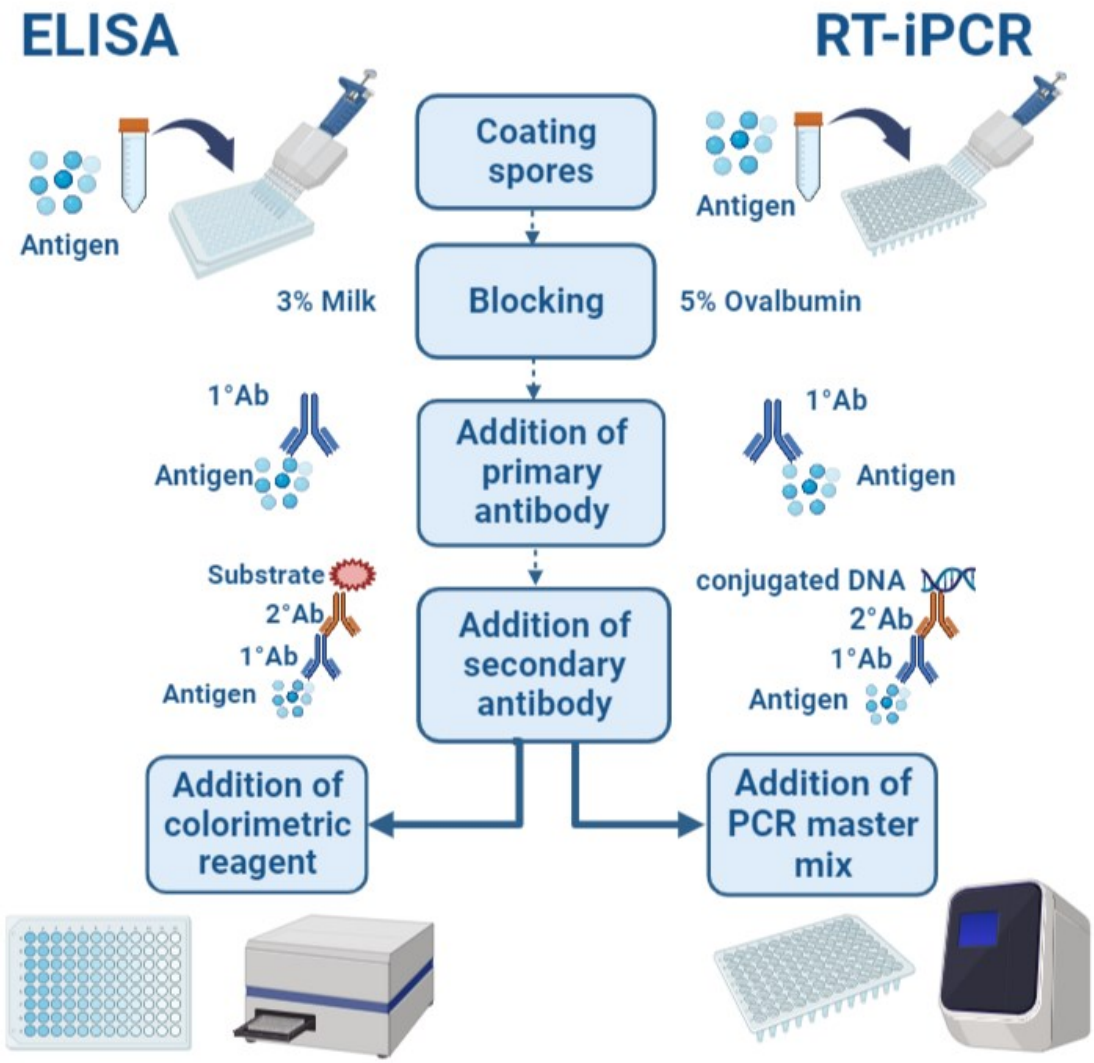

Figure 2.4: Schematic diagram illustrating the steps followed in ELISA (left) including coating spores, blocking, the addition of primary antibody followed by secondary antibody, the addition of colorimetric reagent, and measuring the color developed by spectrophotometry. The steps involved in RT-iPCR (right) include coating spores, blocking, the addition of primary antibody followed by secondary antibody, and finally the addition of PCR master mix and amplification on the qPCR instrument. Created with BioRender.com

Wells were again washed three times with 200 µL of PBS-T manually. A secondary antibody (Horseradish Peroxidase (HRP) Goat Anti-Rabbit) (100 µL / well) of 1 : 5000 dilution in PBS was added and incubated in the dark for 1 h at room temperature. The wells were manually washed with 200 µL of PBS-T thrice and ABTS solution (100 µL / well) was added and incubated for 30 min until color developed at RT. Prior to reading, the plate was shaken once and the absorbance was read at 405 nm using a plate reader (SPECTRAmax® 340PC, Molecular Devices corporation) (Figure 2.4). Absorbance ranging from 0.1 to 4 were found to be in a linear detection range according to the manufacturer's guidelines. However, an absorbance value of 1 indicates 90% light absorption and the solutions with higher concentrations would result in absorbance values greater than 1 (Thiha and Ibrahim 2015).

2.2.6 Optimization and characterization of ELISA

In order to obtain maximum binding capacity, different coating concentrations for each spore at different antibody concentrations were assessed. The known concentration of 3 spores to 1×10^4 *Ptr* spores / mL, 1000 spores to 2×10^5 *Fg* spores / mL, and 200 spores to 5×10^5 *Pst* spores / mL were assessed. The polyclonal antibody concentration varied at a range starting from 1 : 100 to 1 : 2000 for all three antibodies and the secondary antibody concentration were tested at different levels starting from 1 : 1000 to 1 : 5000. Two different wash buffers, PBS-T and Tris-buffered saline – Tween (TBS-T), were also evaluated. Two washing techniques (Plate washer and manual hand wash) were also tested.

2.2.7 Cross reactivity assays – ELISA

Cross reactivity assays were performed to assess the specificity of the ELISA. The experiments were performed with three target spores of *Ptr, Fg,* and *Pst* against their non-specific antibodies. For example, *Ptr,* and *Fg* spores were assessed against *Pst*-specific polyclonal antibodies and vice-versa. For each experiment, a positive control of a specific spore and its specific-antibody was included. A negative control with only PBS was also included. A spore concentration of 3500 spores / well for *Fg* and *Pst* spores and 1750 spores / well for *Ptr* spores was maintained for these experiments to verify cross reactivity.

2.2.8 Antibody-DNA conjugate preparation

The secondary antibody, AffiniPure Goat Anti-Rabbit IgG (H+L) was conjugated to Thunder-Link oligonucleotide (a previously published 90 basepair DNA sequence - CAGCATGTCAGTCAGTCA TGATATCGCAGTATATCGCAGAG AG ACTCTCTCCCCGAGAGATCG CAGT CACAGTCACAGTCAACTAGCATG) (Gaudet et al. 2015) using Thunder-Link® Plus Oligo Conjugation Kit as per the instructions provided by the manufacturers. The secondary antibody conjugated to the oligonucleotide was then purified using Amicon Ultra-0.5 mL Centrifugal Filters (Ultracel-100).

2.2.9 RT-iPCR

The RT-iPCR assay was optimized for *Ptr, Fg,* and *Pst* spores. The RT-iPCR assay was carried out by coating the fungal spores (antigen) in 96-well microtiter plates, then adding rabbit sera specific to the fungal spore (primary antibody), followed by secondary

antibody conjugated to a DNA oligonucleotide based on the Thunder-Link^{R} PLUS oligo Antibody Conjugation Kit. Finally, a PCR master mix (forward primer (FWD 5' TGATATCGCAGTATATCGCAGAG 3'), Reverse primer (REV 5' CATGCTAGTTGACTGTGACTGTG 3'), and probe (5'-[6FAM] ACTCTCTCCCCGAGAGATCG [BHQ1]-3') was added and amplified in a QuantStudio3 qPCR instrument (Applied Biosystems™ QuantStudio™ 3 Real-Time PCR System, Thermo Fisher Scientific) (Figure 2.4) (Gaudet et al. 2015). RT-iPCR assay was used to detect the *Ptr, Fg,* and *Pst* spores. These spores were diluted using two-fold dilutions in filter sterilized PBS starting from a spore concentration of 2.5×10^4 spores / mL for *Ptr*, 2×10^6 / mL for *Fg*, and 6.5×10^5 spores / mL for *Pst* spores. Additionally, *Pst* spores were dissolved in PBS, frozen in liquid nitrogen, and thawed at RT four times to obtain a homogeneous spore suspension. Axygen 96-well plates (96-well PCR Microplate, Axygen PCR- 96-LP-AB-C) were coated with the spores and some wells with no spores acted as negative controls (containing PBS (4 wells) and LCB (2 wells)). The control wells were sealed using plate sealers (Polyester sealing film non-sterile, VWR 60941-062) to avoid contamination, and the 11 two-fold dilutions of spores were coated with a volume of 30 µL / well starting from an initial concentration of 750 spores / well for *Ptr* reaching until 1 spore, 6×10^4 spores / well for *Fg* until 60 spores, and 2×10^4 spores / well for *Pst* spores down to 20 spores. The plate was sealed and incubated overnight at 37°C (Figure 2.4). After overnight incubation, the plate was washed 4× with 175 µL PBS-T 0.05% through manual washing using a multi-channel pipettor. The plate was centrifuged upside down to 1000 rpm (168 × g) for 5 s in Thermo Scientific Centrifuge using clean Kimwipes to dry the plate. Then, the plate was blocked

with 5% OVA (150 µL / well), covered with the plate sealer, and incubated at 37°C for 1h.

After incubation, the plate was washed 4× with PBS-T 0.05% through manual washing and centrifuged upside down at 1000 rpm (168 × g) for 5 s. Primary antibody of 1 : 1000 dilution in LCB was added to each well (30 µL / well) except for negative control wells, covered using a plate lid, and placed on a rocking platform for 1 h at RT. After 1 h incubation, the plate was washed 4× with PBS-T 0.05% through manual washing and centrifuged upside down at 1000 rpm (168 × g) for 5 s in the centrifuge. Secondary antibody of 1 : 5000 dilution in LCB was added to each well (30 µL / well) except for negative control wells, covered using a plate lid, and placed on a rocking platform for 1 h at RT. For the final wash, the plate was washed 8× with PBS-T and 8× with Milli-Q water (200 µL / well - the well size of the plate used was 200 µL and the block in the qPCR instrument was designed for the same), for a total of 16 washes.

The plate was again centrifuged upside down at 1000 rpm (168 × g) for 5 s to dry the plate. PCR master mix of 30 µL was added to each well. The PCR master mix consisted of the following: 15 µL of 2x QuantiTect Master Mix, 0.9 µL of each primer (FWD 5' TGATATCGCAGTATATCGCAGAG3', REV 5' CATGCTAGTTGACTGTGACTGTG3') at a final concentration of 0.3 µM each (Gaudet et al. 2015), 1.8 µL of Taqman probe (5'-[6FAM] ACTCTCTCCCCGAGAGATCG[BHQ1]-3') at a final concentration of 0.3 µM, and sterile Optima Water. The plate was covered with MicroAmp^{TM} Optical Adhesive Film (Applied Biosystem #4360954) and pressed down firmly and carefully to remove air bubbles, using clean Kimwipes. Then, the RT-iPCR was performed using a QuantStudio

3 qPCR instrument (Figure 2.4). The cycle conditions were 95°C for 15 min, 94°C for 15 s, and 60°C for 1 min with 35 cycles. The cycle conditions were optimized previously by Gaudet et al. (2015).

2.2.10 Optimization and characterization of RT-iPCR

In order to obtain maximum binding capacity and reduce non-specific binding / contamination, different coating concentrations for each spore at different antibody concentrations were assessed. For *Ptr* spores, the known concentration of 1 spore to 2.5×10^4 spores / mL, for *Fg* spores, 1000 spores to 2×10^5 spores / mL, and for *Pst* spores, 200 spores to 5×10^5 spores / mL were assessed. The polyclonal antibody concentration varied at a range starting from 1 : 100 to 1 : 2000 for all three antibodies and the secondary antibody concentration were tested at different levels starting from 1 : 1000 to 1 : 5000. Two washing techniques (plate washer and manual hand wash) were tested. The optimized assay conditions were used in all assays.

2.2.11 Cross reactivity assays – RT-iPCR

Cross reactivity assays were performed to assess the specificity of RT-iPCR. The experiments were performed with three target spores of *Ptr, Fg,* and *Pst* against their non-specific antibodies. For example, *Ptr,* and *Fg* spores were assessed against *Pst*-specific polyclonal antibodies and vice-versa. Cross reactivity was also assessed for two non-target pathogens, *Aphanomyces euteiches* (*Ae*) causing pea root rot and *Sclerotinia sclerotiorum* (*Ss*) causing stem rot in wide range of host species. For each experiment, a positive control of specific spore and its specific-antibody was included. A negative control with only PBS (0 spores) were also included. Spore concentrations used were 750

spores / well for *Ptr*, 6×10^4 spores / well for *Fg*, 2×10^4 spores / well for *Pst*, 3000 spores / well for *Ae* and 1×10^4 spores / well for *Ss*. The above-mentioned spore numbers were the maximum possible numbers that the PCR plate could hold / well for *Ptr, Fg* and *Pst* (identified from the method-development experiments) and for *Ae* the amount of spores used were selected as reported in Kaphle (2020). Cross-reactivity assays with just primary antibody, secondary antibody (both conjugated to DNA and non-conjugated secondary antibody), and PCR master mix were also performed to determine the cause of cross-reactivity.

2.3 Statistical analysis

In this study, the statistical analyses were carried out in GraphPad Prism version 9.4.1 for Windows, GraphPad Software (San Diego, California USA). The data from ELISA assays using *Ptr, Fg* and *Pst* spores were subjected to normality testing via Shapiro-Wilk test and Kolmogorov-Smirnov test. Absorbance values obtained through ELISA assays for all three spores were normally distributed. Simple linear regression analysis of ELISA data of three spores were plotted to derive the standard curves with a p-value of 0.001. A repeated-measures One-Way ANOVA followed by Tukey multiple comparisons with a p-value of 0.001 were used to test the significant differences among the different spore concentrations. An ordinary One–Way ANOVA followed by Dunnett's multiple comparisons were used to compare the absorbance values of three different spores against each antibody in the cross-reactivity tests. The symbols *, **, and *** indicate the level of statistical significance in cross-reactivity assays of ELISA (Non-significant $p > 0.12$), (* $p < 0.033$), (** $p < 0.002$), and (*** $p < 0.001$). The data from RT-iPCR assays using *Ptr, Fg,* and *Pst* spores were subjected to normality testing via Shapiro-Wilk test and

Kolmogorov-Smirnov test. Ct values generated through RT-iPCR assays for all three spores were normally distributed. Simple linear regression analysis of RT-iPCR data of three spores was plotted to derive the standard curves with a p-value of 0.0001. An ordinary One-Way ANOVA followed by Tukey multiple comparisons with a p-value of 0.001 was used to test the significant differences between the detectable spore numbers and the control Ct values. RT-iPCR cross reactivity data were subjected to normality testing via Shapiro-Wilk test and the data were normally distributed. An ordinary One – Way ANOVA followed by Dunnett's multiple comparisons were used to compare the Ct values of five different spores against each antibody. The symbols *, **, and *** indicate the level of statistical significance in cross-reactivity assays of RT-iPCR (Non-significant $p > 0.12$), (* $p < 0.033$), (** $p < 0.002$), and (*** $p < 0.001$). It is crucial to distinguish the level of significance as this in turn provides a better understanding of the level of cross reactivity observed between the antibody and non-target spores. However, this could only be a statistical significance and cross-reactivity might be still present when the absorbance values from ELISA / Ct values from RT-iPCR of non-target spores lies within the linear detection range of target spores. The percentage of cross-reactivity in response to the positive control is provided for each spore to give an estimation on cross-reactivity. Percentage difference = (Number of spores detected while using non-target spores / Number of spores in positive control) × 100.

2.4 Results and discussion

2.4.1 Spore numbers counted through a microscope

The spore numbers counted using the microscope are presented in Figure 2.5 with descriptive statistics presented in Table 2.1. In 1 mg of spores, *Ptr* had 3×10^4 spores with a standard deviation (SD) of $\pm 0.4 \times 10^4$, *Fg* contained 8×10^6 spores $\pm 2 \times 10^6$, and *Pst* had 4×10^5 spores $\pm 0.2 \times 10^5$. The variation between replicates (n = 24 for *Ptr*, and n = 48 for *Fg* and *Pst*) were less than 15% for all three spores. The spore numbers indicated above the box plots were resulted after calculations according to the counting chamber used.

For *Ptr* spores, the spore numbers were counted under Fuchs-Rosenthal counting chamber. A volume of 10 µL was pipetted onto the counting chamber. Two grids each with an area of (4 × 4 mm) 16 mm^2 and a volume of 3.2 µL (volume = area × depth (0.2 mm)) were counted and averaged. The average spore number obtained was multiplied by a factor of 312.5 to get spore numbers / mL. For *Fg,* and *Pst* the spore numbers were counted using a Bright-Line Hemacytometer.

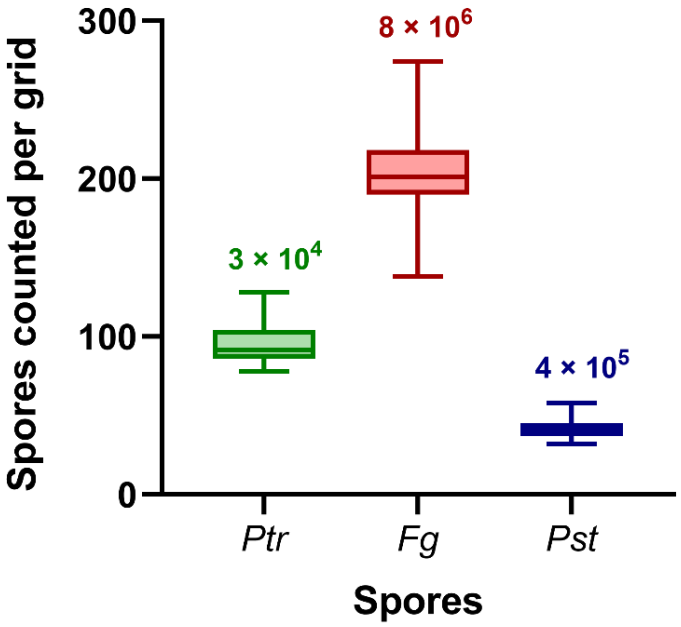

Figure 2.5: Number of *Pyrenophora tritici-repentis* (*Ptr*), *Fusarium graminearum* (*Fg*), and *Puccinia striiformis* (*Pst*) spores counted / grid (3.2 µL for *Ptr*, and 0.1 µL for *Fg* and *Pst* spores) of the counting chamber under a microscope. Calculated spore numbers / mL (/ mg) are indicated above the box plots. The horizontal line inside the box plots indicates the median and whiskers indicate the minimum and maximum spores counted. Colored box plots in green indicate *Ptr,* red indicates *Fg,* and blue indicates *Pst.*

Table 2.1: Descriptive statistics including minimum, maximum, mean, SD values and co-efficient of variation of spore numbers counted through microscope where, n = 12

Descriptive statistics	***Ptr***	***Fg***	***Pst***
Minimum	78	138	32
Maximum	128	274	58
Mean	97	204	41
SD (±)	14.5	25.6	6
Co-efficient of variation	**15%**	**13%**	**14%**

A volume of 10 µL was pipetted onto the hemacytometer. Four grids with an area of (1 × 1 mm) 1 mm^2 and a volume of 0.1 µL (volume = area × depth (0.1 mm)) were counted and averaged. The average spore number obtained was multiplied by 4×10^4 for *Fg* spores (*Fg* spores were diluted 4× before counting because 1 mg of spores had numerous spores making manual counting hard. Hence factor 4 was included in the calculation). For *Pst* spores, the spore numbers counted in four grids and the average was multiplied by 10^4. The majority of this variation is a result of the challenges related to obtaining a homogeneous spore suspension without clumps. These spore counts were used to determine the working concentration of spores for further detection assays in this study.

2.4.2 Detection of *Ptr, Fg,* and *Pst* by ELISA

The assay optimization resulted in using 10 spores to 1×10^4 spores for *Ptr*, 110 spores to 1.15×10^5 spores for *Fg,* and 350 spores to 3.5×10^5 spores for *Pst*; 1 : 1000 dilution of primary antibody; 1 : 5000 dilution of a secondary antibody and PBS-T wash buffer. Manual wash steps were followed for *Ptr* and *Pst* spores whereas plate washer was used for *Fg* spores. These optimized conditions were followed in all the ELISA experiments. Absorbance of 1 indicates 90% absorption of light; however we observed absorbance greater than 1 for concentrated spore samples.

The data obtained from ELISA through spectrophotometry readings were normally distributed for *Ptr, Fg,* and *Pst* spores based on the Shapiro-Wilk and Kolmogorov-Smirnov normality and log normality tests. The standard curve of the average absorbance values of 6 independent replicates were plotted against the log [Spores / well] (Figure 2.6A-C) using simple linear regression analysis.

A repeated-measures one-way ANOVA with Tukey's multiple comparison tests was used to compare the significant differences among different spore concentrations. The linear detection range was 1000 to 30 spores for *Ptr* (Figure 2.6A), 6×10^4 to 1800 spores for *Fg* (Figure 2.6B), and 3.5×10^4 to 2200 spores for *Pst* (Figure 2.6C). Tables 2.2, 2.3, and 2.4 indicate the mean, standard deviation, and % co-efficient of variability (CV) of data obtained through ELISA.

CV (%) was ≤ 7% for *Ptr* and *Pst* spores throughout the dilutions whereas *Fg* had a higher variation (18%) (Table 2.2 – 2.5). The reason for this circumstance could be the use of higher spore numbers for *Fg* than the other two spores. Higher spore numbers increase the possibility of clumps in the suspension leading to a non-homogeneous spore solution. Thus, leading to a lesser R^2 value for *Fg* spores (0.64) compared to *Ptr* and *Pst* spores (0.95 and 0.93 respectively) (Figure 2.6 A-C).

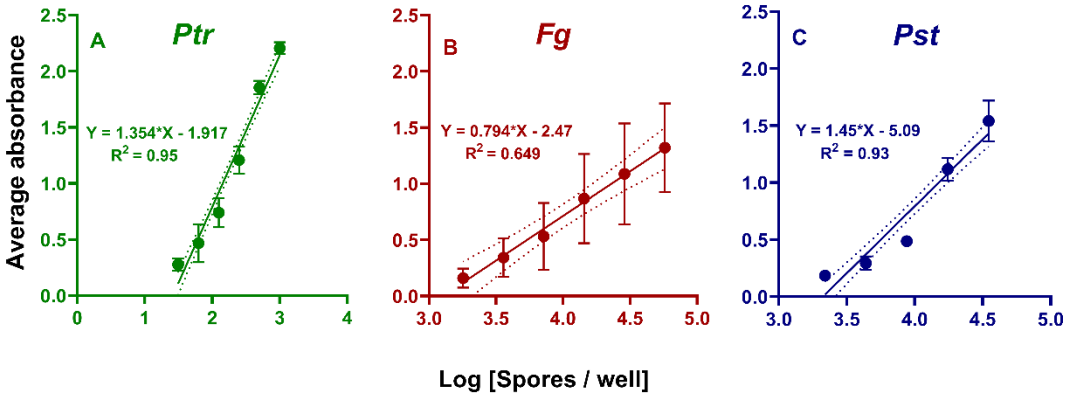

Figure 2.6: Linear regression analysis of the *Pyrenophora tritici-repentis* (*Ptr*) (A), *Fusarium graminearum* (*Fg*) (B), and *Puccinia striiformis* (*Pst*) (C) – ELISA assays. The average absorbance of 6 replicates were plotted against the log[Spores / well]. The relationship between spore numbers (log) and absorbance values were linear and significant ($p < 0.001$). Data points and error bars represent the mean and standard deviation of 6 independent replicate measurements and the dashed lines are 95% confidence intervals of the linear regression.

Table 2.2: Mean, SD, and co-efficient of variability of absorbance for *Pyrenophora tritici-repentis* spores through ELISA

***Ptr* Spores / well**	**Mean (absorbance)**	**SD**	**CV %**	**SEM**
1000	2.200	0.053	2	0.022
500	1.850	0.059	2	0.024
250	1.210	0.122	5	0.050
125	0.739	0.130	5	0.052
60	0.467	0.170	7	0.069
30	0.277	0.054	2	0.022

Descriptive statistics of 6 replicates (n=6), where SD – standard deviation, CV – Coefficient of variability, and SEM – standard error of mean at $p < 0.001$

Table 2.3: Mean, SD, and co-efficient of variability of absorbance for *Fusarium graminearum* spores through ELISA

***Fg* Spores / well**	**Mean (absorbance)**	**SD**	**CV %**	**SEM**
57500	1.320	0.395	16	0.161
28750	1.090	0.449	18	0.183
14375	0.866	0.397	16	0.162
7188	0.531	0.298	12	0.122
3594	0.342	0.173	7	0.071
1800	0.159	0.084	3	0.035

Descriptive statistics of 6 replicates (n=6), where SD – standard deviation, CV – Coefficient of variability, and SEM – standard error of mean at $p < 0.001$

Table 2.4: Mean, SD, and co-efficient of variability of absorbance for *Puccinia striiformis* spores through ELISA

***Pst* Spores / well**	**Mean (absorbance)**	**SD**	**CV %**	**SEM**
35000	1.540	0.178	7	0.073
17500	1.120	0.100	4	0.041
8750	0.486	0.026	1	0.011
4375	0.292	0.059	2	0.024
2200	0.183	0.0290	1	0.012

Descriptive statistics of 6 replicates (n=6), where SD – standard deviation, CV – Coefficient of variability, and SEM – standard error of mean at $p < 0.001$

2.4.3 Cross reactivity assays – ELISA

The antibody's specificity was assessed by conducting cross reactivity assays using ELISA. The spores of *Ptr, Fg,* and *Pst* were evaluated with each antibody. A spore concentration of 35,000 spores / mL was used for *Fg,* and *Pst* spores, and 17,500 spores / mL for *Ptr* spores. An ordinary one-way ANOVA with Dunnett's multiple comparison tests indicated significant differences between positive control (target spores reacted with target antibodies) and the other two species (Figure 2.7A-C). In ELISA cross-reactivity assays, the symbols * with $p < 0.033$, ** with $p < 0.002$, and *** with $p < 0.001$ denote the statistical significance level, which improves comprehension of how antibodies react with non-target spores. Cross-reactivity is still present when the absorbance value of non-target spores is within the linear detection range of target spores, though this could just be a statistical significance. To determine the level of cross-reactivity, an absolute difference is determined and the percentage of cross-reactivity in response to the positive control is given for each spore. Difference in percentage is calculated as follows: (Number of spores detected using non-target spores / Number of spores in positive control) / 100. The heat map (Figure 2.8 A-C) shows the cross-reactivity data where red to blue color mapping indicates higher to lower cross reaction, respectively. The positive control data lies on the left most position in every cross-reactivity graph to render a better comparison.

When *Ptr* antibody was evaluated, the *Fg* and *Pst* spores showed no statistical cross-reactivity. Absorbance values compared to the positive control (*Ptr* spores+ *Ptr* antibody) were significantly lower suggesting minimal cross-reactivity with the *Ptr* antibody (Figure 2.7A). The average absorbance for positive control was 2.55 ± 0.02

(corresponding to 2,016 spores), whereas *Fg* spores with *Ptr* antibody had an average absorbance of 0.07 ± 0.003 a value below the linear range for *Fg* detection (30 spores) contributing to 2% of positive control suggesting low cross reaction (The spore numbers provided in brackets were calculated for the absorbance values of non-target spores by interpolating in the linear curves of target spores (Figure 2.6)), and *Pst* spores with *Ptr* antibody resulted in an average absorbance of 0.65 ± 0.27 (80 spores) which is only 4% of positive control; however, the number of spores detected lies within the detection range of *Ptr* spores suggesting occurrence of cross-reaction (Figures 2.7A and 2.8A).

When *Fg* antibody was assessed, the *Ptr* and *Pst* spores were not significantly different from the positive control (*Fg* spores + *Fg* antibody) (Figure 2.7B) The average absorbance for positive control was 0.93 ± 0.75 (19,092 spores), whereas *Ptr* spores with *Fg* antibody had an average absorbance of 0.58 ± 0.20 (6,744 spores) contributing to 35% of positive control suggesting higher cross reaction and *Pst* spores with *Fg* antibody resulted in an average absorbance of 0.17 ± 0.02 (2,109 spores) 11% of positive control (Figures 2.7B and 2.8B).

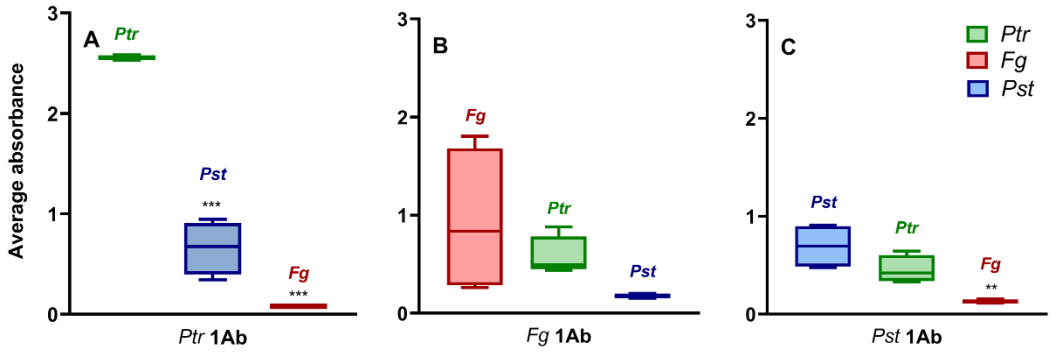

Figure 2.7: ELISA cross reactivity with *Pyrenophora tritici-repentis* (*Ptr*), *Fusarium graminearum* (*Fg*) and *Puccinia striiformis* (*Pst*) against *Ptr* antibody (A), *Fg* antibody (B), and *Pst* antibody (C). Significant differences observed between the positive control and the other two species were indicated with * above each box plot. The horizontal line inside the box plots indicates the median and whiskers indicate the minimum to maximum values and the box plots without * above indicate that the species is not significantly different from the positive control. The symbols *, **, and *** indicate the level of statistical significance (Non-significant $p > 0.12$), (* $p < 0.033$), (** $p < 0.002$), and (*** $p < 0.001$).

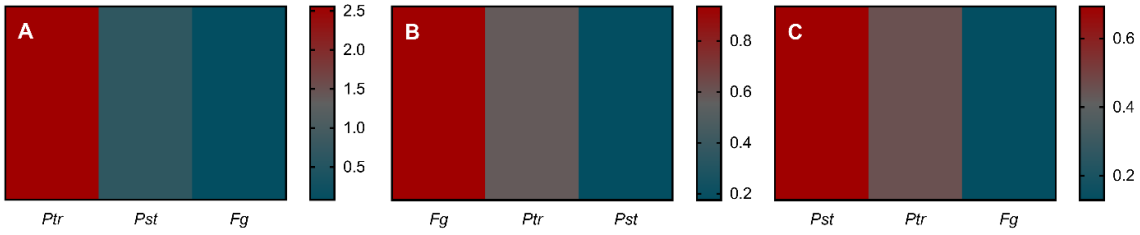

Figure 2.8: Heat map of ELISA cross-reactivity with *Pyrenophora tritici-repentis* (*Ptr*), *Fusarium graminearum* (*Fg*), and *Puccinia striiformis* (*Pst*) spores against *Ptr* antibody (A), *Fg* antibody (B), and *Pst* antibody (C). Red to blue color mapping indicates higher to lower cross reaction.

When *Pst* antibody was used, the *Ptr* spores were not significantly different from the positive control (*Pst* spores + *Pst* antibody) (Figure 2.7C) whereas absorbance of *Fg* spores were significantly lower than the positive control compared to *Ptr* spores. The average absorbance for positive control was 0.69 ± 0.22 (9,517 spores), whereas *Ptr* spores with *Pst* antibody had an average absorbance of 0.45 ± 0.143 (6,507 spores) contributing to 68% of positive control suggesting strong cross reaction and *Fg* spores with *Pst* antibody resulted in an average absorbance of 0.13 ± 0.02 (3,892 spores) which is 41% of positive control leading to a strong cross reaction (Figures 2.7C and 2.8C).

A cross-reaction is an immunologic reaction in which antibodies react with two or more antigens that share epitopes (the part of an antigen where the antibody gets attached) but are otherwise dissimilar in structure (Frank 2002). Cross-reactivity also occurs when antibodies with specificity to one epitope bind to another epitope that has a structural resemblance but is not identical to the actual epitope (Frank 2002). Cross-reacting antibodies can cause problems by providing false positives when an antibody is used to detect a specific antigen. In the above-mentioned results, *Ptr* antibody did not statistically cross react with any other spores and could be potentially used to detect *Ptr* spores through ELISA. This is a cross-reactivity test with these two distinct target spores, as we did not test for responses with other non-target spores, so there may be reactions with other fungal spores as well. As a result, the ELISA application for *Ptr* spores should be used with caution. Conversely, *Fg* and *Pst* antibodies had significant cross-reactions with other spores (Figure 2.7 B and C) and are incapable in ELISA to obtain the specific detection of the *Fg* and *Pst* spores. These cross-reacting antibodies could also possibly

interfere with other antigens (fungal spores) sharing a common epitope or the epitopes with a structural resemblance.

2.4.4 Detection of *Ptr, Fg,* and *Pst* by RT-iPCR

The assay optimization resulted in using 1 spore to 750 spores / well for *Ptr*, 60 spores to 6×10^4 spores / well for *Fg* and 20 spores to 2×10^4 spores / well for *Pst*, 1 : 1000 dilution of primary antibody, and 1 : 5000 dilution of secondary antibody. Manual wash steps were followed for all three spores. These optimized conditions were followed in all the assays.

The data obtained from RT-iPCR were found to be normally distributed for *Ptr, Fg,* and *Pst* spores using Shapiro-Wilk and Kolmogorov-Smirnov normality and log normality tests. The standard curve of the average Ct values of 15 replicates were plotted against the log [spores / well] (Figure 2.9A-C) using simple linear regression analysis. The Ct values obtained from the qPCR amplification were inversely proportional to the spore concentrations used. An ordinary one-way ANOVA with Tukey's multiple comparison tests was used to compare significant differences among different spore concentrations and determine the LOD.

The linear detection ranges were 94 to 1 spore for *Ptr* spores (Figure 2.9A), 60,000 to 938 for *Fg* spores (Figure 2.9B), and 12,000 to 188 for *Pst* spores (Figure 2.9C). Tables 2.5-2.7 indicate the mean, standard deviation, and % co-efficient of variability of data obtained through RT-iPCR. R^2 values were 0.95, 0.89, and 0.76 for *Ptr, Fg,* and *Pst* respectively.

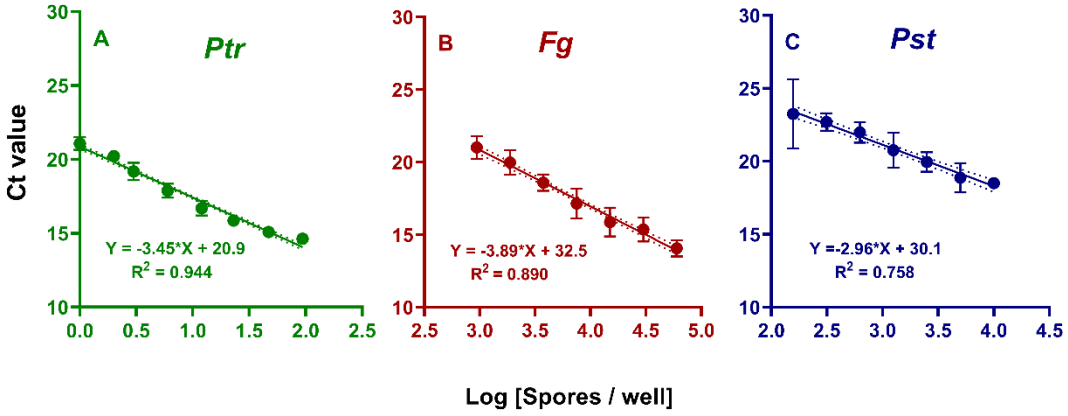

Figure 2.9: Linear regression analysis of the *Pyrenophora tritici-repentis* (*Ptr*) (A), *Fusarium graminearum* (*Fg*) (B), *and Puccinia striiformis* (*Pst*) (C) – RT-iPCR assays. The average Ct values of 15 (3×5) replicates were plotted against the log [Spores / well]. The relationship between spore numbers (log) and Ct values were linear and significant ($p < 0.0001$). Data points and error bars represent the mean and standard deviation of 15 replicate measurements and the dashed lines are 95% confidence intervals of the linear regression. In a few data points of A, the error bars and confidence intervals are smaller than the data points and regression line and thus cannot be seen.

While comparing the CVs of RT-iPCR experiments, all three spores had a higher variability rate of more than 20% with 15 replicates (Table 2.5 – 2.7). Direct comparison of variability between ELISA and RT-iPCR becomes difficult because of the different sample sizes for the two methods. When SEM is compared between ELISA and RT-iPCR, the highest SEM for *Ptr* ELISA was 0.069 whereas, in RT-iPCR, *Ptr* spores had the highest SEM of 0.225; the highest SEM value for *Fg* spores through ELISA was 0.183 whereas through RT-iPCR it had 0.298, and for *Pst* spores the highest SEM observed through ELISA was 0.073 and via RT-iPCR was 0.386.

Comparing the LODs of *Ptr, Pst,* and *Fg* through RT-iPCR (1, 188, and 938 spores respectively) to the LODs of previously published methods using qPCR detection techniques reveals the sensitivity of RT-iPCR assay. Araujo et al. (2020) achieved a LOD of 1 spore each for *Ptr* and *Pst* and 35 spores for *Fg* through qPCR. However, qPCR requires DNA extraction prior to quantification. Since the RT-iPCR quantifies spores coated directly without needing to extract DNA from the fungal spores, this method has a potential advantage over PCR amplification techniques.

In a previous study by Gangneux et al. (2014) a pea root rot pathogen, *Ae* was quantified using qPCR where the authors achieved a limit of detection of 10 spores / g of soil whereas a RT-iPCR assay by Kaphle (2020) achieved a limit of detection of 100 spores / g of soil without a need to perform DNA extraction. The trade-off between sensitivity and ease-of-use, cost, and efficiency that these two methods presents should be guided by the specific application or research question being considered.

Table 2.5: Mean, SD, and co-efficient of variability of *Pyrenophora tritici-repentis* spore Ct values through RT-iPCR

***Ptr* Spores / well**	**Mean**	**SD**	**CV %**	**SEM**
94	15.0	0.593	12	0.119
47	15.5	0.617	12	0.123
23	16.3	0.769	15	0.154
12	17.3	0.944	19	0.189
06	18.2	0.997	20	0.199
03	19.6	0.926	19	0.185
2	20.5	0.997	20	0.199
1	21.5	1.130	22	0.225

Descriptive statistics of 15 replicates (n=15), where SD – standard deviation, CV – Coefficient of variability, and SEM – Standard error of Mean at $p < 0.001$

Table 2.6: Mean, SD, and co-efficient of variability of *Fusarium graminearum* spore Ct values through RT-iPCR

***Fg* Spores / well**	**Mean**	**SD**	**CV %**	**SEM**
60,000	14.9	1.24	25	0.248
30,000	16.1	1.19	24	0.238
15,000	16.7	1.37	27	0.274
7500	18.0	1.49	30	0.298
3750	19.2	1.19	24	0.238
1875	20.5	1.21	24	0.243
938	21.3	1.30	26	0.260

Descriptive statistics of 15 replicates (n=15), where SD – standard deviation, CV – Coefficient of variability, and SEM – Standard error of Mean at $p < 0.001$

Table 2.7: Mean, SD and co-efficient of variability of *Puccinia striiformis* spore Ct values through RT-iPCR

***Pst* Spores / well**	**Mean**	**SD**	**CV %**	**SEM**
12,000	18.2	0.52	10	0.103
6,000	18.8	0.83	17	0.167
3,000	19.9	0.98	20	0.196
1500	20.7	1.05	21	0.210
750	21.4	1.17	23	0.234
375	22.4	1.66	33	0.331
188	23.2	1.93	39	0.386

Descriptive statistics of 15 replicates (n=15), where SD – standard deviation, CV – Coefficient of variability, and SEM – Standard error of Mean at $p < 0.001$

However, there are other factors beyond just those discussed above that should be considered. Chapter 3 of this thesis will describe qPCR, and the challenges involved with DNA extraction and will include a detailed comparison of the qPCR and RT-iPCR assays.

2.4.5 Cross reactivity RT-iPCR

The specificity of RT-iPCR was assessed by conducting cross reactivity assays. The three target spores, *Ptr, Fg,* and *Pst* were evaluated against each antibody. In addition, two non-target spores, *Ae,* and *Ss* were assessed for cross-reactivity with the three target antibodies. Spore concentrations used were 750 spores / well for *Ptr*, 6×10^4 spores / well for *Fg*, 2×10^4 spores / well for *Pst*, 3000 spores / well for *Ae,* and 1×10^4 spores / well for *Ss.* The above-mentioned spore numbers were the maximum detection limit under the linear range for *Ptr, Fg,* and *Pst* spores (determined from the method-development experiments) and for *Ae* the number of spores used were selected as reported in Kaphle (2020). An ordinary one-way ANOVA with Dunnett's multiple comparison test indicated significant differences between the positive control and the other two species (Figure 2.10A-C). In cross-reactivity experiments of RT-iPCR, the symbols, * with $p < 0.033$, ** with $p < 0.002$, and *** with $p < 0.001$ indicate the level of statistical significance, which improves comprehension of how antibodies react with non-target spores. Cross-reactivity is still present when the Ct value of non-target spores is within the linear detection range of target spores, however this does not necessarily have a statistical significance. To estimate cross-reactivity, an absolute difference is determined and the percentage of cross-reactivity in response to the positive control is given for each spore. Difference in percentage is calculated with the following formula:

(Number of spores detected using non-target spores / Number of spores in positive control) / 100. When there is a stronger reaction of non-target spores with an antibody it leads to higher cross reactivity and when there is negative to very low reaction of antibodies to non-target spores then the cross-reactivity is negligible. The heat map (Figure 2.11 A-C) shows the cross-reactivity data where red to blue color mapping indicates higher to lower cross reaction, respectively. The positive control data lies on the left most position in every cross-reactivity graph to render a better comparison.

When *Ptr* antibody was assessed, the *Ae, Fg,* and *Pst* spores were significantly different from the positive control (*Ptr* spores + *Ptr* antibody) with higher Ct values as shown in Figure 2.10A. *Ss* was the only spore that produced Ct values not significantly different from the positive control.

The average Ct value for positive control (*Ptr* spores + *Ptr* antibody) was 14.98 ± 1.36 (corresponding to 51 spores), whereas *Fg* spores with *Ptr* antibody had an average Ct value of 16.47 ± 1.51 (19 spores) contributing to 37% of positive control. The spore numbers provided in brackets were calculated for the Ct values of non-target spores by interpolating from the linear curves of target spores (Figure 2.9). *Pst* spores with *Ptr* antibody resulted in an average Ct value of 19.75 ± 1.58 (2 spores) which is only 4% of positive control (Figure 2.10A). The non-target spore *Ae* had an average Ct value of 19.83 ± 0.82 (2 spores) which is only 4% of positive control whereas *Ss* had a Ct of 15.57 ± 1.07 (34 spores) which is 67% of positive control against *Ptr* antibody (Figures 2.10A and 2.11A).

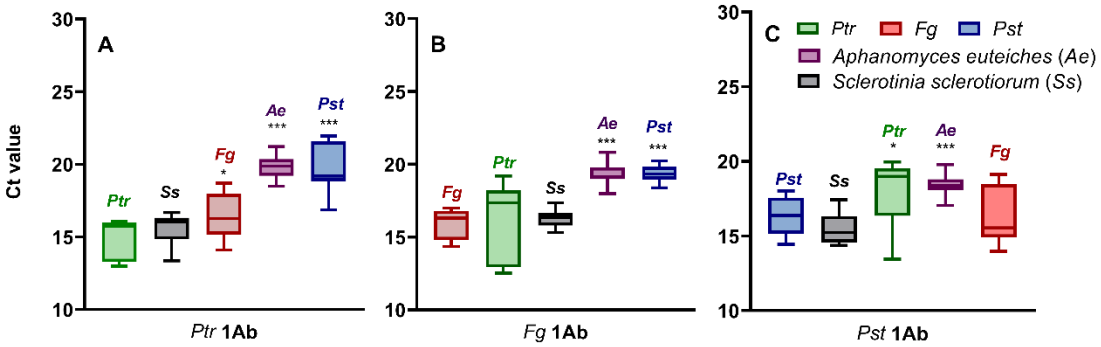

Figure 2.10: Cross reactivity of RT-iPCR with *Pyrenophora tritici-repentis, Fusarium graminearum, Puccinia striiformis, Aphanomyces euteiches,* and *Sclerotinia sclerotiorum* against *Pyrenophora tritici-repentis* antibody (A), *Fusarium graminearum* antibody (B), and *Puccinia striiformis* antibody (C). Significant differences observed between the positive control (target spore with target antibody) and the other spores were indicated with * above each box plot. The horizontal line inside the box plots indicates the median and whiskers indicate the minimum to maximum values and the box plots without * above indicate that the species is not significantly different from the positive control. Symbols *, **, and *** indicate the level of statistical significance (Non-significant $p > 0.12$), (* $p < 0.033$), (** $p < 0.002$), and (*** $p < 0.001$).

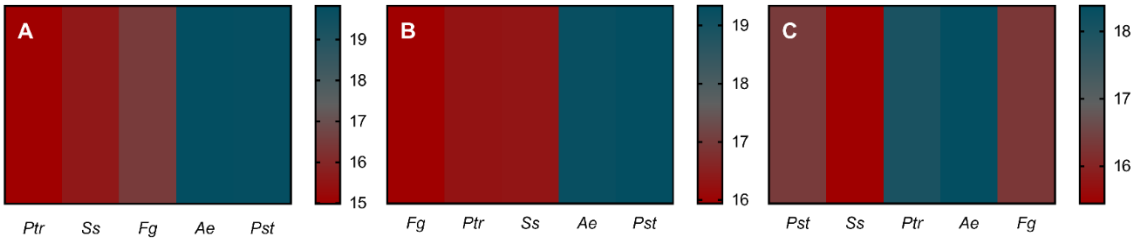

Figure 2.11: Heat map of RT-iPCR cross-reactivity with *Pyrenophora tritici-repentis (Ptr), Fusarium graminearum (Fg),* and *Puccinia striiformis (Pst)* spores against *Ptr* antibody (A), *Fg* antibody (B), and *Pst* antibody (C). Red to blue color mapping indicates higher to lower cross reaction based on Ct values.

When *Fg* antibody was used, the *Ae* and *Pst* spores were significantly different from the positive control (*Fg* spores + *Fg* antibody) with a higher Ct value as shown in Figure 2.10B. In comparison, both *Ptr* and *Ss* were not statistically different from the positive control (*Fg* spores) as shown in Figure 2.10B. The average Ct value for positive control was 15.94 ± 0.99 (18,115 spores), whereas *Ptr* spores with *Fg* antibody had an average Ct value of 16.27 ± 2.68 (14864 spores) contributing to 82% of positive control suggesting a strong cross reaction. *Pst* spores with *Fg* antibody resulted in an average Ct value of 19.34 ± 0.5 (2422 spores) which is only 13% of positive control but still lies within the detection range of *Fg* spores (Figure 2.10B). The non-target spore *Ae* had an average Ct value of 19.24 ± 0.82 (2567), 14% of the positive control. While minimal, the number *Ae* of spores still lies within the detection range of *Fg* spores. *Ss* had a Ct of 16.30 ± 0.56 (14,629) which is 81% of positive control against *Fg* antibody indicating a strong cross reaction (Figures 2.10B and 2.11B).

When *Pst* antibody was evaluated, *Ptr spores* had a higher Ct value compared to the positive control (*Pst* spores + *Pst* antibody), however, it had cross reactivity due to a single low Ct value measurement (not determined to be an outlier in the ROUT test) skewing the variability of *Ptr* measurement. *Ss* spores had a lower Ct value than the positive control and were not significantly different from the positive control, as shown in Figure 2.10C. *Fg* spores had a Ct value that was nearly equal to the positive control thus not significantly different from the positive control. In contrast, *Ae* had higher Ct values and were significantly different from the positive control. The average Ct value for positive control was 16.34 ± 1.26 (43,185 spores), whereas *Ptr* spores with *Pst* antibody had an average Ct value of 18.02 ± 2.05 (11,726 spores) contributing to 27% of positive

control. *Fg* spores with *Pst* antibody resulted in an average Ct value of 16.27 ± 1.88 (45,589 spores) which is 105% of positive control which indicates a higher cross reaction (Figure 2.10C). The non-target spore *Ae* had an average Ct value of 18.38 ± 0.7 (8,840 spores) which is 20% of positive control whereas *Ss* had a Ct of 15.44 ± 0.96 (86,757 spores) contributing to 200% of positive control against *Pst* antibody which suggests a higher cross-reaction (Figures 2.10C and 2.11C).

As discussed earlier in the results of ELISA cross-reactivity, the antibody cross reacts when an antigen shares the same type of epitope with another antigen or when an antigen has an epitope that resembles another epitope but is not identical in nature (Frank 2002; Murphy and Weaver 2017). This cross-reaction can provide false positives while these cross-reacting antibodies are used in antigen specific detection. Cross-reaction can be minimized by producing monoclonal antibody (Frank 2002; Murphy and Weaver 2017). Immune cells that are all clones of the same parent cell create monoclonal antibodies. They are intended to bind to the epitope of a single antigen (a small, specific region). Monoclonal antibodies are highly selective and can be used in targeted therapies, diagnostic tests, and research. Polyclonal antibodies, on the other hand, are created by many immune cells that identify different epitopes of the same antigen. Polyclonal antibodies are less selective than monoclonal antibodies because they bind to several sites on an antigen. But polyclonal antibodies have their own advantage of being able to detect very low concentrations of antigens as they bind to multiple sites of the same antigen, are less expensive, and are easier to produce. Additionally, if the target antigen shares comparable epitopes with other molecules, cross-reactivity with monoclonal antibodies can still occur, thus may not offer a perfect solution to the cross reactions compared to

polyclonal antibodies. Several factors influence an antibody's cross-reactivity, including the specificity of the antigen-antibody interaction and the degree of similarity across diverse antigens.

Based on the results of cross-reactivity assays through RT-iPCR, all three antibodies had significant reactions with other spores indicating varying degrees of cross reactivity. This implies that these antibodies are lacking the specificity to detect the antigen they were developed for and thus may react with other spores and produce inaccurate results. More research into the development of more specific antibodies is needed to further advance this technique.

Fischer et al. (2007) and Mondal et al. (2020) reported that bacterial enterotoxins can be quantified through RT-iPCR without any cross-reactions with other bacterial enterotoxins when monoclonal antibodies are used. These results indicate a possible advantage of using monoclonal antibodies over polyclonal antibodies. It also implies that fungal spores could be possibly sharing a common epitope on their cell wall suggesting higher cross-reactions among the fungal spores. *Ae* did not react with any antibody possibly because it belongs to a lower-class fungi division – Oomycota and the cell wall may be different among true fungi (higher-class fungi) and lower-class fungi. On the other hand, all three antibodies reacted against *Ss* causing a higher cross-reactivity. This could be because *Ss* belongs to a higher fungi division Ascomycota to which two of the target pathogens in this study – *Ptr* and *Fg* belong (Figures 2.1 and 2.2). However, *Pst* antibody also reacted against *Ss* which is not consistent with the above statement because *Pst* belongs to the division – Basidiomycota which is a distinct division and still belongs to a higher class of fungi (Figure 2.3). Further research is required to explore the causes of this cross-

reactivity and approaches for developing more specific antibodies toward target fungal spores.

In order to minimize cross-reactivity purification methods were carried out using serum antibody purification kit using protein G protocol and by cross absorbing the non-specific antigens (i.e reacting a primary antibody against a cross-reacting antigen for a specific period of time (4 h) and collecting the supernatant); however these methods couldn't help with reducing cross-reactivity of antibodies.

2.4.6 Comparison of ELISA and RT-iPCR

2.4.6.1 Comparison of limit of detection

Comparing the LOD of RT-iPCR to the previously calculated LOD of ELISA, the sensitivity was significantly improved with the RT-iPCR for all three spores (Table 2.8).

RT-iPCR improved the LODs by 2-fold for *Fg*, 12-fold for *Pst*, and 30-fold for *Ptr,* compared to the corresponding LODs obtained by ELISA (Table 2.8). While our data does suggest that the RT-iPCR assay has significantly improved sensitivity over the ELISA method for quantifying fungal spores, the increase in sensitivity falls well short of the 10,000-fold increase as mentioned in the review by Niemeyer et al. (2005).

The previously reported studies had a 10,000-fold increase in quantified tumor marker proteins, bacterial colony forming units, and human interleukin proteins. However, proteins can be quantified in a very low concentration compared to whole fungal spores; thus, the increased sensitivity of more than 10,000-fold for proteins was not expected to be replicated here for fungal spores.

Table 2.8: The LOD of three target spores through ELISA and RT-iPCR and the gain in sensitivity is calculated as the ratio of RT-iPCR's LOD to that of the ELISA's

Spores	**LOD ELISA**	**LOD RT-iPCR**	**Gain in sensitivity**
Ptr	30	1	30×
Fg	1800	938	2×
Pst	2200	188	12×

2.4.6.2 Comparison of cross-reactivity of ELISA and RT-iPCR

Since the cross-reactivity assays had varying results between ELISA and RT-iPCR, cross-reactivity assays with only primary antibody, secondary antibody (both conjugated to DNA and non-conjugated secondary antibody), and PCR master mix were also performed to determine potential causes of cross-reactivity. Higher cross reactivity with just the secondary antibody conjugated to DNA was observed against spores containing no primary antibody, while no cross reactivity was observed with other tested controls, including only primary antibody and secondary antibody without DNA conjugate and PCR master mix (data not shown). The reaction with the secondary antibody and the spores varied with spore numbers in a linear relation (i.e., higher cross reaction with maximum spores and lower reaction with minimum spores). This may implies that the DNA conjugated to the secondary antibody may play a role in causing cross-reactivity among antibodies and their non-specific antigens.

Future research focused on optimizing these assays and avoiding cross-reactions caused by primary antibodies, cell surface proteins specific to a target fungal spore should be used to develop the primary antibody instead of using the whole spore for antibody production. This could help in minimizing the cross-reactions that occur with antigens sharing a common epitope.

A secondary antibody alone wouldn't yield a signal since no label is conjugated to it. So, the above results clearly demonstrated that the DNA attached to a secondary antibody has a significant part in causing cross-reactions against fungal spores. To achieve a highly specific detection, one could conjugate the DNA of the target antigen to the secondary

antibody and use the probes and primers that detect the specific target-antigen. However, more studies are needed at this point to develop this fairly new technique for highly specific and sensitive detection of fungal spores.

2.5 Conclusion

An RT-iPCR assay was developed for the rapid and sensitive detection of three airborne fungal pathogens – *Ptr, Fg,* and *Pst*. The developed RT-iPCR assay was able to detect as low as single spore of *Ptr*, 938 spores of *Fg,* and 188 spores of *Pst*. The assay had significantly improved sensitivity and linear working range for all three spores compared to ELISA. RT-iPCR provided 2-fold increased sensitivity for *Fg,* 12-fold for *Pst,* and 30-fold for *Ptr* compared to ELISA using the same polyclonal antibodies. RT-iPCR does not require genomic DNA extraction as it measures spores coated directly, representing a major benefit over alternative qPCR techniques (discussed in Chapter 3). The increased sensitivity of RT-iPCR over the corresponding ELISA further suggests this is a promising new technique for direct spore detection. However, the specificity of the polyclonal antibodies still remains a challenge. In order to fully utilize this assay to accurately detect air-borne fungal spores, more research should be carried out to produce target specific primary antibodies and using a specific DNA tag to conjugate with the secondary antibody which would result in a more highly specific, sensitive, and rapid detection tool to quantify fungal pathogens.

Chapter 3 Detection of three airborne fungal pathogens by real-time quantitative PCR and determination of DNA extraction efficiency

3.1 Introduction

Immunoassays and PCR are two common techniques for detecting plant pathogens. Immunoassays or serological testing, depend on the specificity of the antigen-antibody reaction and the foundation of PCR testing is the identification of specific nucleic acid sequences (DNA or RNA). Immunoassays related limitations due to cross-reactivity were discussed in the previous chapter. Examples of diagnostic procedures that depend on the identification of specific nucleic acids include polyacrylamide gel electrophoresis, nucleic acid hybridization, and PCR. In this chapter, the detection of *Pyrenophora tritici-repentis* (*Ptr*)*, Fusarium graminearum* (*Fg*)*,* and *Puccinia striiformis* (*Pst*) spores using quantitative PCR (qPCR) and a potential approach to determine DNA extraction efficiency will be discussed.

Since the 1980s, PCR has been frequently used for identifying plant diseases due to its high sensitivity and comparatively simple procedure. PCR assays involve the selection of primers, which are short DNA fragments that can pair with specific areas of the pathogen's genome. Moreover, primers should be designed to recognize a specific disease or pathogen race. Similar to serological testing where specific antibodies are produced for a specific antigen, different primers must be identified and validated for every pathogen, or even for strains or biotypes of a specific pathogen for PCR assays (Schumann and D'Arcy 2006).

PCR benefits include a more sensitive and more specific detection than immunoassays. To conduct PCR tests, specialized, expensive equipment is required. However, new developments in technology such as qPCR have shortened the test's turnaround time to less than one day.

qPCR which is so far the most common method used for pathogen detection and to date, quantification has produced higher sensitivity and specificity using pathogen specific primers (Mayer et al. 2003; Araujo et al. 2020). However, analysis by qPCR requires extraction of DNA from the target spores, which are involved and introduce uncertainties in the measurements (Schrader et al. 2012). A major research gap that exists with this approach is the determination of DNA extraction efficiency. Most researchers tend to optimize the procedures of DNA extraction to obtain maximum DNA quantity but fail to determine actual extraction recovery in total (Liu et al. 2015; Araujo et al. 2020; Morcia et al. 2020; Yang et al. 2021). In many cases, it is assumed that the optimized extraction protocol achieves 100% efficiency while extracting DNA, which is not feasible for fungal spores using existing DNA extraction procedures. In order to accurately quantify the number of spores present in a given sample, it is crucial to determine the DNA extraction efficiency from a known quantity of spores, and thus allow for corrections due to DNA losses during extraction. In this chapter, qPCR assays are validated for the three target fungal spores and a potential approach to determine the DNA extraction efficiency is discussed, which involves a series of calculations and derived formulas.

The basic fungal reproductive biology and the relationship with the quantification of spore numbers are discussed in this section (Figure 3.1). Spores are used by fungi to spread their range and colonize new host plants in close and far away environments.

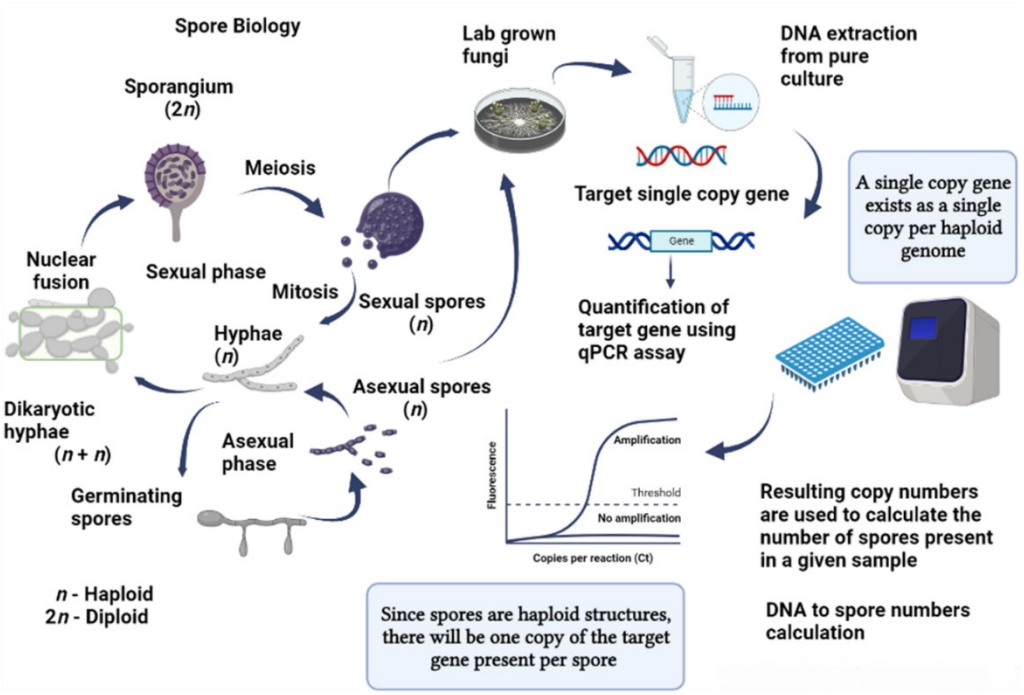

Figure 3.1: Basic fungal reproductive biology and its relationship with quantification of spore numbers. Adapted from Nwe et al. (2011). Created with BioRender.com

Fungi are capable of sexual and asexual reproduction. Fungi produce spores for both sexual and asexual reproduction, and these spores can either be dispersed through wind or water or travel on an agent or vector to leave the host organism. Fungal spores are lighter and smaller than plant seeds. Parent fungi expel trillions of spores as a result of reproduction which increases the chances of finding conducive locations, host and environment for survival according to the concept of disease triangle (Figure 1.1).

In Figure 3.1, the diploid stage is indicated as 2n whereas the haploid stage is indicated as n. The following three phases are present in all fungal sexual reproduction systems. The dikaryotic stage, in which two haploid hyphae coexist in a single cell, is first formed when two complementary haploid hyphae join during plasmogamy. During karyogamy, the dikaryotic hyphae undergo nuclear fusion to form the sporangium, a diploid sac-like structure in which the spores are stored (Schumann and D'Arcy 2006). Meiosis finally takes place in the sporangium and haploid spores are then disseminated into the environment. Spores germinate and divide by mitosis which results in hyphae formation and the cycle continues. Fungi reproduce asexually by fragmentation, budding, or by producing haploid spores. The most common mode of asexual reproduction is spore formation. The hyphae germinate to produce haploid asexual spores. So regardless of sexual / asexual stages, spores are haploid structures.

Spores are grown under lab conditions for some species and on host plants for biotrophic species to extract DNA and perform qPCR. In qPCR when a single copy gene is targeted, (a single copy gene is a gene that exists as a single copy in a haploid cell) it amplifies the specific gene and detects the amount of copies present in the particular sample of DNA. Since spores are haploid structures there will be only one copy of the target gene present /

spore which implies, quantified copy numbers can be used directly to calculate the spore numbers in a given sample.

3.2 Materials and methods

3.2.1 DNA extraction

DNA extraction was optimized by performing extractions from *Ptr, Fg,* and *Pst* spores using a DNeasy PowerSoil kit from QIAGEN. Initially, 5 mg of spores were weighed and added to the 1.5 mL power bead tube provided with the kit. A volume of 60 µL of C1 solution (lysis buffer) was added to each tube and the sample was incubated at 65℃ for 10 min to increase cell lysis. After 10 min, the sample was ground in the PRECELLYS® 24 (Bertin Instruments) programmed at 5000 rpm; 2 times for 30 s; with a 5 s gap period. Then the sample was centrifuged at 15,000 × g for 2 min. The supernatant was collected, transferred to a fresh tube and 250 µL of solution C2 (binding buffer) was added and vortexed for 5 s; then incubated at 4℃ for 5 min. The sample was centrifuged at 15,000 × g for 2 min and the supernatant was collected and transferred to a fresh tube. A volume of 200 µL of solution C3 (wash buffer) was added and vortexed briefly for 5 s. The sample was incubated again for 5 min at 4℃. After incubation, it was centrifuged at 15,000 × g for 2 min and the supernatant was collected, transferred to a fresh tube and 1200 µL of solution C4 was added and vortexed for 5 s. From this mixture, 675 µL of solution was loaded on to the spin column provided and centrifuged at 15,000 × g for 1 min. The flow-through was discarded and the remaining sample left from the mixture was processed using the same spin column until all of the solution has passed through the spin column. Then 500 µL of solution C5 was added and centrifuged for 1 min at 15,000 × g. Flow

through was discarded and the spin column was placed in a clean collection tube and centrifuged again for 2 min at 16,000 × g. Finally, the spin column was placed in the elution tube provided by the kit and 60 µL of elution buffer (solution C6) was added to the spin column and centrifuged at 15,000 × g for 1 min. The spin column was discarded and flow through DNA was collected in the elution tube. DNA quantity and quality (A260 / A280, A260 / A230) were measured using a NanoDrop™ One UV-Vis Spectrophotometer by multiple measurements (n=15; 3 samples with 5 measurements each) and stored at -20℃ until further use.

Few adaptations were made to the existing QIAGEN protocol (according to the previous research works conducted at the Lethbridge RDC) to maximize the efficiency of DNA extraction in terms of quantity and quality. Spores dissolved with the bead buffer and C1 solution were heated at 65° C for 10 minutes in a digital cooling dry bath (Thermo Scientific). *Pst* spores were frozen and thawed in liquid nitrogen 4 times prior to DNA extraction to reduce their aggregation due to hydrophobicity. Spores were ground at RT using PRECELLYS® 24 (Bertin Instruments) (program 5000 – 2 × 30 s grinding with a 10 s pause in between 2 cycles).

3.2.2 qPCR

qPCR assays were carried out to quantify the DNA extracted from all three spores. The materials used for these tests were the PerfeCTa® SYBR® Green SuperMix Low Rox (QantaBio) and pathogen-specific primers were acquired as reported in Araujo et al. (2020) to carry out the experiments (Table included in the appendix). The qPCR instrument used to perform the experiments was an Applied Biosystems QuantStudio™

3. For each assay, 7.5 µL of qPCR master mix and 2.5 µL of DNA template was added. The qPCR cycle conditions were as follows: 1 cycle at 95℃ for 3 min, 40 cycles at 94℃ for 15 s, 55℃ for 30 s, and 72℃ for 30 s. Ct values at DNA amplification, melt curve, and standard curve were calculated by the software QuantStudio™ Design & Analysis Software V1.4.2 at the end of each experiment. Cross reactivity assays were evaluated by testing pathogen specific primers and the genomic DNA (gDNA) of non-specific pathogens and the Ct values were compared.

3.3 Statistical analysis

Data from qPCR assays using extracted DNA of *Ptr, Fg,* and *Pst* spores were subjected to normality testing via Shapiro-Wilk test and Kolmogorov-Smirnov test in GraphPad Prism version 9.4.1 for Windows, GraphPad Software. Ct values generated through qPCR assays for all three spores were normally distributed. A simple linear regression analysis of qPCR data of three spores were plotted to derive the standard curve. A mixed effect analysis followed by Tukey multiple comparisons were used to test the significant differences between the detectable spore numbers and the control Ct values of *Ptr* and *Fg* spores through qPCR. A non-parametric One-Way ANOVA (Kruskal-Wallis test) followed by Tukey multiple comparisons were used to test the significant differences between the detectable spore numbers and the control Ct values of *Pst* spores.

3.4 Results and discussion

3.4.1 DNA extraction optimization and characterization

Different spore amounts (1 mg, 2 mg, 5 mg, and 10 mg) were tested and 5 mg of spores was chosen as the optimal concentration of spores to get the maximum DNA yield and

quality. The DNA extraction was performed using 4 different extraction kits: DNeasy PowerSoil® kit (QIAGEN), DNeasy PowerSoil® Pro kit (QIAGEN), ZymoBIOMICS™ DNA Miniprep Kit (Zymo Research), and Quick-DNA™ Fungal / Bacterial Miniprep kit (Zymo Research) (Methods provided in the appendix). A DNeasy PowerSoil® kit yielded effective DNA quantity and quality with consistent replicate results and was chosen to carry out DNA extraction for this research (Figure 3.2). Different beads such as Garnet and ceramic beads, zirconia beads, beads from the DNeasy PowerSoil® kit, and baked sand were also tested with the DNeasy PowerSoil® (results tabulated in appendix). Ultimately the beads that come in the DNeasy PowerSoil® kit (Garnet beads) were selected for our extraction method as they yielded better DNA quality with all three spores. There was no perfect single extraction method for all three spores, however, the goal was to find a single extraction method that could achieve sufficient DNA quality and quantity for all three spores. This was an important consideration as we wanted to ensure the developed method was efficient, cost-effective, and widely-applicable to end-users. Therefore, three separate extraction methods for each of the target spores was not a viable approach. For example, whereas zirconia beads performed better for extracting a higher quantity of DNA from *Ptr* spores compared to the DNeasy PowerSoil® kit beads, the same was not the case for *Fg* and *Pst* spores. Furthermore, baked sand yielded a higher quantity of DNA with all spores but the quality was poor when tested for A260 / A280 and A260 / A230.

Results comparing the different DNA extraction kits for *Ptr* and *Fg* spores using Nanodrop measurements are reported in Figure 3.2 and results comparing different beads used for extraction are tabulated in the appendix.

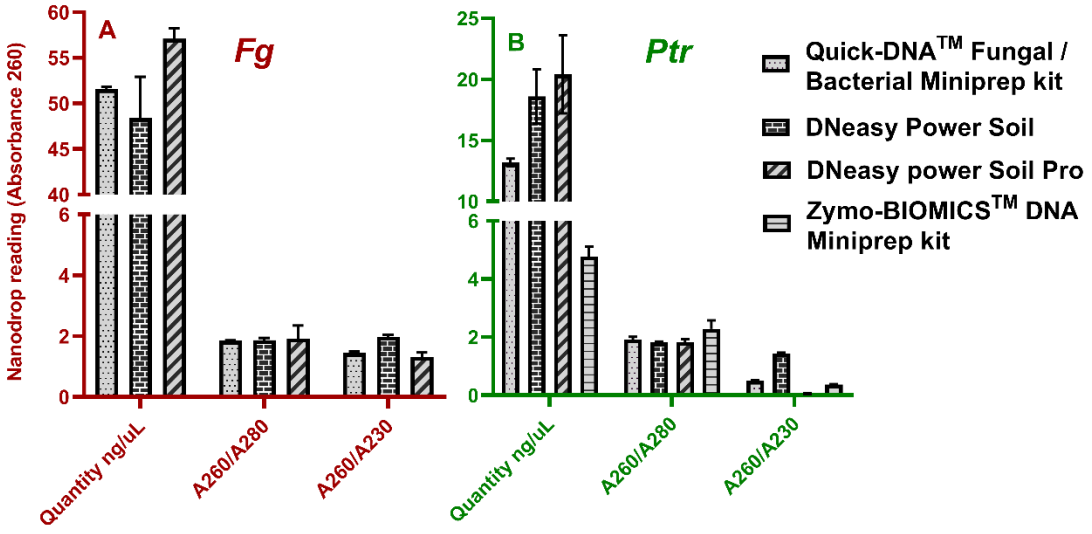

Figure 3.2 Comparison of different DNA extraction kits for *Fusarium graminearum* (*Fg*) and *Pyrenophora tritici-repentis* (*Ptr*) spores using Nanodrop measurements analyzing the quantity in ng / µL and quality via A260 / A280 and A260 / A230 measurements. Interleaved bars indicate the mean with an SD of 5 replicates for each spore. Zymo-BIOMICS™ DNA Miniprep kit was not tested with *Fg* spores as the kit did not yield enough quantity and quality DNA with *Ptr*.

As *Pst* spores were limited as we cannot culture them under lab conditions (biotroph organism) and hence, they were not used for testing with different extraction kits. For this DNA extraction kits comparison, the amount of spores used was 10 mg for both *Ptr* and *Fg* spores.

3.4.2 Calculation of copies of interest and serial dilution preparation from gDNA

Most methodological approaches aimed at determining extraction efficiencies involve the addition of a known quantity of a standard or surrogate that can accurately replicate the behavior (i.e., losses) of the target (i.e., DNA) during the extraction protocol. The unique challenge posed by spore extraction is that it starts with intact spores encapsulating the target DNA. Therefore, spiking a DNA standard into an intact or surrogate spore is a non-trivial task. The method to determine extraction efficiency described here takes a more fundamental approach. The steps involved in converting copies of interest to spore numbers rely on factors that include genome sizes of the pathogen, targeted single copy genes, the total mass of DNA in ng based on NanoDrop™ measurements, the quantity of DNA / reaction, initial number of spores used for DNA extraction, and dilution factor. The first four factors are utilized in a series of derived formulas to obtain copies of interest of a particular pathogen whereas the final two factors will be used as correctional factors in the formula derived to quantify spore numbers (Figure 3.3).

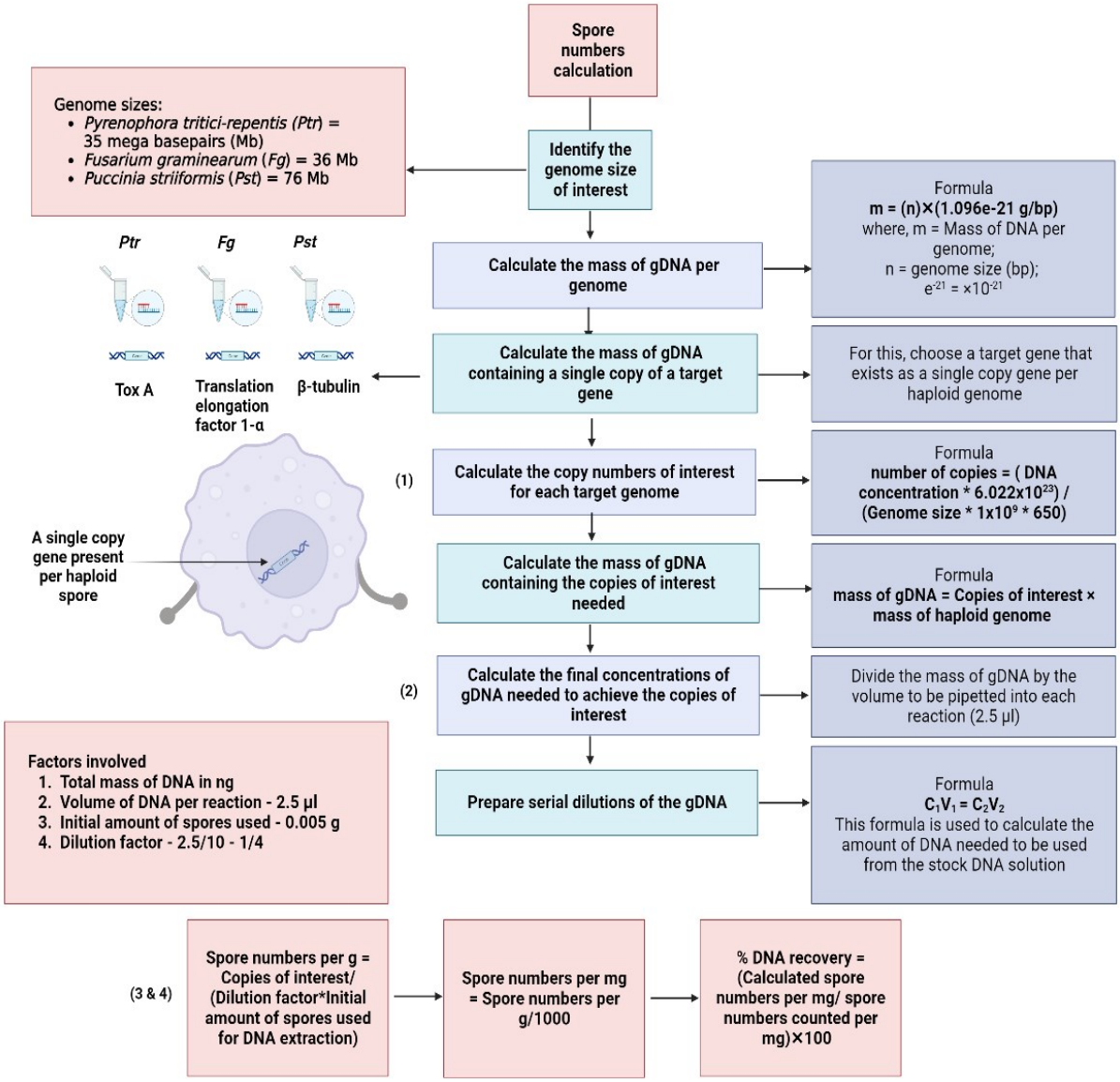

Figure 3.3: The series of steps involved in the calculation of copies of interest using genome sizes, mass of gDNA, target genes, copy numbers, and the derived formula to calculate spore numbers from quantified copies of interests (Applied Biosystems 2003). Created with BioRender.com.

The independent factors that are involved in converting copies of interest to spore numbers from the listed factors are the total mass of DNA in ng – (spectrophotometer measurement), the quantity of DNA / reaction, the initial amount of spores used for DNA extraction, and dilution factor. These independent factors rely on the user's experimental conditions and can vary for each experiment. The total mass of DNA in ng is measured from extracted DNA and the quantity is measured by spectrophotometer. There are uncertainties with NanoDrop spectrophotometer measurement values as they are sensitive to interferences and thus not always accurate, making multiple measurements essential. To try to minimize uncertainties associated with the NanoDrop instrument, we took 15 measurements / spore sample, and we've also did a qubit measurement for *Fg* DNA to cross-check the NanoDrop measurement. Dilution factor is calculated by dividing the volume of DNA / reaction by total volume of the PCR reaction well.

Table 3.1: Initial volume, DNA concentration, total volume of DNA, volume of DNA / reaction, genome size, a gene of interest, and copy number of the target gene to calculate the copies of interest of *Pyrenophora tritici-repentis, Fusarium graminearum,* and *Puccinia striiformis* spores.

Organism of Interest	**Tan spot**	**Fusarium head blight**	**Stripe rust**
Spores used	*Pyrenophora tritici-repentis*	*Fusarium graminearum*	*Puccinia striiformis*
Initial material of spores used (g)	0.00503 ± 0.01	0.00502 ± 0.02	0.00501 ± 0.01
Spore numbers / mg	3×10^4 ± 3715	8×10^6 ± 2×10^5	4×10^5 ± 2×10^4
DNA concentration (ng / µL) measured by Nanodrop	7 ± 0.9	35 ± 3.71	10 ± 0.61
DNA concentration (fg / µL) measured by Nanodrop	7×10^6	3.5×10^7	1×10^7
Total volume of DNA (µL)	60	60	60
Total DNA concentration (ng) measured by Nanodrop	420	2100	600
Total DNA concentration (fg) measured by Nanodrop	4.2×10^8	2.1×10^9	6×10^8
DNA used / qPCR reaction (µL)	2.5	2.5	2.5
Genome size (in base pairs - bp)	3.5×10^7	3.6×10^7	7.6×10^7
Gene of Interest	Tox A	Translation elongation factor 1-α	β - tubulin
Copy number / genome	1	1	1

Dilution factor	2.5/10	2.5/10	2.5/10
References for target genes	(Aboukhaddour et al. 2009)	(Barros et al. 2013)	(Wang et al. 2009)

***Ptr* spores**

Organism of Interest : *Pyrenophora tritici-repentis*

Using the information listed in Table 3.1, the following steps were calculated.

Genome size (n) = 3.5×10^7

Mass of DNA / genome (m) = $[n][\frac{1.096(10)^{-21}g}{bp}]$

Mass of DNA / genome = 3.836×10^{-14} g = 38.36 fg

The formula above was derived as follows:

$$m = [n]\left[\frac{1\ mole}{6.023 \times 10^{23}\ molecules\ (bp)}\right]\left[\frac{660g}{mole}\right] = [n]\left[\frac{1.096 \times 10^{-21}g}{bp}\right]$$

Where:

n= DNA size (bp), m = mass, Avogadro's number = 6.023×10^{23} molecules / 1 mole

Average MW of double-standard DNA molecule = 660 g / mole

Calculation of mass of gDNA containing 1 copy of Tox A gene =

$$\frac{\text{Mass of DNA / genome}}{Copy\ number} = 38.36 \text{ fg}$$

Number of copies in total DNA extracted is obtained by dividing total DNA extracted by mass of DNA containing 1 copy of the target gene.

Number of copies in total DNA extracted (*Ptr*) = 1.09×10^7

Final concentration (fg / µL) of gDNA = $\frac{Mass\ of\ gDNA\ needed\ (fg)}{volume\ of\ DNA\ used\ per\ reaction}$

Table 3.2: Calculation of final concentration of gDNA of *Pyrenophora tritici-repentis* spores. It is obtained by dividing the mass of gDNA needed in fg by volume of DNA used / reaction.

Copies of interest	**mass of gDNA needed (fg)**	**volume of DNA used / reaction (µL)**	**Final concentration (fg / µL) of gDNA**
1×10^7	3.8×10^8	2.5	1.5×10^8
1×10^6	3.8×10^7	2.5	1.5×10^7
1×10^5	3.8×10^6	2.5	**1.5×10^6**
1×10^4	3.8×10^5	2.5	1.5×10^5
1×10^3	3.8×10^4	2.5	1.5×10^4
1×10^2	3.8×10^3	2.5	1.5×10^3
10	3.8×10^2	2.5	1.5×10^2
1	38.36	2.5	15

Serial dilution of gDNA, $C_1V_1 = C_2V_2$ is shown in Table 3.3. Where C_1 is Stock concentration determined by spectrophotometry (fg / µL), V_1 is Volume to be determined (µL), C_2 is Final concentration of gDNA (fg / µL), and V_2 is Total volume (µL). An example calculation for Dilution 1 in Table 3.3 is shown below:

$C_1 = 7 \times 10^6$

$V_1 = ?$

$C_2 = \mathbf{1.5 \times 10^6}$ (chosen from table 3.2, where C1 > C2)

$V_2 = 20$ µL

$V_1 = \frac{C2 \times v2}{C1}$

$V_1 = 4.3$ µL

Volume of diluent (µL) = $V_2 - V_1$

= 15. 7 µL

To obtain the final volume of 20 µL, add 4.3 µL of stock gDNA to 15.7 µL of diluent, followed by serial dilutions prepared as given in Table 3.3 (Applied Biosystems 2003).

Table 3.3: Volume of gDNA and diluent needed to prepare serial dilutions, final concentrations of dilutions, and the copy numbers of Tox A gene / reaction volume for *Pyrenophora tritici-repentis* spores.

Source of gDNA for dilutions	**Initial concentration (fg / µL) (C1)**	**Volume of gDNA (µL) (V1)**	**Volume of diluent (µL)**	**Final volume (µL) (V2)**	**Final concentration of dilution (fg / µL) (C2)**	**Resulting copy numbers of Tox A gene / 2.5 (µL)**
Stock	7×10^6	NA	NA	NA	NA	NA
Dilution 1	7×10^6	4.3	15.7	20.0	1.5×10^6	1×10^5
Dilution 2	1.5×10^6	2.0	18.0	20.0	1.5×10^5	1×10^4
Dilution 3	1.5×10^5	2.0	18.0	20.0	1.5×10^4	1×10^3
Dilution 4	1.5×10^4	2.0	18.0	20.0	1.5×10^3	1×10^2
Dilution 5	1.5×10^3	2.0	18.0	20.0	1.5×10^2	10
Dilution 6	1.5×10^2	2.0	18.0	20.0	15	1

Fg and *Pst* spores

For *Fg* and *Pst* spores, the initial copies of interest were determined the exact same way with all the important information listed in Table 3.1 (calculations are included in the appendix). Tables 3.4 – 3.5 indicates the calculations of the mass of gDNA, final concentration, and the volume of gDNA and the diluent needed to prepare the serial dilutions for *Fg* spores and Tables 3.6 – 3.7 indicates the same calculations used for *Pst* spores (Applied Biosystems 2003).

Table 3.4: Calculation of final concentration of gDNA of *Fusarium graminearum* spores. It is obtained by dividing the mass of gDNA needed in fg by volume of DNA used / reaction.

Copies of interest	**mass of gDNA needed (fg)**	**volume of DNA used / reaction (µL)**	**Final concentration (fg / µL) of gDNA**
5.3×10^7	2.1×10^9	2.5	8.4×10^8
5.3×10^6	2.1×10^8	2.5	8.4×10^7
5.3×10^5	2.1×10^7	2.5	**8.4×10^6**
5.3×10^4	2.1×10^6	2.5	8.4×10^5
5.3×10^3	2.1×10^5	2.5	8.4×10^4
5.3×10^2	2.1×10^4	2.5	8.4×10^3
53	2.1×10^3	2.5	8.4×10^2
5.3	2.1×10^2	2.5	84

Table 3.5: Volume of gDNA and diluent needed to prepare serial dilutions, final concentrations of dilutions and resulting copy numbers of translation elongation factor 1-α gene / reaction volume for *Fusarium graminearum*.

Source of gDNA for dilutions	**Initial concentration (fg / µL) (C1)**	**Volume of gDNA (µL) (V1)**	**Volume of diluent (µL)**	**Final volume (µL) (V2)**	**Final concentration of dilution (fg / µL) (C2)**	**Resulting copy numbers of Translation elongation factor 1-α gene / 2.5 (µL)**
stock	3.5×10^7	NA	NA	NA	NA	NA
Dilution 1	3.5×10^7	4.8	15.2	20	8×10^6	5.3×10^5
Dilution 2	8×10^6	2	18	20	8×10^5	5.3×10^4
Dilution 3	8×10^5	2	18	20	8×10^4	5.3×10^3
Dilution 4	8×10^4	2	18	20	8×10^3	5.3×10^2
Dilution 5	8×10^3	2	18	20	8×10^2	53
Dilution 6	8×10^2	2	18	20	80	5.3

Table 3.6: Calculation of final concentration of gDNA of *Puccinia striiformis* spores. It is obtained by dividing the mass of gDNA needed in fg by volume of DNA used / reaction.

Copies of interest	**mass of gDNA needed (fg)**	**volume of DNA used / reaction (µL)**	**Final concentration (fg / µL) of gDNA**
7.2×10^6	6×10^8	2.5	2.4×10^8
7.2×10^5	6×10^7	2.5	2.4×10^7
7.2×10^4	6×10^6	2.5	**2.4×10^6**
7.2×10^3	6×10^5	2.5	2.4×10^5
7.2×10^2	6×10^4	2.5	2.4×10^4
72	6×10^3	2.5	2.4×10^3
7.2	6×10^2	2.5	2.4×10^2

Table 3.7: Volume of gDNA and diluent needed to prepare serial dilutions, final concentrations of dilutions, and resulting copy numbers of β – Tubulin gene / reaction volume for *Puccinia striiformis* spores.

Source of gDNA for dilutions	**Initial concentration (fg / µL) (C1)**	**Volume of gDNA (µL) (V1)**	**Volume of diluent (µL)**	**Final volume (µL) (V2)**	**Final concentration of dilution (fg / µL) (C2)**	**Resulting copy numbers of β – Tubulin gene / 2.5 (µL)**
Stock	1×10^7	NA	NA	NA	NA	NA
Dilution 1	1×10^7	4.8	15.2	20	2×10^6	7.2×10^4
Dilution 2	2×10^6	2	18	20	2×10^5	7.2×10^3
Dilution 3	2×10^5	2	18	20	2×10^4	7.2×10^2
Dilution 4	2×10^4	2	18	20	2×10^3	72
Dilution 5	2×10^3	2	18	20	2×10^2	7.2

3.4.3 Calculation of spore numbers and DNA extraction efficiency

Calculated spore numbers (C) = $\frac{x}{y \times z}$

Where x = copies of interest,

y = Dilution factor, and

z = Initial amount of spores used for DNA extraction

Relative uncertainty in C, $\Delta C = \frac{(\Delta z)}{|z|} \times |C|$

DNA extraction efficiency (E) (in %) = $\left(\frac{C}{m}\right) \times 100$

Where C = Calculated spore numbers,

m = Spore numbers counted on the microscope

Relative uncertainty in E, **(Δ**E) = |E| $\times \sqrt{(\frac{\Delta C}{C})^2 + (\frac{\Delta m}{m})^2}$

***Ptr* spores**

Spore numbers / g (C) = 1.09×10^5 / (2.5 µL /10 µL) × 0.00503 g

= 8.7×10^7 spores

Relative uncertainty in C, (ΔC) = (0.00001 / 0.00503) × 8.7×10^7

= 1.7×10^5

Calculated spore numbers (C) = $8.7 \times 10^7 \pm 1.7 \times 10^5$ spores

Spore numbers / mg = 8.7×10^4 spores

DNA extraction efficiency = (8.7×10^4 / 3×10^4) × 100

= 290%

Relative uncertainty in E, $\Delta E = |290| \times \sqrt{(\frac{170}{87000})^2 + (\frac{3715}{30000})^2}$

$= |290| \times 0.124$

$= 35.92$

Ptr spore DNA extraction efficiency = 290 ± 36 %

***Fg* spores**

Spore numbers / g (C) = 5.3×10^5 / (2.5 µL / 10 µL) × 0.00502 g

$= 4.2 \times 10^8$ spores

Relative uncertainty in C, $\Delta C = (0.00002 / 0.00502) \times 4.2 \times 10^8$

$= 1.71 \times 10^6$

Calculated spore numbers (C) = $4.2 \times 10^8 \pm 1.71 \times 10^6$ spores

Spore numbers / mg = 4.2×10^5 spores

DNA extraction efficiency = $(4.2 \times 10^5 / 8 \times 10^6) \times 100 = 5\%$

Relative uncertainty in E, $\Delta E = |5| \times \sqrt{(\frac{1710}{420000})^2 + (\frac{200,000}{8000000})^2}$

$= |5| \times 0.025$

$= 0.13$

Fg spore DNA extraction efficiency = 5 ± 0.1 %

***Pst* spores**

Spore numbers / g (C) = 7.2×10^4 / (2.5 µL / 10 µL) × 0.005 g

$= 5.7 \times 10^7$ spores

Relative uncertainty in C, $\Delta C = (0.00001 / 0.00501) \times 5.7 \times 10^7$

$= 1.14 \times 10^5$

Spore numbers / mg = 5.7×10^4 spores

Calculated spore numbers (C) = $5.7 \times 10^7 \pm 1.14 \times 10^5$ spores

DNA extraction efficiency = $(5.7 \times 10^4 / 4 \times 10^5) \times 100$

$= 14\%$

Relative uncertainty in E, $\Delta E = |14| \times \sqrt{(\frac{114}{57000})^2 + (\frac{20000}{400000})^2}$

$= |14| \times 0.050$

$= 0.7$

Pst spore DNA extraction efficiency = 14 ± 0.7 %

The DNA extraction efficiency calculated for *Ptr, Fg,* and *Pst* were 290% ± 36, 5% ± 0.1, and 14% ± 0.7, respectively. The possible reason for >100% extraction efficiency for *Ptr* spores is they tend to clump and aggregate with each other making the visual microscope counting challenging and less accurate. This could have resulted in under estimation of number of spores present / mg when counted under a microscope which plays an important role in the calculation. Additionally, the *Ptr* spores are comparatively much bigger in size than the other two spores and the beads used may have ground the spores more efficiently compared to *Fg* and *Pst* spores. These two factors, microscope counting and DNA extraction, would be consistent with a greater calculated extraction efficiency. On the other hand, the efficiency % is very low for *Fg* (5%) and *Pst* (14%) spores. This impacts the sensitivity and accuracy of the assay. In *Pst* spores, during asexual stage, a mini secondary cycle of reinfection can occur by dihaploid dikaryotic

urediniospores that are n+n (Zheng et al. 2013). In this instance, *Pst* DNA extraction efficiency would change from 14% for haploid to 7% for dihaploid, further decreasing extraction efficiency. Whether a spore is haploid or dihaploid in nature is an important consideration for these calculations. In a situation where both haploid and dihaploid spore cells are thought to be present, a range in extraction efficiencies can be reported. In this case, it is unclear from the literature how common the dihaploid asexual cycle occurs for *Pst*, thus we will assume *Pst* is haploid for the purposes of our calculations.

The inoculum needed to cause an infection lies between 10^5 to 10^6 spores for *Pst* (Araujo et al. 2023) and 8000 to 10^4 for *Fg* (known from Dr. Foroud's lab group at the Lethbridge RDC). Therefore, even with the poor recoveries of both *Pst* and *Fg* < 15%, as long as detection limits lie below 10^4 it is still possible for the growers to detect presence in time to control the disease spread. However, accurate quantification still remains in question. Poor DNA extraction efficiencies would impact the sensitivity and accuracy of the assay and further investigation is required here to improve the very poor extraction efficiencies.

3.4.4 Detection of *Ptr, Fg,* and *Pst* by qPCR

The data obtained from qPCR were found to be normally distributed for *Ptr, Fg,* and *Pst* spores using Shapiro-Wilk and Kolmogorov-Smirnov normality and log normality tests. The standard curve of the average Ct values of 10 replicates were plotted against the log [copies of interest / well] (Figure 3.4A-C) using simple linear regression analysis. The Ct values obtained from the qPCR amplification were inversely proportional to the copies of interests used. The PCR wells with maximum copies of interest had the least Ct value and

the wells with the least copies had the highest Ct values. The copies of interest quantified were converted to spore numbers using the derived formulas above and were corrected to DNA extraction efficiency.

A mixed effect analysis for *Ptr* and *Fg* and a non-parametric one-way ANOVA for *Pst* spores were used. A different analysis was used for *Pst* spores due to the fact that there were only 4 dilutions that had Ct values and other dilutions were undetermined when amplified in qPCR. *Ptr* and *Fg* spores had Ct values for 5 and 6 dilutions, respectively Then the analysis was followed by Tukey's multiple comparison test for all three spores to compare the significant differences among different spore concentrations and determine the LOD. The linear detection ranges for all three spores were 3 to 30,000 for *Ptr* (Figure 3.4A), 85 to 8,512,000 spores for *Fg* (Figure 3.4B), and 411 to 411,429 for *Pst* (Figure 3.4C). Tables 3.8, 3.9, and 3.10 show the mean of Ct values, standard deviation, and co-efficient of variability % of data obtained through qPCR for all three spores. There was no cross reactivity reported when the primers are tested for non-specific pathogens (Data not shown) and hence the higher specific detection is achieved when compared to immunoassays (Melt curve analysis of qPCR detecting *Ptr*, *Fg* and *Pst* spores representing the specificity of the primers included in the appendix). The average % CV for all three spores was ≤ 20% with one exception (55%) (Tables 3.8 – 3.10). The R^2 values were 0.99, 0.99, and 0.95 for *Ptr*, *Fg*, and *Pst* spores, respectively providing a highly sensitive linear range of detection (Figure 3.4A-C).

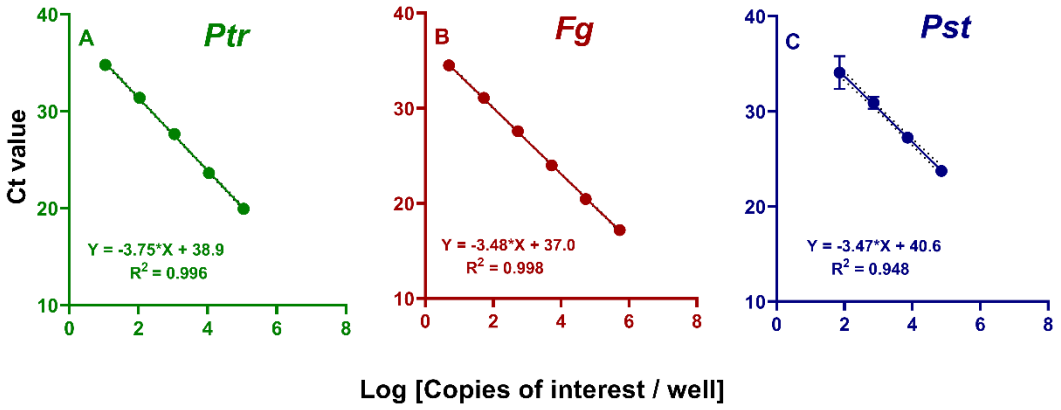

Figure 3.4: Simple linear regression analysis of the *Pyrenophora tritici-repentis* (a), *Fusarium graminearum* (b), *and Puccinia striiformis* (c) through qPCR assays. The average Ct values of 10 replicates were plotted against the log [copies of interest / well]. Data points and error bars represent the mean and standard deviation of 10 replicate measurements and the dashed lines are 95% confidence intervals of the linear regression. In A and B, the error bars and confidence intervals are smaller than the data points and regression line and thus cannot be seen. The relationship between copies of interest (log) and Ct values were linear and significant ($p < 0.001$).

Table 3.8: Mean, SD, and co-efficient of variability of Ct values for *Pyrenophora tritici-repentis* spores through qPCR

***Ptr* Spores / well**	**Ct Mean**	**SD**	**CV %**
3×10^4	19.9	0.102	3
3×10^3	23.6	0.137	4
3×10^2	27.7	0.105	3
30	31.4	0.36	11
3	34.81	0.5680	20

Descriptive statistics of 10 replicates (n=10), where SD – standard deviation, CV – Coefficient of variability at $p < 0.001$

Table 3.9: Mean, SD, and co-efficient of variability of Ct values for *Fusarium graminearum* spores through qPCR

***Fg* Spores / well**	**Ct Mean**	**SD**	**CV %**
8.5×10^6	17.2	0.07	2
8.5×10^5	20.4	0.13	4
8.5×10^4	24	0.05	1
8.5×10^3	27.6	0.06	2
8.5×10^2	31.1	0.31	10
85	34.5	0.49	17

Descriptive statistics of 10 replicates (n=10), where SD – standard deviation, CV – Coefficient of variability at $p < 0.001$

Table 3.10: Mean, SD, and co-efficient of variability of Ct values for *Puccinia striiformis* spores through qPCR

***Pst* Spores / well**	**Ct Mean**	**SD**	**CV %**
4.1×10^5	23.7	0 0.26	8
4.1×10^4	27.2	0.39	12
4.1×10^3	30.9	0.62	20
4.1×10^2	34.1	1.73	55

Descriptive statistics of 10 replicates (n=10), where SD – standard deviation, CV – Coefficient of variability at $p < 0.001$

The LODs of previously published methods using qPCR detection techniques by Araujo et al. (2020) achieved a LOD of 1 spore each for *Ptr* and *Pst* spores and 35 spores for *Fg* spores using the same set of primers used in this study. However, the DNA extraction efficiency was not considered, with 100% extraction efficiency assumed and directly quantified from the amount of DNA used. Therefore, it is possible that the LODs estimated by Araujo et al. (2020) have been underestimated, and are actually higher than reported.

In a previous study by Morcia et al. (2020), *Fg* was detected and quantified using dPCR and the limit of detection was 13 copies / µL. Again, the DNA extraction efficiency was not considered and the authors only reported copies of interest instead of actual spore numbers, thus direct comparison is challenging. Liu et al. (2015) detected and quantified cereal rust pathogens, reporting a limit of detection of 5 pg / µL of DNA of *Pst* spores, but again spore numbers were not calculated. Research by Mayer et al. (2003) focused on quantifying copy numbers of the *nor-1* gene and its correlation with the quantification of colony forming units (cfu) of *Aspergillus flavus*. The limit of detection reported was 10^4 copies / g of sample. A known concentration of the target pathogen was used to infect the host tissue and the DNA was extracted to perform real-time PCR and calculate the recovery rate. The recovery rate was calculated by directly correlating the copy numbers to the inoculated spore numbers without involving any conversion factors (Mayer et al. 2003). The reported recovery rates ranged from 98.3 – 115.5 % across different dilutions of the pathogen. Our findings of extraction efficiency percentage for *Fg* and *Pst* were far below the reported values by Mayer et al. (2003) and for *Ptr* spores, the extraction efficiency was more than double due to underestimation of spore numbers.

To our knowledge, there are no studies that have conducted a comprehensive assessment of absolute extraction recoveries of DNA from fungal spores for qPCR. Yang et al. (2021) investigated the impact of plant tissue matrix on the extraction recovery of DNA. While the authors do not directly assess extraction efficiencies of DNA from pathogenic cells, the results are informative and useful for comparisons. They used three model plant pathogens; *Pectobacterium atrosepticum, Plasmodiophora brassicae,* and *Botrytis cinerea* to determine matrix effects during DNA extraction. It is important to consider that the pathogens selected were entirely three different organisms belonging to different kingdoms. Extracted genomic DNA from each pathogen was measured separately and also mixed in aliquots of DNA with healthy plant tissues and extracted again (mixed DNA). qPCR was performed using both DNA samples and the matrix effect on recovery was calculated by the difference between the quantified original DNA of the pathogen (containing no plant tissue matrix) and the quantified mixed DNA (pathogen and host tissue). The overall matrix effect on DNA recovery rate ranged from 2.7 – 63.8% in this study (Yang et al. 2021). The authors acknowledge that their experiments fail to assess actual recovery of pathogenic DNA from plant cells and that the true recovery rate is likely even lower than their reported matrix effects. When comparing the matrix effect determined by Yang et al. (2021), they achieved a range from 23-64% for fungal spores, which is higher than the extraction efficiency achieved in this study for *Fg* and *Pst* spores 5% and 14% respectively. *Ptr* spores had an extraction efficiency of 290%, however, we think it could be resulted due to underestimation of spore numbers under a microscope as they tend to clump with each other. Each clump had varied spore numbers thus, only approximate values could be obtained. Yang et al. (2021) achieved a higher extraction

efficiency because of a fact that they didn't consider calculating extraction efficiencies from the intact spore, but only the matrix effect from the presence of plant tissue.

Our results have demonstrated a derivation of a formula and approach that can be utilized in the calculation of DNA extraction efficiency and subsequent quantification of fungal spores. There are important implications of these findings that will improve the ability to quantify pathogens by qPCR more accurately. Even though our detection limits lie far below the amount of inoculum needed to cause an infection in the field, and thus these extraction losses may not be relevant at spore levels during infection, accurate quantification of spore numbers is still significant in plant disease diagnosis. Additionally, these results could have broader implications for other applications of qPCR, for example, in clinical settings. While more research is needed in this area, in the immediate term, there simply needs to be a much greater acknowledgment of the uncertainties introduced to qPCR when DNA extraction efficiency is not being considered.

3.4.5 Comparison of LODs of qPCR and RT-iPCR

In general, LODs from real-time immunoPCR (RT-iPCR) and qPCR (Table 3.11) were comparable, varying with the target spore. *Ptr* spores had a 3-fold improved sensitivity with RT-iPCR over the corresponding qPCR. *Fg* spores had an 11-fold increased sensitivity when detected through qPCR compared to RT-iPCR. *Pst* spores showed an increased sensitivity of 2.2-fold by RT-iPCR compared to qPCR (Table 3.11).

Table 3.11: The LOD of three target spores through RT-iPCR and qPCR experiments.

Spores	**LOD RT-iPCR**	**LOD qPCR**	**Sensitivity comparison**
Ptr	1	3	3.0 × (RT-iPCR)
Fg	938	85	11 × (qPCR)
Pst	188	411	2.2 × (RT-iPCR)

3.5 Conclusion

A qPCR assay was evaluated for the rapid and sensitive detection of three airborne fungal pathogens – *Ptr, Fg,* and *Pst*. The qPCR method was able to detect as low as 3 spores of *Ptr*, 80 spores of *Fg,* and 411 spores of *Pst* and significantly improved linear working range for all three spores and provided a highly specific detection without any cross reactions, unlike immunoassays that were discussed in the previous chapter. More accurate detection ranges are possible when DNA extraction efficiency is calculated and implemented in the quantification of spore numbers. Determination of DNA extraction efficiency is an important finding of this project and would enable accurate quantification of fungal pathogens. To our knowledge, there was no study conducted so far to determine the DNA extraction efficiency and to calculate spore numbers from the quantified DNA. We have used a classical approach (Applied Biosystems 2003) to calculate DNA extraction efficiency and quantification of spore numbers involving genome size, copy numbers of the targeted genes, extracted DNA concentrations, volume of DNA, and dilution factors. These used formulas are applicable to any other pathogenic fungal spores to determine the DNA extraction efficiency and quantification of spore numbers when genome size and identification of single or low copy genes are available.

Chapter 4 Quantitative detection of *Pst* spores in field samples: comparing microscopy, RT-iPCR, and qPCR results

4.1 Introduction

4.1.1 Rust species

The three rusts of wheat, leaf (*Puccinia triticina*), stem (*Puccinia graminis*), and stripe rust (*Puccinia striiformis*) spores are prevalent across Canada (Araujo et al. 2020). Stripe rust is more common in western Prairie provinces which have cool and dry weather conditions whereas leaf and stem rusts have a higher impact in the eastern Prairie region where the environmental conditions are warm and humid (Xi et al 2015). Rust fungi are obligate biotrophic basidiomycetes that cause infection mainly through asexual urediniospores. A single growing season can produce an enormous amount of inoculum through several cycles of urediniospores infection in susceptible wheat varieties. They are wind dispersed and are able to travel a long distance (Araujo et al. 2020).

The three rusts share highly similar urediniospore morphologies, including germ pores (3–13 on the surface), outer hyaline walls varying in thickness from 0.8 to 1.8 µm, shapes from round to obovoid, and diameters from 26–30 µm × 18–32 µm (Liu and Hambleton 2010; Araujo et al. 2020). Stripe rust infects foliage, which has spores that are yellow to orange in colour. Leaf rust, which also affects leaves, has spores that are reddish to brown in colour. Stem rust has spores that are brown to black in colour and infects stem and leaves (Agrios 2005). Spores from wild related wheat species could also be present in these samples (Liu and Hambleton 2010). However, microscope identification becomes hard when doing it manually as most of them appear in reddish orange and brown colors.

Stem and leaf rusts were once severe disease, but because of extensive breeding programs, wheat in Western Canada is no longer significantly affected by these two rusts. Stripe rust is the most threatening rust species in Western Canada due to a lack of widespread genetic resistance (Zheng et al. 2014).

When available, disease forecasting tools should be utilized to identify probable wheat diseases. This will help farmers decide whether to select varieties with genetic resistance or to apply fungicides or other preventative steps to control the infections. The disease triangle concept states that for a disease to emerge, there must be a susceptible host, a virulent infection, and the right environmental factors (Scholthof 2007). It takes a significant number of pathogen propagules to predict if hazardous disease levels would emerge in fields (Scholthof 2007; Araujo et al. 2023). Determining the regional concentrations of pathogen propagules in crop areas, such as spores, is becoming more and more important for disease forecasting systems (Cao et al. 2016). It is common practise to monitor and measure fungal plant pathogen airborne inoculum using spore trapping techniques. There are many spore trapping techniques available, such as wax-coated film, double-sided adhesive tape, and air sampling instruments. These techniques are critical for spores / pathogen monitoring, understanding disease progression, and predicting crop diseases (Cao et al. 2016).

In this chapter, quantification of airborne fungal spores of *Puccinia striiformis* (*Pst*) spores from real-time air samples are discussed. Airborne spores were collected from two different wheat field trials at the Lethbridge Research and Development Centre (RDC), AB; disease nursery (49°, 42’9” N, 112°, 45’40” W) is located approximately 200 m to the north-east of the Lethbridge RDC main building and Fairfield (49°, 42’31” N, 112°,

41’51” W) is located approximately 2.5 km to the east of the Lethbridge RDC. *Pst* and *Tilletia tritici* causing wheat bunt are the two spores studied in the disease nursery but *Tilletia tritici* wouldn’t interfere with the spores collected from the sampler as they aren’t air-borne instead it is a seed born disease and we didn’t see any bunt spores during microscopic screening. In Fairfield, the diseases studied are stripe, stem, and leaf rusts; but the stripe rust was the only rust species seen during the sampling year. Only *Pst* spores were selected because these two fields were inoculated with *Pst* spores and based on initial microscopic and molecular screening, *Pyrenophora tritici-repentis* (*Ptr*) and *Fusarium graminearum* (*Fg*) spores weren’t detected while using pathogen-specific primers in qPCR.

4.2 Materials and methods

Airborne spores were collected from two different wheat field trials at Lethbridge RDC, AB, the disease nursery, and Fairfield, using the Burkard automatic cyclone air sampler (Burkard Manufacturing Co. Ltd., Rickmansworth, Hertfordshire, UK) (Figure 4.1). The Burkard cyclone air sampler captures all particles that are present in the air. The upper section of the sampler is connected to the rotating wind-pane which rotates constantly and keeps the sampling orifice facing the wind. The particles are collected in 1.5 mL micro-centrifuge tubes that are placed inside the sampler. At the Lethbridge RDC, both single and multi-vial cyclone samplers are present and they actively sample air and airborne particles at a rate of 16.5 L / min.

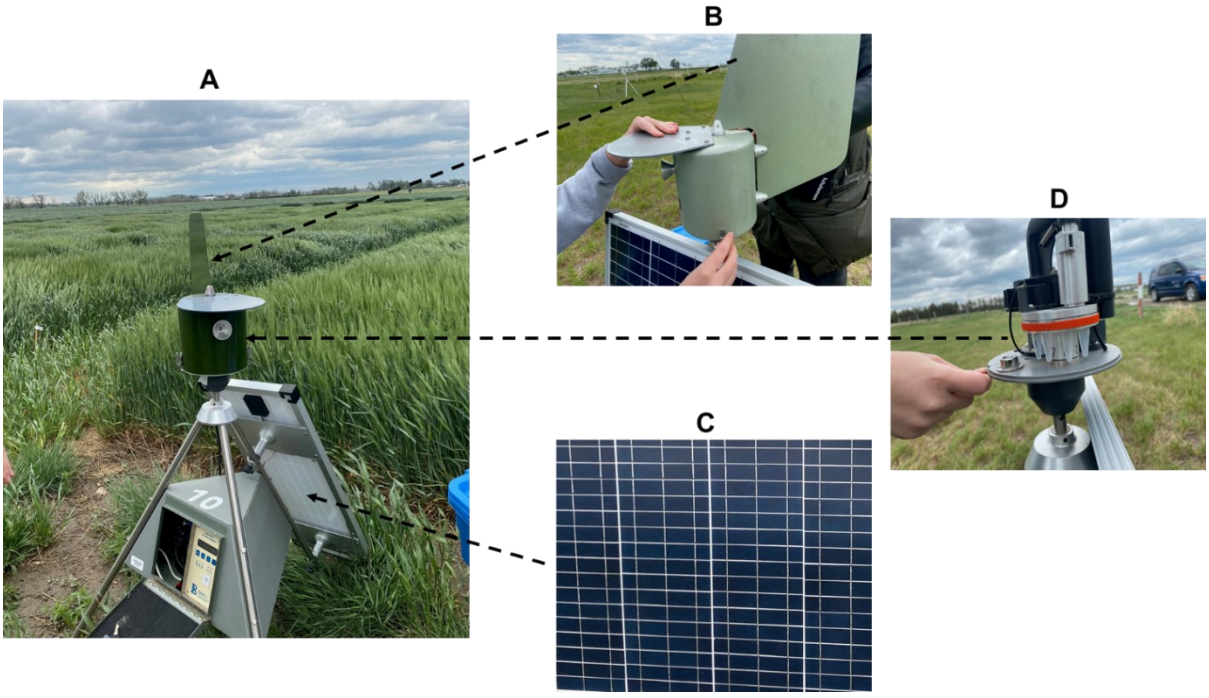

Figure 4.1: Burkard cyclone air sampler used to collect airborne spores (A), Rotating wing to orient collecting orifice facing the wind to collect airborne spores (B), Battery operated collector via a solar power panel (C), Spores collected for 24 h in micro-centrifuge tubes placed inside the collecting device (D).

The multi-vial sampler is connected to a multi-functional timer which automatically shifts from one tube to another for spore collection. This instrument has the capacity to hold 8 tubes which allows up to 8 samplings / week. The instrument automatically switches to a different tube at a 24 h time interval. The samples were collected approximately once / week according to the timer set-up and tubes were replaced with a fresh set of tubes after each collection. This instrument is connected to a battery which is operated by a solar power panel (Figure 4.1).

Spores were collected from the disease nursery and Fairfield locations and the *Pst* spores were detected and quantified using microscope counting, Real-Time immunoPCR (RT-iPCR), and quantitative PCR (qPCR). Only *Pst* spores were quantified due to the fact that both fields were inoculated only with *Pst* spores. The inoculation dates for the disease nursery and Fairfield fields were week of June 1st and July 6th respectively. The validated methods from previous chapters (2 and 3) were used for quantitative detection of *Pst* spores. The spore collector present in the disease nursery was a single-vial sampler providing 1 sample tube / week whereas the Fairfield collector used a muti-vial sampler which collected 8 sample tubes / week.

4.2.1 Spore sample preparation

4.2.1.1 Disease nursery

The samples were collected from a single-vial sampler located in the disease nursery from mid-May to July 2022 for 8 weeks (exact collection dates shown in the graphs). The tubes containing air samples were re-suspended in 1 mL of PBS and subjected to liquid nitrogen treatment 4 times. The 1 mL field sample suspension was divided into 3 tubes as

100 µL for microscope counting, 450 µL for RT-iPCR, and 450 µL for qPCR. The sample tubes were stored at - 20° C until further experiments.

4.2.1.2 Fairfield

The samples were collected from a multi-vial sampler located in the Fairfield from July to August 2022 for 8 weeks (exact collection dates shown in Figure 4.2B). The 8 sample tubes / week were combined and re-suspended in a single tube with 2.5 mL of PBS and subjected to liquid nitrogen treatment 4 times. The 2.5 mL field sample suspension was divided into 4 tubes as 100 µL for microscope counting, 450 µL for RT-iPCR, and 450 µL for qPCR. The remaining sample tubes were stored at - 20° C.

4.2.2 Determination of spore concentration

Pst spore concentrations were determined using a Bright-Line hemacytometer under a brightfield microscope (Leica Microsystems DM6000 B) and the pictures were taken using an attached camera (Leica Microsystems DFC310 FX) to identify the morphology of the spores. For each count, 10 µL of the spore suspension was pipetted into the counting chamber, covered with a cover glass, and the spores were counted under the microscope using a hemocytometer. The four outside corner grids out of nine grids (1 mm × 1mm each) were counted under the microscope / count. Each spore sample was counted four times for a total of 16 counts. The spore numbers counted / 10 µL (4 grids out of 9) were multiplied by 10^4 to calculate the number of spores / mL.

4.2.3 RT-iPCR

The RT-iPCR assay was optimized for *Pst* spores in Chapter 2 (section 2.2.4) and was carried out to generate the standard curve for interpolating the unknown air samples from

the disease nursery and Fairfield fields. For the standard curve, standard spores were diluted in doubling dilutions in filter sterilized PBS starting from a spore concentration of 6.5×10^5 spores / mL of PBS of *Pst* spores. These spores were frozen in liquid nitrogen and thawed at RT four times to obtain a homogeneous spore suspension. A 96-well plate was coated with the spores and some wells with no spores acted as controls (containing PBS (4 wells) and LCB (2 wells)). The control wells were sealed using plate sealers to avoid contamination and the spores were coated in doubling dilutions with a volume of 30 µl / well starting from an initial concentration of 2×10^4 spores / well for *Pst* spores. There was some evidence that having the standard spore dilutions run on the same plate as the unknowns could introduce the possibility of contamination. Thus, it was decided to run the unknown samples and standard spore dilution curves in separate plates; however the plates were run on the same instrument. The plate was sealed and incubated overnight at 37°C. After overnight incubation, the experiment was carried out as mentioned in Chapter 2 (section 2.2.4) (Gaudet et al. 2015).

4.2.4 DNA extraction

The optimized DNA extraction from Chapter 3 was performed for extractions of DNA from unknown field samples from disease nursery and Fairfield using a DNeasy PowerSoil kit from QIAGEN. The prepared sample solution of 450 µL (from section 4.2.1) was centrifuged at 12,000 × g for 2 min and the supernatant was discarded. An equal volume of bead buffer from the kit was used to re-suspend the sample solution (this step was performed to avoid further dilution of field samples with bead buffers). From this step, the extraction was carried out as mentioned in Chapter 3 section 3.2.1.

4.2.5 qPCR

qPCR assays were carried out to quantify the spores from air samples. The materials used for these tests were the PerfeCTa® SYBR® Green SuperMix Low Rox (QantaBio) and pathogen-specific primers for *Pst* spores were acquired as reported in Araujo et al. (2020) to carry out the experiments (section 3.2.2). The qPCR instrument used to perform the experiments was an Applied Biosystems™ QuantStudio™ 3. For each condition, 7.5 µL of qPCR master mix and 2.5 µL of DNA template was added. The qPCR cycle conditions were as follows: 1 cycle at 95℃ for 3 min, 40 cycles at 94℃ for 15 s, 55℃ for 30 s, and 72℃ for 30 s. Ct values at DNA amplification, melt curve, and standard curve were calculated by the software QuantStudio™ Design & Analysis Software V1.4.2 at the end of each experiment. DNA extraction efficiency calculated in chapter 3, section 3.4.3 is applied to the calculation of spore numbers in air samples of both disease nursery and Fairfield locations.

4.3 Statistical analysis

The data from RT-iPCR assays using *Pst* spores were subjected to normality testing via the Shapiro-Wilk test and Kolmogorov-Smirnov test. Ct values generated through RT-iPCR assays for *Pst* spores were normally distributed. Simple linear regression analysis of RT-iPCR data of *Pst* spores were plotted to derive the standard curve. Ct values obtained from the unknown field samples were used to interpolate the corresponding spore numbers from the standard curve. The data resulting from qPCR assays using extracted DNA of *Pst* spores were subjected to normality testing via the Shapiro-Wilk test and Kolmogorov-Smirnov test. Ct values generated through qPCR assays for *Pst*

spores were normally distributed. Simple linear regression analysis of qPCR data of *Pst* spores were plotted to derive the standard curve. Ct values obtained from the unknown field samples were used to interpolate the corresponding spore numbers from the standard curve and corrected to DNA extraction efficiency. Comparison among the three real-time detection methods was carried out using the Pearson-correlation test and the Pearson-correlation matrix was used to determine the r coefficients to compare the spore numbers detected through each method with the other.

4.4 Results and discussion

4.4.1 Rust spore numbers counted through a microscope

The *Pst* spore numbers from the field samples were counted using microscopy and are illustrated in Figure 4.2 with descriptive statistics presented in Table 4.1. It is important to note that these spore counts potentially represent all rust species in the sample as it is difficult to achieve species level identification of *Pst* spores using a microscope. Most of the rust species including stem, leaf, and stripe rust look similar in shape and size, representing a source of uncertainty in these measurements. Rust spores infecting wild related wheat species could be also present. In both disease nursery and Fairfield, when the disease was rated, stripe rust was the dominant infection observed. However, the likely more significant source of variation in microscope counts is a result of the challenges related to obtaining a homogeneous spore suspension without clumps in field samples. The environmental debris and dust present in the field samples make manual counting under the microscope challenging (Table 4.1 and 4.2).

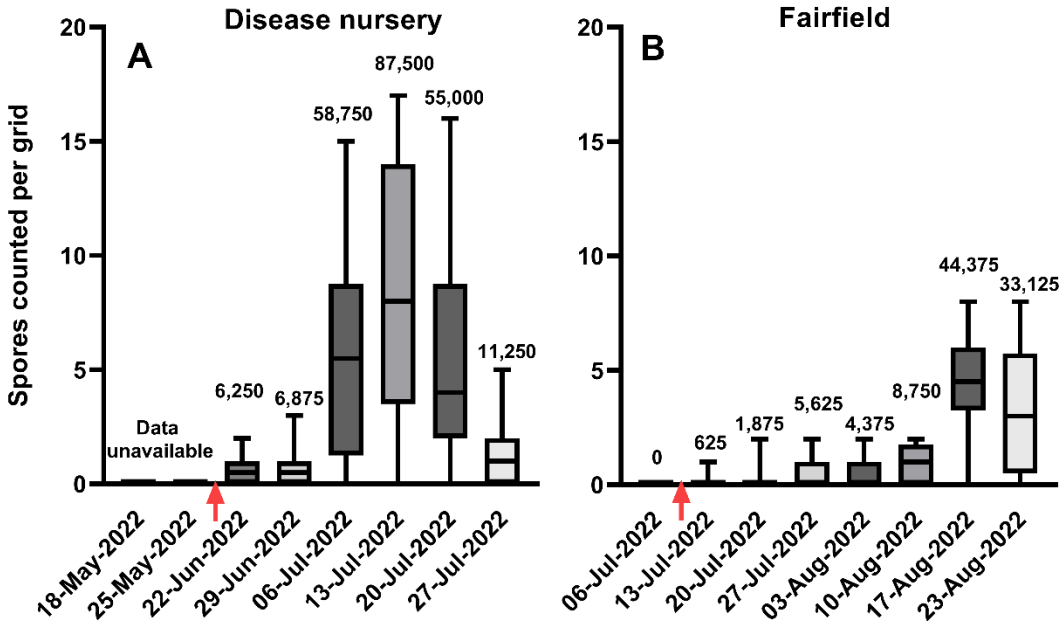

Figure 4.2: Number of *Puccinia striiformis* spores in field samples counted / grid (0.1 µL of suspension) of the counting chamber under a microscope. Calculated spore numbers / mL are indicated above the box plots. The horizontal line inside the box plots indicates the median and whiskers indicate the minimum and maximum spores counted. A – Disease nursery and B – Fairfield. The red arrow on the graphs indicates the inoculation dates of *Puccinia striiformis* spores in both fields.

Table 4.1: Descriptive statistics of *Puccinia striiformis* spores from disease nursery counted with a light microscope / 0.1 µL of the field sample where n = 16

Date (2022)	Minimum	Maximum	Mean	SD	CV (%)
18-May	N/A	N/A	N/A	N/A	N/A
25-May	N/A	N/A	N/A	N/A	N/A
22-Jun	0	2	0.6	0.7	115
29-Jun	0	3	0.7	0.9	127
06-Jul	0	15	5.9	4.8	82
13-Jul	0	17	8.8	5.4	62
20-Jul	0	16	5.5	4.4	80
27-Jul	0	5	1.1	1.4	125

Table 4.2: Descriptive statistics of *Puccinia striiformis* spores from Fairfield counted with a light microscope / 0.1 µL of the field sample where n = 16

Date (2022)	Minimum	Maximum	Mean	SD	CV (%)
06-Jul	0	0	0	N/A	N/A
13-Jul	0	1	0.1	0.3	400
20-Jul	0	2	0.2	0.5	290
27-Jul	0	2	0.6	0.7	129
03-Aug	0	2	0.4	0.7	166
10-Aug	0	2	0.9	0.8	92
17-Aug	0	8	4.4	2.2	50
23-Aug	0	8	3.3	2.6	79

In the samples of disease nursery, the first two weeks had an unusually high amount of soil and plant debris which made the counting process unfeasible; thus the data were unavailable for the first two weeks. The highest total amount of spores / sample (87,500 ± 33,603) was counted for the week of July 13th which is 4 weeks after inoculation and the lowest count (6,250 ± 1,443) was observed for the week of 22nd June which is right after inoculation (Figure 4.2A) (Table 4.1).

In the samples of Fairfield, the highest amount of spores (44,375 ± 16,504) were counted for the week of August 17th which is 6 weeks after inoculation, and the lowest count (0) was observed for the week of 6th July which is right before inoculation (Figure 4.2B) (Table 4.2). As mentioned previously, species-level identification of *Pst* spores is not possible here and the spore numbers reported could result from interference of other rust spp in both the fields.

The CV % ranged between 60 – 125 % for all microscope counts of disease nursery air samples and ranged between 50 – 400 % for the Fairfield air samples. As indicated in Tables 4.1 and 4.2, the minimum values were 0 for all the samples with the maximum ranging from 0 – 17, leading to higher variability in this data set. Potential clumping together of spores with environmental debris, misidentification / miss counting due to debris and dust, and also just the very small number of spores counted (a count of 0 or 2) is a relatively small difference in an actual number of spores, but has a large impact on the SD. This also illustrates the challenge of using environmental spore counts using microscopic observations.

The inherent difficulties and inefficiencies of manual microscope counting, including the inability to differentiate species-level identification and heterogenous spore suspensions,

the microscope data should be considered qualitative. A similar challenge of manual counting and distinguishing between species-level variation was previously reported in Araujo (2018). As mentioned in the study by Liu and Hambleton (2010), there could be spores from wild related wheat species present in the environmental samples which would make the manual counting very hard to distinguish between spores. Consequently, this method is not presented as a viable real-time quantification tool for pathogen detection. It is used strictly for comparison to the other techniques studied here, RT-iPCR and qPCR.

4.4.2 Detection of *Puccinia striiformis* by RT-iPCR

The data obtained from RT-iPCR were found to be normally distributed for *Pst* spores using Shapiro-Wilk and Kolmogorov-Smirnov normality and log normality tests. The standard curve of the average Ct values of 16 replicates were plotted against the log [spores / well] (Figure 4.3) using simple linear regression analysis. Ct values obtained from the unknown field samples were used to interpolate the corresponding spore numbers from the standard curve. The RT-iPCR assay was carried out to generate the standard curve for interpolating the unknown air samples from the fields of disease nursery and Fairfield. The interpolated spore numbers are presented in Figure 4.4 (A – disease nursery and B – Fairfield). Higher incidence of spore numbers was detected in both fields 5 weeks after inoculation with *Pst* spores. The percentage of variability was < 98% for the air samples in both fields, still far less than the variability observed in the microscope counts (Tables 4.3 and 4.4).

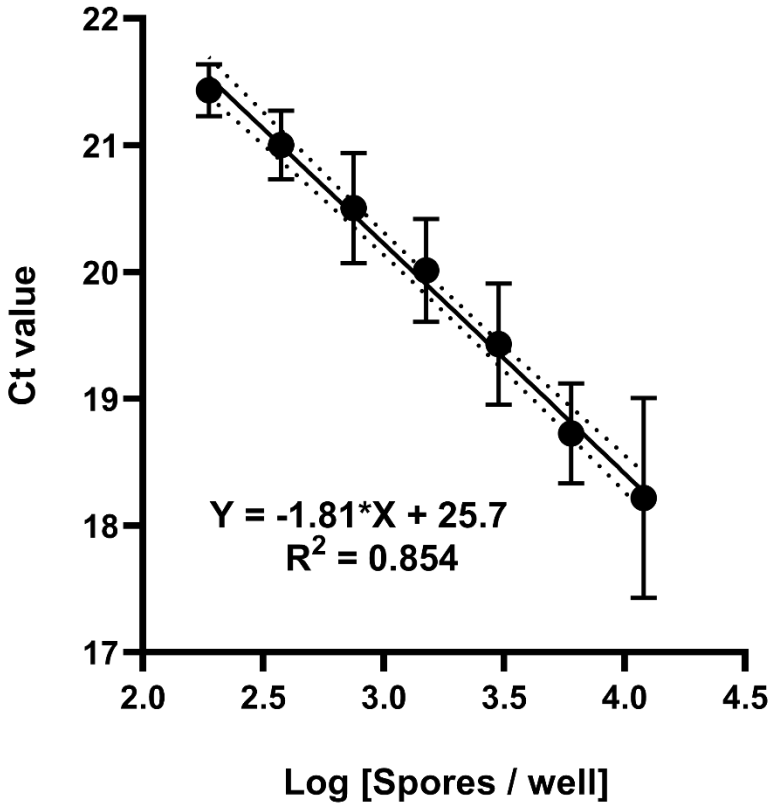

Figure 4.3: Linear regression analysis of the *Puccinia striiformis* – RT-iPCR assays. The average Ct values of 16 replicates were plotted against the log[spores / well]. The relationship between spore numbers (log) and Ct values is linear and significant ($p < 0.0001$).

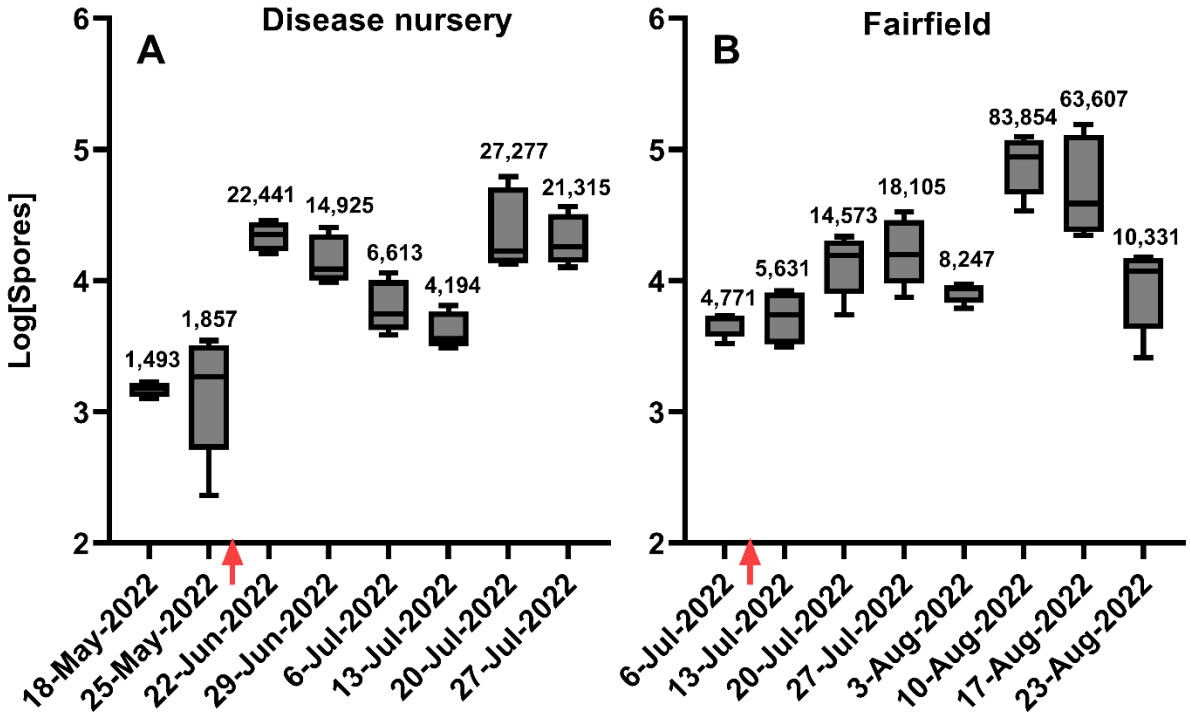

Figure 4.4: Number of *Puccinia striiformis* spores detected in field samples interpolated from the standard curve of known spore amounts through RT-iPCR. Calculated spore numbers / mL are indicated above the box plots. The horizontal line inside the box plots indicates the median and whiskers indicate the minimum and maximum spores counted. A – Disease nursery and B – Fairfield. The red arrow on the graphs indicates the inoculation dates of *Puccinia striiformis* spores in both fields.

Table 4.3: Descriptive statistics of *Puccinia striiformis* spores from the disease nursery location detected through RT-iPCR where n = 4

Date (2022)	Minimum	Maximum	Mean	SD	CV (%)
18-May	1,256	1,685	1,493	197	13
25-May	232	3,500	1,857	1,392	75
22-Jun	16,102	28,728	22,441	5,837	26
29-Jun	9,739	25,496	14,925	7,225	48
06-Jul	3,840	11,472	6,613	3,346	51
13-Jul	3,083	6,463	4,194	1,543	37
20-Jul	13,411	62,085	27,277	23,354	86
27-Jul	12,651	36,565	21,315	10,510	49

Table 4.4: Descriptive statistics of *Puccinia striiformis* spores from the Fairfield location detected through RT-iPCR where n = 4

Date (2022)	Minimum	Maximum	Mean	SD	CV (%)
06-Jul	3,306	5,424	4771	987	21
13-Jul	3,142	8,374	5631	2,600	46
20-Jul	5,501	21,644	14,573	6,697	46
27-Jul	7,451	33,328	18,105	10,890	60
03-Aug	6,159	9,399	8,247	1,429	17
10-Aug	34,055	125,763	83,854	38,390	46
17-Aug	22,089	155,070	63,607	62,098	98
23-Aug	2,584	15,169	10,331	5,759	56

In the samples of disease nursery, the highest amount of spores (27,277 ± 23,354) were detected for the week of July 20th which is 5 weeks after inoculation, and the lowest count (1493 ± 197) was observed for the week of May 18th, prior to inoculation (Figure 4.4A) (Table 4.3).

In the samples of Fairfield, the highest amount of spores (83,854 ± 38,390) were detected for the week of August 10th which is again 5 weeks after inoculation and the lowest numbers detected (4,771 ± 987) were observed for the week of 6th July which is just prior to inoculation (Figure 4.4B) (Table 4.4).

The CV % ranged between 13 – 86 % for all the disease nursery air samples through RT-iPCR and the highest variation was with the highest spore numbers detected in the week of 20th July. The CV % ranged between 17 – 98 % for all the Fairfield air samples through RT-iPCR. The higher CV % was with the week of 17th August were the second highest spore numbers were detected through RT-iPCR. These higher variability percentages were due to variable minimum and maximum values of spores detected were likely due to the challenge of obtaining a homogeneous spore suspension (Table 4.3 and 4.4).

4.4.3 Detection of *Puccinia striiformis* by qPCR

The data obtained from qPCR were found to be normally distributed for *Pst* spores using Shapiro-Wilk and Kolmogorov-Smirnov normality and log normality tests. The standard curve of the average Ct values of 24 replicates were plotted against the log [copies of interest / well] (Figure 4.5) using simple linear regression analysis. The Ct values were obtained for the log of copies of interest / well and converted to spore numbers using the

calculations derived in Chapter 3, section 3.4.3. The DNA extraction efficiency was also considered and the spore numbers calculated were corrected to the extraction efficiency of 14% (Calculated in Chapter 3, section 3.4.3 for *Pst* spores). Ct values obtained from the unknown field samples were used to interpolate the corresponding spore numbers from the standard curve.

The qPCR assay was carried out to generate the standard curve for interpolating the unknown air samples from the fields of the disease nursery and Fairfield. Unlike in RT-iPCR, the standards were run for both fields on the same plate where unknowns were analyzed. The DNA standard did not interfere with unknowns on the qPCR. This could be because in RT-iPCR the spores were directly coated and there are a series of bindings and washing steps involved whereas in qPCR the assay itself is simpler by just adding the PCR master mix and the extracted DNA in the appropriate wells (Gaudet et al. 2015; Araujo et al. 2020). The interpolated spore numbers are presented in Figure 4.6 (A – disease nursery and B – Fairfield). Higher incidence of spore numbers were detected in both fields 4-5 weeks after inoculation with *Pst* spores. Tables 4.5 and 4.6 indicates the minimum, maximum, mean, SD, and CV of *Pst* spores through qPCR at both locations.

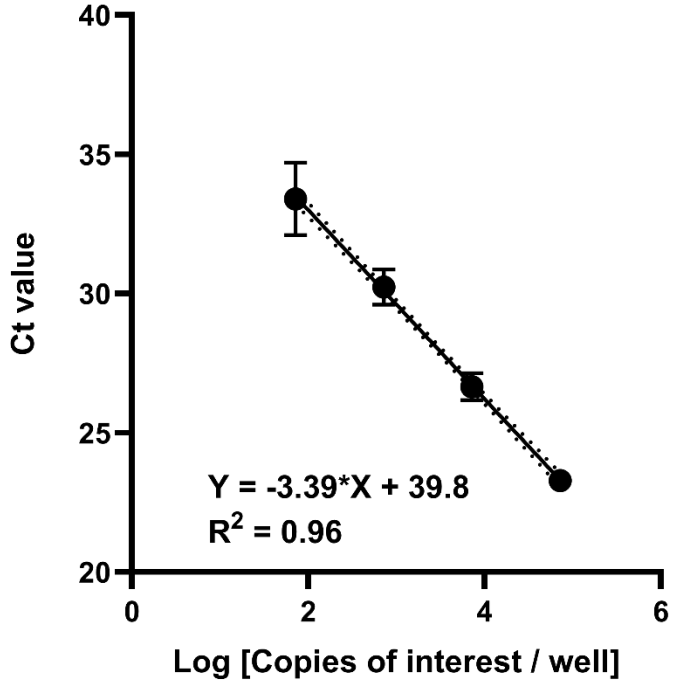

Figure 4.5: Linear regression analysis of the *Puccinia striiformis* – qPCR assays. The average Ct values of 24 replicates were plotted against the log [copies of interest / well]. The relationship between spore numbers (log) and Ct values is linear and significant ($p < 0.0001$).

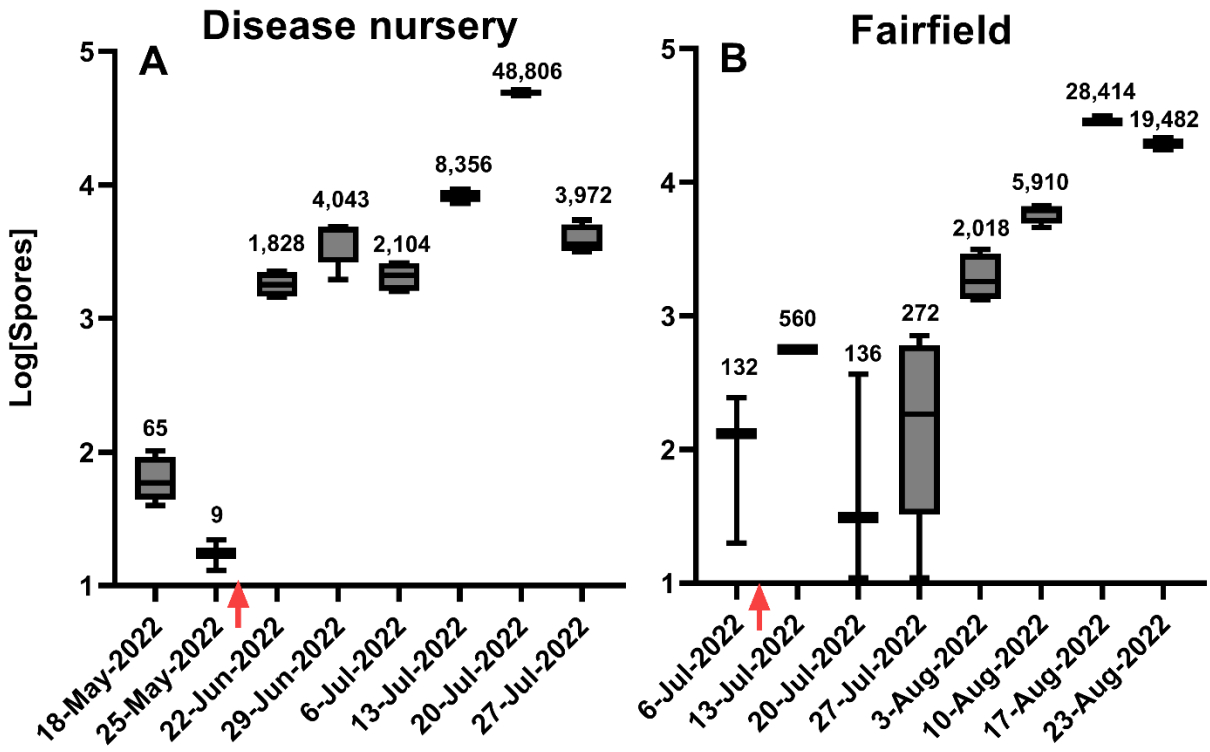

Figure 4.6: Number of *Puccinia striiformis* spores detected in field samples interpolated from the standard curve of known spore amounts through qPCR. Calculated average spore numbers / mL are indicated above the box plots. The horizontal line inside the box plots indicates the median and whiskers indicate the minimum and maximum spores counted. A – Disease nursery and B – Fairfield. The red arrow on the graphs indicates the inoculation dates of *Pst* spores in both fields.

Table 4.5: Descriptive statistics of *Puccinia striiformis* spores from disease nursery location detected through qPCR where n = 4

Date (2022)	Minimum	Maximum	Mean	SD	CV (%)
18-May	40	102	65	26	40
25-May	13	22	18	6	36
22-Jun	1,456	2,260	1,828	414	23
29-Jun	1,967	4,885	4,043	1389	34
06-Jul	1,602	2,599	2,104	546	26
13-Jul	7,285	9,319	8,356	875	10
20-Jul	46,601	51,340	48,806	2102	4
27-Jul	3,166	5,471	3,972	1045	26

Table 4.6: Descriptive statistics of *Puccinia striiformis* spores from Fairfield location detected through qPCR where n = 4

Date (2022)	Minimum	Maximum	Mean	SD	CV (%)
06-Jul	20	244	132	158	120
13-Jul	560	560	560	N/A	N/A
20-Jul	11	366	136	199	147
27-Jul	11	709	272	311	114
03-Aug	1316	3139	2018	847	42
10-Aug	4579	6702	5910	946	16
17-Aug	27090	31463	28414	2057	7
23-Aug	17608	21599	19482	1750	9

In the samples of disease nursery, the highest amount of spores (48,806 ± 2102) were detected for the week of July 20th which is 5 weeks after inoculation, and the lowest count (9 ± 6) was observed for the week of 25th May which just prior to inoculation (Figure 4.6A) (Table 4.5).

In the samples of Fairfield, the highest amount of spores (28,414 ± 38,390) were detected for the week of August 17th which is 6 weeks after inoculation and the lowest numbers detected (132 ± 120) were observed for the week of July 6th which is just prior to inoculation (Figure 4.6B) (Table 4.6).

The CV % ranged between 4 – 40 % for all the disease nursery air samples through qPCR and the highest variation was with the second lowest spore numbers detected in the week of 18th May and this could have resulted because the first two weeks samples had more debris. The CV % ranged between 7 – 147 % for all the Fairfield air samples through qPCR. The higher CV % was with the week of 20th July and the week of 13th July did not provide a variability percentage because only one of the 4 replicates were amplified and all other replicates were undetermined by the qPCR assay. Overall, the variability percentage was lower in qPCR and RT-iPCR when compared to a microscope. The average CV% for qPCR (44%) < RT-iPCR (48%) < microscope (138%) as qPCR deals with extracted DNA and not the whole spores like in the former methods and does not include washing steps like in RT-iPCR (Table 4.5 and 4.6). Potential clumping together of spores with environmental debris, misidentification / miss counting, and counting a small number of spores could have led to the higher variation in the microscope counts.

4.4.4 Comparison of *Puccinia striiformis* spores detected in the field samples through Microscopy, RT-iPCR, and qPCR

The spore numbers detected through all three detection techniques were compared and analyzed using the Pearson correlation test. The stacked bar graph (Figure 4.7) indicates the mean and SD of the spore numbers detected through microscopy, RT-iPCR, and qPCR. A higher incidence of spore numbers was observed in both fields 4 to 6 weeks after inoculation, suggesting the ability of all three techniques to at least capture a consistent trend in spore numbers through time. The Pearson correlation matrix indicates the strength of linear relationship between two variables. Here the strength of linear relationship between microscopy vs RT-iPCR, microscopy vs qPCR and RT-iPCR vs qPCR were compared for both disease nursery and Fairfield spore numbers (Figure 4.8). In the disease nursery field samples, the microscopy vs RT-iPCR had a R coefficient value of -0.04 indicating no correlation between the two techniques making them incomparable whereas microscopy vs qPCR had a R coefficient of 0.43 and RT-iPCR vs qPCR with R value of 0.59 having moderate correlation among these techniques (Figure 4.8A).

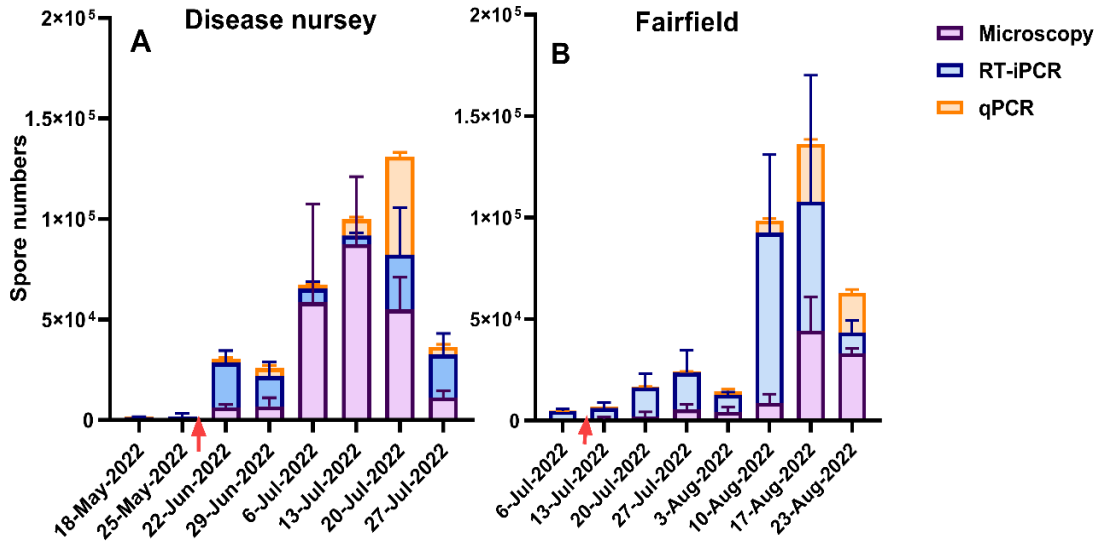

Figure 4.7: The stacked graphs compare the mean and SD of the spore numbers detected through microscope counting, RT-iPCR, and qPCR in the fields of disease nursery (A) and Fairfield (B) through bar graphs The error bars indicate the variability of replicates where n = 16, and the red arrow on the graphs indicate the inoculation dates of *Puccinia striiformis* spores in both fields. The replicates where 16 for the RT-iPCR and qPCR whereas 14 for the microscope with 2 missing values in the disease nursery field due to the sample with excess plant and soil debris.

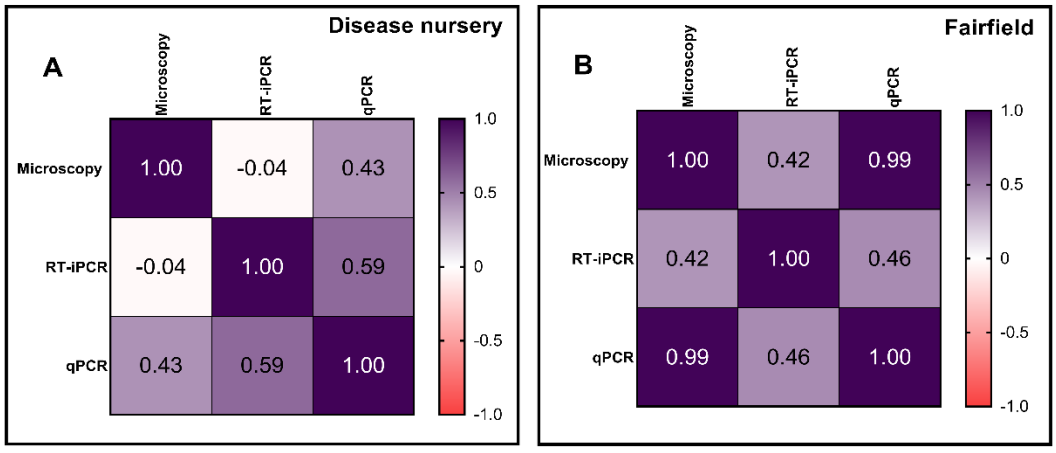

Figure 4.8: Pearson correlation matrices comparing each detection technique with the other: microscopy vs RT-iPCR, microscopy vs qPCR, and RT-iPCR vs qPCR for disease nursery (A) and Fairfield (B) samples.

Microscopy vs RT-iPCR had a poor correlation because the microscopy values were very high in the weeks of 6 and 13th July and values were not available for the first two weeks before inoculation. The higher spore numbers in microscopy counts could be a result of other rust spores being counted. This could have resulted in the absence of correlation between the two techniques (Figure 4.8A). However, these microscopy counts have been used to compare with qPCR results and a moderate correlation is obtained. The absence of correlation could have resulted from RT-iPCR spore counts as well. However, there are uncertainties in accurate detection using RT-iPCR due to cross reactivity and non-homogeneous spore suspension. The *Pst* antibody used for detection could also possibly interfere with other fungal spores sharing a common epitope or the epitopes with structural resemblance resulting in cross reactivity (Murphy and Weaver 2017).

In the Fairfield air samples, the microscopy vs RT-iPCR had a R coefficient of 0.42 and RT-iPCR vs qPCR had a R coefficient of 0.46 leading to a moderate correlation among these techniques. The microscopy vs qPCR comparison with R value of 0.99 explains an excellent linear correlation between microscopy and qPCR for the Fairfield air samples (Figure 4.8B).

The reason for different correlation co-efficient between the locations could be the presence of other rust species in disease nursery and their absence in the Fairfield. This might have increased the microscopy counts where species-level identification is hard in disease nursery samples and thus the negative correlation when compared to other techniques. Fairfield samples might have other spores / any species (other than rust) that might have potentially cross-reacted with *Pst* antibodies resulting in increased spore numbers in RT-iPCR which explains the variation in spore numbers through different

techniques in both the fields. This could have impacted the correlation factors and resulted in huge differences between both locations.

In Figure 4.9, the systematic difference between the spore numbers detected through the three techniques becomes more evident and the scatter plots highlighted the uncertainties in those measurements. In Figure 4.9, panels A and B highlight a number of points that are high in number for microscopy. This increased spore numbers on the microscope counts are consistent with the uncertainty in microscopy counting and its high potential for false positives from other rust species. In Figure 4.9A (disease nursery), the plot highlights the increased spore numbers in the microscopy counts than RT-iPCR. This is consistent with the poor correlation seen in Figure 4.8A similar trend can be seen for spore numbers comparison between microscopy and qPCR techniques (Figure 4.9B, disease nursery), again indicating higher microscope spore numbers.

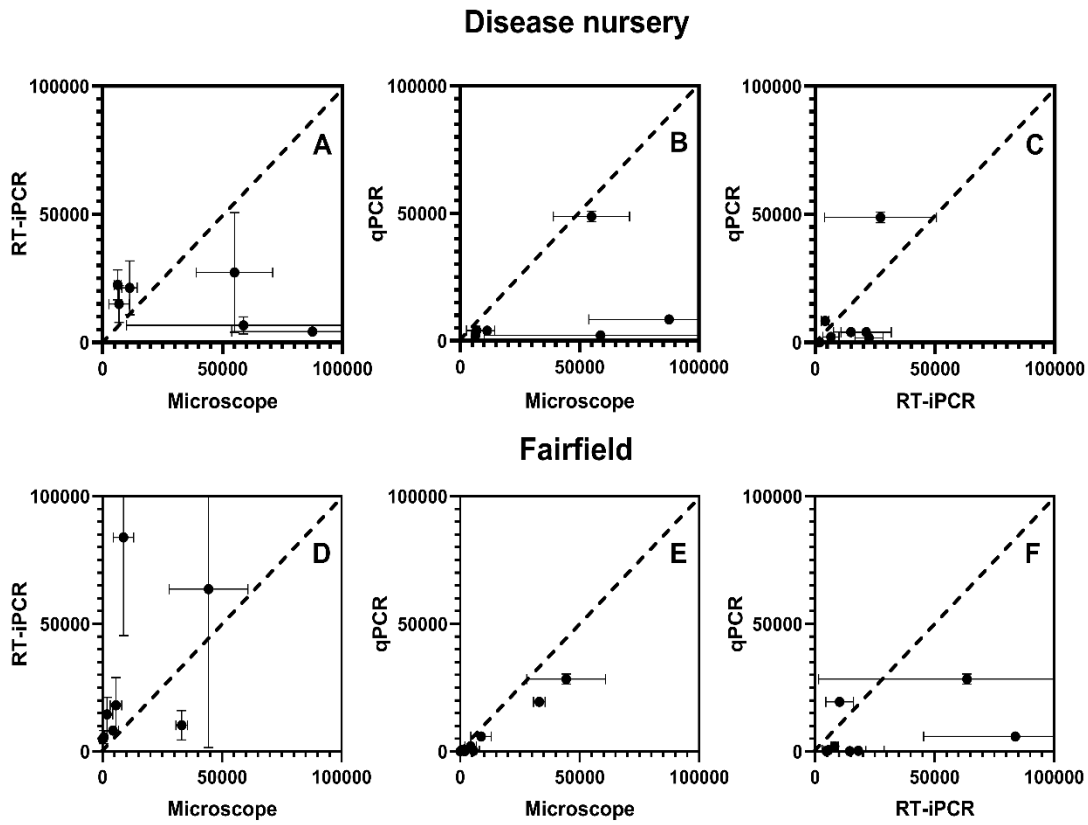

Figure 4.9: The spore numbers detected through microscopy, RT-iPCR, and qPCR were compared using scatter plots. The dashed lines indicate the theoretical linear line of slope = 1 (i.e., x = y) for the spore numbers. Each data point represents the mean ± SD of 4 replicates of each field sample. Spore numbers detected through microscopy vs RT-iPCR in disease nursery (A), Spore numbers detected through microscopy vs qPCR in disease nursery (B), Spore numbers detected through RT-iPCR vs qPCR in disease nursery (C), Spore numbers detected through microscopy vs RT-iPCR in the Fairfield (D), Spore numbers detected through microscopy vs qPCR in the Fairfield (E), Spore numbers detected through RT-iPCR vs qPCR in the Fairfield (F).

Panels D and F show a number of points that indicate increased spore numbers detected through RT-iPCR. High spore numbers detected through RT-iPCR could have resulted from potential cross-reactivity. The cross-reactivity of antibodies with non-target spores is briefly discussed in chapter 2 (section 2.4.5) and here the spore numbers obtained through RT-iPCR in quantifying real air samples support the potential cross-reactivity issue identified with environmental samples involving other fungal spores and perhaps environmental debris. As mentioned in chapter 2 section 2.4.5, cross reactivity issues can be minimized by producing more specific antibodies either by employing monoclonal antibodies instead of polyclonal antibodies (Frank 2002; Murphy and Weaver 2017) or by studying the surface proteins in detail Volterson et al. (2018) and producing a highly specific antibody.

In Figure 4.9D, where spore numbers detected through microscopy and RT-iPCR in Fairfield are compared, a majority of the data points on the RT-iPCR side had maximum spore numbers detected with high variability which could have resulted from cross-reactivity and the on-going challenge of obtaining a homogeneous spore suspension. When spore numbers of RT-iPCR and qPCR of Fairfield were compared (Figure 4.9F), again more data points fall on the RT-iPCR with high spore numbers and increased variability which explains the moderate correlation between the two techniques. When spore numbers of microscopy and qPCR of the Fairfield were compared (Figure 4.9E), the data points fall nearly close to the 1:1 line on both sides leading to a much better correlation between the two methods with R coefficient of 0.99 (Figure 4.8B).

In Figure 4.9, plots indicate a high variability with RT-iPCR and microscopy counts. The high variability in these two detection methods could be resulting in failure in obtaining a

homogeneous solution as both these methods use whole spores to quantify. This suggests that using whole spores in a homogeneous suspension is critical for accurate detection. In contrast, qPCR had very tight replicates with less variation as this method amplifies DNA to quantify the spores than using the whole spores. This suggests that qPCR could be the most applicable method in the field when DNA extraction efficiencies are considered.

4.5 Conclusion

In this chapter, field samples from disease nursery and Fairfield were evaluated for the *Pst* spores using three detection techniques of microscopy, RT-iPCR, and qPCR and results were compared. The major challenge observed with all three methods was to obtain a homogeneous suspension when different air samples were resuspended. Though liquid nitrogen treatments were given prior to any procedure, this problem persisted with methods of RT-iPCR and microscopy counting, where sample suspensions of whole spores are used directly. This issue was minimized in qPCR as it used extracted DNA to perform the analysis. Another challenge encountered with microscopy was the species level identification of rust spores and the incapability in differentiating them. This may have produced inaccuracies in the microscope results due to false positive identifications. With RT-iPCR, the spore numbers detected in Fairfield were higher when compared to the other two methods and this could be a result of cross-reactivity as discussed in Chapter 2 (section 2.4.5). Finally, qPCR had less variation within its replicates and seemed to produce accurate results compared to the other two techniques. However, it is important to know that the qPCR data presented is corrected for DNA extraction efficiency and that copies of interest converted to spore numbers using the derived formula from Chapter 3 (sections 3.4.3 and 4.2.5) and *Pst* spores were considered haploid

in this calculations and it is crucial to know the haploid / dihaploid nature of the spores. To accurately quantify and calculate the spores field samples it is important to carefully consider the technique being used and the associated uncertainties. Namely, cross reactivity issues with immunoassay techniques to avoid false detections and extraction and conversion calculation factors when using qPCR detection techniques.

Chapter 5 Summary and future directions

In this thesis, the importance of early detection of important plant diseases of wheat was discussed, which plays a crucial role in plant disease management that could reduce the losses caused by disease causing pathogens worldwide. Conventional detection and identification methods based on disease symptom visualization or laboratory identification could be time-consuming, expensive, and require professionals with specific experience. Moreover, the screening of plant disease to determine the occurrence of diseases includes logistical factors such as the cost of a single test, availability of on-site evaluation, and pre- and post-probability of disease risk. In recent years, many tools have emerged to efficiently diagnose on time plant diseases. However, we still face challenges to identify and detect different pathotypes involved in causing a disease. A better understanding of pathogens including their morphology and conducive environmental conditions and robust and reliable detection of pathogens to the species or strain level are significant requirements of disease monitoring and management. The development of more rapid and cost-effective tools to detect pathogens before the appearance of symptoms is needed to manage the diseases effectively. To overcome these difficulties, recent advances in new molecular techniques coupled with the benefits of immunological methods have been proposed in this thesis for the early detection of three important fungal pathogens of wheat. This would pave a better understanding for current and future scientists to develop similar assays to detect other plant pathogens to limit their spread.

In summary, **Chapter 2** describes the development of real-time immunoPCR (RT-iPCR) to detect three important airborne fungal pathogens of wheat: *Pyrenophora tritici-*

repentis (*Ptr*)*, Fusarium graminearum* (*Fg*)*,* and *Puccinia striiformis* (*Pst*) causing tan spot, Fusarium head blight, and stripe rust respectively. The limit of detection were 2, 188, and 938 spores for *Ptr, Pst,* and *Fg* respectively. This novel technique has greatly improved the sensitivity and also eliminates the need for tedious DNA extraction procedures required in other molecular approaches. However, cross reactivity challenges led to uncertainties in the specific detection of the target pathogens. This could be the major limitation of RT-iPCR being used as a detection tool leading to false positives. This issue could be potentially avoided by producing more specific primary and secondary antibodies specific to the target antigen.

Chapter 3 describes the evaluation of quantitative PCR (qPCR) for the same target fungal spores for rapid and sensitive detection. The developed qPCR was able to detect as low as 6 spores of *Ptr*, 80 spores for *Fg,* and 411 spores of *Pst* and had significantly improved the sensitivity and linear working range for all three spores and provided a highly specific detection without any cross reactions as observed with the immunoassays, ELISA and RT-iPCR in chapter 2. Although DNA extraction is required to perform qPCR, this chapter derived a formula to calculate the DNA extraction efficiency and the conversion of copies of interest to spore numbers. This approach considered the spore reproductive biology and derived conversion factors for DNA concentration, volume of DNA used, dilution factor, target gene, and genome size of the pathogens to enable accurate quantification of spore numbers for all three fungal pathogens.

Chapter 4 described the quantification of *Pst* spores in field samples of two locations: disease nursery and Fairfield at the Lethbridge RDC. The *Pst* spores were quantified using three real-time detection techniques, microscopy, RT-iPCR, and qPCR and the

results were compared. The challenges involved were species-level identification while using microscopy detection and cross-reactivity issues when using RT-iPCR; these challenges were discussed and qPCR is so far the most accurate method to quantify fungal spores when appropriate correction and conversion calculations are used.

There were a number of challenges encountered throughout this research project that helps to pave a platform for better understanding and future directions of development for this project.

The main challenge encountered in the development of a novel RT-iPCR for the detection of plant pathogens is cross-reactivity. As discussed in chapter 2, this issue may be avoided by producing more specific primary and secondary antibodies. Polyclonal antibodies have the advantage of being able to detect very low concentrations of antigens since they bind to numerous locations on the same antigen, being less expensive, and being simple to make are the main reasons for utilizing the polyclonal antibodies in this research. In order to produce a primary antibody specific to a fungal spore or any pathogen the surface proteins must be studied thoroughly before antibody production. A previous attempt of raising monoclonal antibodies against *Pst* spores led to the identification of low titer IgM (unpublished data). The epitope that is specific to the antigen must be selected and the production of monoclonal or recombinant antibodies should be considered rather than polyclonal antibodies to reduce non-specific reactivities. Polyclonal antibodies have the ability to bind to a wide range of antigens with comparable epitopes, resulting in cross-reactivity. Monoclonal antibodies, on the other hand, are intended to bind to a single, particular epitope of a single antigen, reducing the possibility of cross-reactivity. However, a different approach is needed.

Proteomic analysis could be carried out on the target antigen to identify the surface protein that is very specific to the target antigen. This protein could be selected by isolating the surface proteins and selecting a specific protein (specific to the target antigen) to produce an antibody. In order to pick a surface protein that is specific to a fungal antigen first, all the surface proteins have to be isolated and that can be done by using buffers or trypsin digestion. Trypsin digestion can remove any proteins that are not bound to the surface of the fungal antigen. Then the remaining proteins on the fungal surface could be isolated and analyzed by mass spectrometry to identify the specific proteins that could be picked up by matching their identity against protein databases using bioinformatic tools (Volterson et al. 2018). A previous study reported by Volterson et al. (2018) has identified a conidial surface protein CcpA responsible for the virulence of *Aspergillus fumigatus*, an important human pathogenic fungi, using the above-mentioned method. Hydrogen-fluoride (HF)–pyridine extraction and a trypsin-shaving approach to isolate surface proteins from the target fungi and liquid chromatography-tandem mass spectrometry (LC-MS / MS) to identify the protein were used.

In terms of secondary antibodies, the DNA conjugated to the secondary antibody played an important role in causing cross-reactivity. To achieve a highly specific detection, one could consider conjugating the DNA of the target antigen to the secondary antibody and use the probes and primers specific to the target-antigen. However, more studies are needed to develop this fairly new technique of conjugating a target antigen DNA for a highly specific and sensitive detection of fungal spores as this kind of technique has never been employed before to detect any fungal pathogens. Another potential solution could be conjugating the DNA to the primary antibody instead of a secondary antibody

(if appropriate conjugation kits are commercially available) as this could eliminate a problematic step and eases the process by eliminating one step in the method. Again the question of what is the optimal DNA probe to conjugate remains; the target antigen's DNA or a non-homologous DNA strand as was used in this study. If a target antigen's DNA is coupled with the secondary antibody, appropriate primers must be developed and each antigen would require a distinct secondary antibody. This method could be time-consuming and labor intensive, however a highly specific and sensitive detection is possible with pathogen-specific primers. More experiments must be carried out to develop a highly specific method to detect the antigen without any cross-reactions.

So far, the best method to quantify fungal spores is the qPCR technique which has produced highly specific and sensitive detection without any cross reactions. However, qPCR analysis first requires DNA extraction from the spores, which is a non-trivial process. This research demonstrated that more accurate detection is possible when DNA extraction efficiency is calculated and applied to the quantification of spore numbers. The formula derived as part of this thesis would help achieve the quantification of any organism that requires DNA extraction in an accurate manner. This is also an important contribution to this thesis. More studies are required to fully employ the potential of the derived formulas, and these formulas must be extended to other pathogenic fungal spores in order to analyze DNA extraction efficiency and spore number quantification.

By utilizing the above described methods, growers could be benefitted by detecting the pathogenic micro-organisms in their crop field at early stages, before the appearance of symptoms, and make timely decisions depending on the pathogen prevalence and the other factors that are described in the disease triangle including the virulent pathogen,

susceptible / resistant host, environmental factors favoring the spread of the disease and time of the year. This in turn would also reduce the spread of diseases resulting in major crop losses and ultimately increase crop production to meet the challenge of feeding the global population by 2050.

References

Abdullah, A. S., Turo, C., Moffat, C. S., Lopez-Ruiz, F. J., Gibberd, M. R., Hamblin, J., et al. 2018. Real-time PCR for diagnosing and quantifying co-infection by two globally distributed fungal pathogens of wheat. Frontiers in Plant Science 9:1086.

Aboukhaddour, R., Cloutier, S., Ballance, G. M., and Lamari, L. 2009. Genome characterization of *Pyrenophora tritici-repentis* isolates reveals high plasticity and independent chromosomal location of *ToxA* and *ToxB*. Molecular Plant Pathology 10: 201–212.

Aboukhaddour, R., Turkington, T. K., and Strelkov, S. E. 2013. Race structure of *Pyrenophora triciti-repentis* (tan spot of wheat) in Alberta, Canada. Canadian Journal of Plant Pathology 35:256-268.

Aboukhaddour, R., Fetch, T., McCallum, B. D., Harding, M. W., Beres, B. L., and Graf, R. J. 2020. Wheat diseases on the prairies: A Canadian story. Plant Pathology 69:418-432.

Adler, M., Schulz, S., Fischer, R., and Niemeyer, C. M. 2005. Detection of rotavirus from stool samples using a standardized immuno-PCR ("Imperacer") method with end-point and real-time detection. Biochemical and Biophysical Research Communications 333:1289-1294.

Agrios, G.N. 2005. *Plant pathology*. 5th edition. San Diego (CA): Elsevier Inc – Academic Press.

Alberta Agriculture and Forestry, G.O.A. 2020. Fusarium head blight of barley and wheat. Ag-Info Centre © 2020 Government of Alberta. https://open.alberta.ca/dataset/107529dc-b4fd-4950-

9fbfe963f5af988c/resource/c3ff2518-471d-4709-b753-88efb4d3ae41/download/af-Fusarium-head-blight-barley-and-wheat.pdf. Accessed on “11 May 2023”.

Ali, S., Gladieux, P., Leconte, M., Gautier, A., Justesen, A.F., Hovmøller, M.S., Enjalbert, J., and Vallavieille-Pope, C. 2014. Origin, migration routes and worldwide population genetic structure of the wheat yellow rust pathogen *Puccinia striiformis* f.sp. *tritici*. PLOS Pathogens 10:e1003903.

Araujo G. T. 2018. Determination of the incidence of fungal spores for important wheat pathogens in western Canada [M.Sc. thesis]. Alberta (Canada): University of Lethbridge.

Araujo, G. T., Amundsen, E., Frick, M., Gaudet, D. A., Aboukhaddour, R., Selinger, B., et al. 2020. Detection and quantification of airborne spores from six important wheat fungal pathogens in southern Alberta. Canadian Journal of Plant Pathology 43: 439-454.

Araujo, G. T., Gaudet, D. A., Amundsen, E., Frick, M., Aboukhaddour, R., Selinger, B. L., et al. 2023. Inoculum threshold for stripe rust infection in wheat. Canadian Journal of Plant Pathology. 1-16

Aslam, S., Tahir, A., Aslam, M. F., Alam, M. W., Shedayi, A. A., and Sadia, S. 2017. Recent advances in molecular techniques for the identification of phytopathogenic fungi – A mini review. Journal of Plant Interactions 12:493-504.

Asseng, S., Ewert, F., Martre, P., Rötter, R. P., Lobell, D. B., Cammarano, D., et al. 2014. Rising temperatures reduce global wheat production. Nature Climate Change 5:143-147.

Atkins, and Clark, I. M. 2004. Fungal molecular diagnostics: A mini review. Journal of Applied Genetics 45:3-15.

Bankina, B., and Priekule, I. 2011. A review of tan spot research in the Baltic countries: occurrence, biology and possibilities of control. Žemdirbystė (Agriculture) 98:3-10.

Barletta, J. M., Edelman, D. C., and Constantine, N. T. 2004. Lowering the detection limits of HIV-1 viral load using real-time immuno-PCR for HIV-1 p24 antigen. American Journal of Clinical Pathology 122:20-27.

Barros, G.G., Alaniz Zanon, M.S., Chiotta, M.L., Reynoso, M.M., Scandiani, M.M., and Chulze, S.N. 2013. Pathogenicity of phylogenetic species in the *Fusarium graminearum* complex on soybean seedlings in Argentina. European Journal of Plant Pathology 138:215-222.

Beddow, J. M., Pardey, P. G., Chai, Y., Hurley, T. M., Kriticos, D. J., Braun, H. J., et al. 2015. Research investment implications of shifts in the global geography of wheat stripe rust. Nature Plants 1:15132.

Bonot, S., Ogorzaly, L., El Moualij, B., Zorzi, W., and Cauchie, H.M. 2014. Detection of small amounts of human adenoviruses in stools: comparison of a new immuno real-time PCR assay with classical tools. Clinical Microbiology and Infection 20:1010-6.

Borer, E. T., Laine, A. L., and Seabloom, E. W. 2016. A multiscale approach to plant disease using the metacommunity concept. Annual Review of Phytopathology 54:397-418.

Brar, G. S., and Kutcher, H. R. 2016. Race characterization of *Puccinia striiformis* f. sp. *tritici,* the cause of wheat stripe rust, in Saskatchewan and southern Alberta, Canada and virulence comparison with races from the United States. Plant Disease 100:1744-1753.

Braun, E. J., and Howard, R. J. 1994. Adhesion of fungal spores and germlings to host plant surfaces. Protoplasma 181:202-212.

Cao, X., Yao, D., Zhou, Y., West, J. S., Xu, X., Luo, Y., et al. 2016. Detection and quantification of airborne inoculum of *Blumeria graminis* f. sp. *tritici* using quantitative PCR. European Journal of Plant Pathology 146:225–229.

Chakraborty, S., and Newton, A. C. 2011. Climate change, plant diseases and food security: An overview. Plant Pathology 60:2-14.

Chapagain, T., and Good, A. 2015. Yield and production gaps in rainfed wheat, barley, and canola in Alberta. Frontiers in Plant Science 6:990.

Chen, X. 2020. Pathogens which threaten food security: *Puccinia striiformis*, the wheat stripe rust pathogen. Food Security 12:239-251.

Chen, X., Penman, L., Wan, A., and Cheng, P. 2010. Virulence races of *Puccinia striiformis* f. sp.*tritici* in 2006 and 2007 and development of wheat stripe rust and distributions, dynamics, and evolutionary relationships of races from 2000 to 2007 in the United States. Canadian Journal of Plant Pathology 32:315-333.

Chen, Y., and Zhou, M.-G. 2009. Characterization of *Fusarium graminearum* isolates resistant to both carbendazim and a new fungicide JS399-19. Phytopathology 99:441-446.

Ciuffetti, L.M., Manning, V.A., Pandelova, I., Faris, J.D., Friesen, T.L., Strelkov, S. E.,

et al. 2014. *Pyrenophora tritici-repentis*: A plant pathogenic fungus with global impact. *Genomics of plant-associated fungi: monocot pathogens* 1-39.

Cruz, C. D., and Valent, B. 2017. Wheat blast disease: Danger on the move. Tropical Plant Pathology 42:210-222.

Dawson A., 2016. Fusarium conference hears of disease resurgence. Alberta: Manitoba Cooperator. Published: December 2, 2016.

Dietzel, K., Valle, D., Fierer, N., U'Ren, J. M., and Barberán, A. 2019. Geographical distribution of fungal plant pathogens in dust across the United States. Frontiers in Ecology and Evolution 7:304.

Dinh, H. X., Singh, D., Periyannan, S., Park, R. F., and Pourkheirandish, M. 2020. Molecular genetics of leaf rust resistance in wheat and barley. Theoretical and Applied Genetics 133:2035-2050.

Enghiad, A., Ufer, D., Countryman, A. M., and Thilmany, D. D. 2017. An overview of global wheat market fundamentals in an era of climate concerns. International Journal of Agronomy 2017:1-15.

Epstein, L., and Nicholson, R. 2016. Adhesion and adhesives of fungi and oomycetes. In *Biological adhesives. Springer International Publishing Switzerland 2016*, ed. Smith A.M: Springer, p. 25-55.

Feng, P., Wang, B., Liu, D.L., Xing, H., Ji, F., Macadam, I., et al. 2018. Impacts of rainfall extremes on wheat yield in semi-arid cropping systems in eastern Australia. Climatic Change 147:555-569.

Fernandez, M. R., Stevenson, C. F., Hodge, K., Dokken-Bouchard, F., Pearse, P. G., Waelchli, F., et al. 2016. Assessing effects of climatic change, region and

agronomic practices on leaf spotting of bread and durum wheat in the Western Canadian Prairies, from 2001 to 2012. Agronomy Journal 108:1180-1195.

Figueroa, M., Hammond-Kosack, K. E., and Solomon, P. S. 2018. A review of wheat diseases-a field perspective. Molecular Plant Pathology 19:1523-1536.

Fischer, A., Eiff, C.V., Kuczius, T., Omoe, K., Peters, G., and Becker, K. 2007. A quantitative real-time immuno-PCR approach for detection of staphylococcal enterotoxins. Journal of Molecular Medicine 85:461–469.

Food and Agriculture Organization (FAO) of the United Nation. 2020. Wheat production. FAO Cereal Supply and Demand Brief | World Food Situation | Food and Agriculture Organization of the United Nations. Accessed on "11 May 2023".

Frank SA. 2002. Specificity and Cross-Reactivity. In *Immunology and Evolution of Infectious Disease*. Princeton, New Jersey, USA. Princeton University Press.

Gangneux, C., Cannesan, M.A., Bressan, M., Castel, L., Moussart, A., Vicré-Gibouin, M., Driouich, A., Trinsoutrot-Gattin, I., and Laval, K. 2014. A sensitive assay for rapid detection and quantification of *Aphanomyces euteiches* in soil. Phytopathology 104:1138-47.

Gaudet, D., Nilsson, D., Lohr, T., and Sheedy, C. 2015. Development of a real-time immuno-PCR assay for the quantification of 17β-estradiol in water. Journal of Environmental Science and Health, Part B 50:683-690.

Ghanbarnia, K., Gourlie, R., Amundsen, E., and Aboukhaddour, R. 2021. The changing virulence of stripe rust in Canada from 1984 to 2017. Phytopathology 111:1840-1850.

Gilbert, J., and Tekauz, A. 2000. Review: Recent developments in research on Fusarium head blight of wheat in Canada. Canadian Journal of Plant Pathology 22:1-8.

Golan, J., and Pringle, A. 2017. Long-distance dispersal of fungi. Microbiology Spectrum 5:4-5.

He, X., Qi, W., Quiñones, B., McMahon, S., Cooley, M., and Mandrell, R.E., 2011. Sensitive detection of Shiga Toxin 2 and some of its variants in environmental samples by a novel immuno-PCR assay. Applied and Environmental Microbiology 77: 3558-64.

He, J., Evers, D.L., O'Leary, T.J., and Mason, J.T. 2012. Immunoliposome-PCR: a generic ultrasensitive quantitative antigen detection system. Journal of Nanobiotechnology 10:26-42.

Hu, C., Chen, P., Zhou, X., Li, Y., Ma, K., Li, S., et al. 2022. Arms Race between the Host and Pathogen Associated with Fusarium Head Blight of Wheat. Cells, 11: 2275-2302.

Jain, A., Sarsaiya, S., Wu, Q., Lu, Y., and Shi, J. 2019. A review of plant leaf fungal diseases and its environment speciation. Bioengineered 10:409-424.

Kaphle. S. 2020. Development of a real-time immuno-PCR assay for the detection of pea root rot causal agent, *Aphanomyces euteiches* [M.Sc. thesis]. Alberta (Canada): University of Lethbridge.

Keller, M. D., Bergstrom, G. C., and Shields, E. J. 2013. The aerobiology of *Fusarium graminearum*. Aerobiologia 30:123-136.

Kim, H. J., McCoy, M. R., Majkova, Z., Dechant, J. E., Gee, S. J., Tabares-da Rosa, S., et al. 2012. Isolation of alpaca anti-hapten heavy chain single domain antibodies for development of sensitive immunoassay. Analytical Chemistry 84:1165-1171.

Kumar, K., Xi, K., Turkington, T. K., Aljarrah, M., and Capettini, F. 2019. Yield responses in spring wheat and barley cultivars, varying in stripe rust resistance in central Alberta. Canadian Journal of Plant Pathology 42:3 344-352.

Kuzdralinski, A., Kot, A., Szczerba, H., Nowak, M., and Muszynska, M. 2017. A review of conventional PCR assays for the detection of selected phytopathogens of wheat. Journal of Molecular Microbiology and Biotechnology 27:175-189.

Lamari, L., and Bernier, C. C. 1991. Genetics of tan necrosis and extensive chlorosis in tan spot of wheat caused by *Pyrenophora tritici-repentis*. Phytopathology 81:1092-1095.

Line, R. F. 2002. Stripe rust of wheat and barley in North America: A retrospective historical review. Annual Review of Phytopathology 40:75-118.

Liu, M., and Hambleton, S. 2010. Taxonomic study of stripe rust, *Puccinia striiformis sensu lato*, based on molecular and morphological evidence. Fungal Biology 114:881-899.

Liu, M., McCabe, E., Chapados, J. T., Carey, J., Wilson, S. K., Tropiano, R., et al. 2015. Detection and identification of selected cereal rust pathogens by TaqMan® real-time PCR. Canadian Journal of Plant Pathology 37:92-105.

Malou, N., and Raoult, D. 2011. Immuno-PCR: A promising ultrasensitive diagnostic method to detect antigens and antibodies. Trends in Microbiology 19:295-302.

Mayer, Z., Bagnara, A., Farber, P., and Geisen, R. 2003. Quantification of the copy number of nor-1, a gene of the aflatoxin biosynthetic pathway by real-time PCR, and its correlation to the cfu of *Aspergillus flavus* in foods. International Journal of Food Microbiology 82:143-151.

McCartney, H. A., Foster, S. J., Fraaije, B. A., and Ward, E. 2003. Molecular diagnostics for fungal plant pathogens. Pest Management Science 59:129-142.

Moffat, C. S., and Santana, F. M. 2018. Diseases affecting wheat: Tan spot. In *Integrated disease management of wheat and barley: Burleigh Dodds Science Publishing, Cambridge, UK, 2019,* ed. Oliver, R: Burleigh Dodds Science Publishing Limited, p. 95-107.

Mondal, B., Ramlal, S., Setlem, K., Mahadeva, A., Aradhya, S., and Parid, M. 2020. A real-time immunocapture PCR (RT-IPCR) without interference of protein A for convenient detection of staphylococcal enterotoxin B from food and environmental samples. Annals of Microbiology 70:25.

Morcia, C., Tumino, G., Gasparo, G., Ceresoli, C., Fattorini, C., Ghizzoni, R., et al. 2020. Moving from qPCR to chip digital PCR assays for tracking of some *Fusarium* species causing Fusarium head blight in cereals. Microorganisms 8:1307-1318.

Moreno, M. V., Stenglein, S. A., and Perelló, A. E. 2012. *Pyrenophora tritici-repentis*, causal agent of tan spot: A review of intraspecific genetic diversity. In *The molecular basis of plant genetic diversity*. *InTech March, 2012,* ed. M. Caliskan: InTech p. 374.

Muhammad, M. 2018. Plant disease epidemiology: Disease triangle and forecasting mechanisms in highlights. Hosts and Viruses 5:7-11.

Murphy, K., and Weaver, C. eds. 2017. *Janeways Immunobiology.* Garland Science: Taylor & Francis Group, LLC, New York, NY, 10017, USA.

Narayan, H., Srivasatava, P., Bhatt, S. C., Joshi, D., and Soni, R. 2022. Plant pathogenesis and disease control. *Plant Protection: From Chemicals to Biologicals*, Walter de Gruyter GmbH & Co KG, 2022, Berlin, Germany.

Nwe, N., Furuike, T., and Tamura, H. 2011. Production, properties and applications of fungal cell wall polysaccharides: chitosan and glucan. Advances in Polymer Science 244:187–208.

Niemeyer, C. M., Adler, M., and Wacker, R. 2005. Immuno-PCR: High sensitivity detection of proteins by nucleic acid amplification. Trends in Biotechnology 23:208-216.

Osborne, L. E., and Stein, J. M. 2007. Epidemiology of Fusarium head blight on small-grain cereals. International Journal of Food Microbiology 119:103-108.

Quan, P. L., Sauzade, M., and Brouzes, E. 2018. dPCR: A technology review. Sensors (Basel) 18:1271-1297.

Salipante, S. J., and Jerome, K. R. 2020. Digital PCR - an emerging technology with broad applications in microbiology. Clinical Chemistry 66:117-123.

Sano, T., Smith, C.L., and Cantor, C.R. 1992. Immuno-PCR: very sensitive antigen detection by means of specific antibody-DNA conjugates. Science 258:120-122.

Sanoubar, R., Bauer, A., and Seigner., L. 2015. Detection, identification and quantification of *Fusarium graminearum* and *Fusarium culmorum* in wheat kernels by PCR techniques. Journal of Plant Pathology and Microbiology 6:287.

Santana, F.M., and Friesen, T.L., 2008. Tan spot disease of wheat : race characterization. Passo-Fundo Embrapa Trigo 84.

Statistics Canada. 2020. Table 32-10-0359-01 Estimated areas, yield, production, average farm price and total farm value of principal field crops, in metric and imperial units. https://doi.org/10.25318/3210035901-eng Accessed on "11 May 2023" .

Schrader, C., Schielke, A., Ellerbroek, L., and Johne, R., 2012. PCR inhibitors - occurrence, properties and removal. Journal of Applied Microbiology 113:1014-1026.

Scholthof, K.-B. G. 2007. The disease triangle: Pathogens, the environment and society. Nature Reviews: Microbiology 5:152-156.

Schumann, G. L., and D'Arcy, C. J. 2006. *Essential plant pathology*, 2nd edition American Phytopathological Society (APS Press), St. Paul, Minnesota, U.S.A.

Shin, J., Chang, Y. K., Quang, T. N., Heung, B., and Ravichandran, P. 2019. Optimizing parameters for image processing techniques using machine learning to detect powdery mildew in strawberry leaves. American Society of Agricultural and Biological Engineers Annual International Meeting 1901347. Boston, Massachusetts July 7- July 10, 2019.

Snehi, S. K., Raj, S. K., Prasad, V., and Singh, V. 2015. Recent research findings related to management strategies of Begomoviruses. Journal of Plant Pathology and Microbiology, 6:1-12.

Tang, D, DeVit, M., and Johnston, S. A. 1992. Genetic immunization is a simple method for eliciting an immune response. Nature 356:152-154.

Tewari, S., and Sharma, S. 2019. Molecular techniques for diagnosis of bacterial plant pathogens. In *Microbial diversity in the genomic era. January 2019:* Elsevier Inc, p. 481-497.

Thiha, A., & Ibrahim, F. 2015. A colorimetric enzyme-linked immunosorbent assay (ELISA) detection platform for a point-of-care dengue detection system on a lab-on-compact-disc. Sensors 15:11431-11441.

Trail, F. 2009. For blighted waves of grain: *Fusarium graminearum* in the postgenomics era. Plant Physiology 149:103-110.

Voltersen, V., Blango, M. G., Herrmann, S., Schmidt, F., Heinekamp, T., Strassburger, M., et al. 2018. Proteome analysis reveals the conidial surface protein CcpA essential for virulence of the pathogenic fungus *Aspergillus fumigatus*. American Society for Microbiology 9:e01557-18.

Walter, S., Nicholson, P., and Doohan, F. M. 2010. Action and reaction of host and pathogen during Fusarium head blight disease. New Phytologist 185:54-66.

Wang, Y., Zhu, M., Zhang, R., Yang, H., Wang, Y., Sun, G., Jin, S., and Hsiang, T. 2009. Whole genome amplification of the rust *Puccinia striiformis* f. sp. *tritici* from single spores. Journal of Microbiological Methods 77:29–234.

Ward, T. J., Clear, R. M., Rooney, A. P., O'Donnell, K., Gaba, D., Patrick, S., et al. 2008. An adaptive evolutionary shift in Fusarium head blight pathogen populations is driving the rapid spread of more toxigenic *Fusarium graminearum* in North America. Fungal Genetics and Biology 45:473-484.

Wei, B., Despins, T., Fernandez, M. R., Strelkov, S. E., Ruan, Y., Graf, R., et al. 2021. Race distribution of *Pyrenophora tritici-repentis* in relation to ploidy level and

susceptibility of durum and winter bread wheat. Canadian Journal of Plant Pathology 43:582-598.

Wessels, E., Rusman, L. G., van Bussel, M. J., and Claas, E. C. 2014. Added value of multiplex Luminex gastrointestinal pathogen panel (xTAG® GPP) testing in the diagnosis of infectious gastroenteritis. Clinical Microbiology and Infection 20:O182-O187.

Xi, K., Kumar, K., Holtz, M. D., Turkington, T. K., and Chapman, B. 2015. Understanding the development and management of stripe rust in central Alberta. Canadian Journal of Plant Pathology 37:21-39.

Yang, F., Jacobsen, S., Jorgensen, H. J., Collinge, D. B., Svensson, B., and Finnie, C. 2013. *Fusarium graminearum* and its interactions with cereal heads: studies in the proteomics era. Frontiers in Plant Science 4:37.

Yang, Y., Zhou, Q., Zahr, K., Harding, M.W., Feindel, D., and Feng, J. 2021. Impact of DNA extraction efficiency on the sensitivity of PCR-based plant disease diagnosis and pathogen quantification. European Journal of Plant Pathology 159:583–591.

Zhang, P., Liu, Y., Liu, W., Massart, S., and Wang, X. 2017. Simultaneous detection of wheat dwarf virus, northern cereal mosaic virus, barley yellow striate mosaic virus and rice black-streaked dwarf virus in wheat by multiplex RT-PCR. Journal of Virological Methods 249:170-174.

Zhao, J., Huang, L., Huang, W., Zhang, D., Yuan, L., Zhang, J., et al. 2014. Hyperspectral measurements of severity of stripe rust on individual wheat leaves. European Journal of Plant Pathology 139:407-417.

Zheng, W., Huang, L., Huang, J., Wang, X., Chen, X., Zhao, J., et al. 2014. High genome heterozygosity and endemic genetic recombination in the wheat stripe rust fungus. Nature Communications 4:2673-2682.

Appendix

Additional information for chapter 3

Fg spores

Organism of Interest : *Fusarium graminearum*

Genome size (n) = 3.6×10^7

Mass of DNA / genome (m) = $[n][\frac{1.096(10)^{-21}g}{bp}]$

Mass of DNA / genome = 3.9456E-14 = 39.45 fg

Calculation of mass of gDNA containing 1 copy of Translation elongation factor 1-α gene = $\frac{\text{Mass of DNA / genome}}{Copy\ number}$ = 39.45 fg

Number of copies in total DNA extracted (*Fg*) = 5.3×10^7

Pst spores

Organism of Interest : *Puccinia striiformis*

Genome size (n) = 7.6×10^7

Mass of DNA / genome (m) = $[n][\frac{1.096(10)^{-21}g}{bp}]$

Mass of DNA / genome = 8.3296E-14 = 83.30 fg

Calculation of mass of gDNA containing 1 copy of β - Tubulin gene = $\frac{\text{Mass of DNA / genome}}{Copy\ number}$ = 83.30 fg

Number of copies in total DNA extracted (*Pst*) = 7.2×10^6

Materials and methods

Different DNA extraction kits used

The optimized DNA extraction kit (DNeasy PowerSoil) procedure was given in the methods section of chapter 3 (Section 3.2.1) and the procedures of other three kits used for testing are provided here.

1. **DNeasy PowerSoil Pro kit**

DNA extraction was performed by extractions from *Ptr,* and *Fg,* spores using a DNeasy PowerSoil Pro kit from QIAGEN. Initially, 10 mg of spores were weighed and added to the 1.5 mL PowerBead Pro tube provided with the kit. A volume of 800 µL of CD1 solution was added to each tube and the sample was incubated at 65°C for 10 min to increase cell lysis. After 10 min, the sample was ground in the Precellys grinder at 5000 rpm; 2 times for 30 s; with a 5 s gap period. Then the sample was centrifuged at 15,000 × g for 2 min. The supernatant of 500 µL was collected, transferred to a fresh tube and 200 µL of solution CD2 was added and vortexed for 5 s. The sample was centrifuged at 15,000 × g for 1 min and the supernatant of 700 µL was collected and transferred to a fresh 2 mL microcentrifuge tube. A volume of 600 µL of solution CD3 was added and vortexed briefly for 5 s. From this mixture, 650 µL of solution was loaded on to the spin column provided and centrifuged at 15,000 × g for 1 min. The flow-through was discarded and the remaining sample left from the mixture was processed using the same spin column until all of the solution has passed through the spin column. Then 500 µL of solution EA was added and centrifuged for 1 min at 15,000 × g. Flow through was discarded and then 500 µL of solution C5 was added and centrifuged at 15,000 × g for 1

min. Flow through was discarded and spin column was placed in a clean collection tube and centrifuged again for 2 min at 16,000 × g. Finally, the spin column was placed in the elution tube provided by the kit and 60 µL of elution buffer (solution C6) was added to the spin column and centrifuged at 15,000 × g for 1 min. The spin column was discarded and flow through DNA was collected in the elution tube. DNA quantity and quality (A260 / A280, A260 / A230) were measured using a NanoDrop™ One UV-Vis Spectrophotometer by multiple measurements (n=15; 3 samples with 5 measurements each) and stored at -20℃ until further use.

2. ZymoBIOMICS™ DNA Miniprep Kit (ZYMO RESEARCH)

DNA extraction was performed by extractions from *Ptr,* spores using a ZymoBIOMICS™ DNA Miniprep Kit from ZYMO RESEARCH. Initially, 10 mg of spores were weighed (wet weight = 70.5 mg) and added to a ZR BashingBead™ lysis tube. A volume of 750 µL of ZymoBIOMICS lysis was added to the tube. The sample was ground in the Vortex Genie® for 40 min of continuous bead beating. Then the sample was centrifuged at 10,000 × g for 1 min. The supernatant of 400 µL was collected, transferred to a Zymo-Spin™ III-F filter in a collection tube and centrifuged at 8,000 × g for 1 min and the Zymo-Spin™ III-F filter was discarded. A volume of 1200 µL of ZymoBIOMICS™ DNA binding buffer was added to the filtrate in the collection tube and vortexed briefly for 5 s. From this mixture, 800 µL of solution was transferred to the Zymo-Spin™ IICR column provided in a collection tube and centrifuged at 10,000 × g for 1 min. The flow-through was discarded and the remaining sample left from the mixture was processed by repeating the above step until all of the solution has passed through the column. Then 400 µL of ZymoBIOMICS™ DNA wash buffer 1 was added

to the Zymo-Spin™ IICR column in a new collection tube and centrifuged for 1 min at 10,000 × g. Flow through was discarded and then 700 µL of ZymoBIOMICS™ DNA wash buffer 2 was added to the Zymo-Spin™ IICR column in a collection tube and centrifuged at 10,000 × g for 1 min. Flow through was discarded and the column was placed in a collection tube and 200 µL of ZymoBIOMICS™ DNA wash buffer 2 was again added to the Zymo-Spin™ IICR column and centrifuged for 1 min at 10,000 × g. Finally, the column was placed in a clean 1.5 mL microcentrifuge tube and 100 µL of ZymoBIOMICS™ DNase/RNase free water was added directly to the column matrix and incubated for 1 min at RT. After incubation, the sample was centrifuged at 10,000 × g for 1 min to elute the DNA. A Zymo-Spin™ III-HRC filter was placed in a new collection tube and 600 µL of ZymoBIOMICS™ HRC prep solution was added and centrifuged at 8,000 × g for 3 min. The eluted DNA in previous step was transferred to the prepared Zymo-Spin™ III-HRC filter in a clean 1.5 mL microcentrifuge tube and centrifuged at 16,000 × g for 3 min. DNA quantity and quality (A260 / A280, A260 / A230) were measured using a NanoDrop™ One UV-Vis Spectrophotometer by multiple measurements (n=15; 3 samples with 5 measurements each) and stored at -20℃ until further use.

3. Quick-DNA™ Fungal / Bacterial Miniprep kit (ZYMO RESEARCH)

DNA extraction was performed by extractions from *Ptr,* and *Fg* spores using a Quick-DNA™ Fungal / Bacterial Miniprep kit from ZYMO RESEARCH. Initially, 500 µL beta-mercaptoethanol was added to the 100 mL of genomic lysis buffer that came with the kit to a final dilution of 0.5 % (volume / volume) for optimal performance of the kit. Then, 10 mg of spores were weighed (resuspended in 200 µL of PBS, wet weight *Ptr* =

67.5 mg and *Fg* = 40.6 mg) and added to a ZR BashingBead™ lysis tube. A volume of 750 µL of ZR BashingBead™ buffer was added to the tube. The sample was ground in the Vortex Genie® for 40 min of continuous bead beating. Then the sample was centrifuged at 10,000 × g for 1 min. The supernatant of volume 400 µL was collected, transferred to a Zymo-Spin™ III-F filter in a collection tube and centrifuged at 8,000 × g for 1 min and the Zymo-Spin™ III-F filter was discarded. A volume of 1200 µL of genomic lysis buffer was added to the filtrate in the collection tube and vortexed briefly for 5 s. From this mixture, 800 µL of solution was transferred to the Zymo-Spin™ IICR column provided in a collection tube and centrifuged at 10,000 × g for 1 min. Then 200 µL of DNA pre-wash buffer was added to the Zymo-Spin™ IICR column in a new collection tube and centrifuged for 1 min at 10,000 × g. Flow through was discarded and then 500 µL of g-DNA wash buffer was added to the Zymo-Spin™ IICR column in a collection tube and centrifuged at 10,000 × g for 1 min. Finally, the Zymo-Spin™ IICR column was placed in a clean 1.5 mL microcentrifuge tube and 100 µL of DNA elution buffer was added directly to the column matrix and centrifuged at 10,000 × g for 30 s to elute the DNA. DNA quantity and quality (A260 / A280, A260 / A230) were measured using a NanoDrop™ One UV-Vis Spectrophotometer by multiple measurements (n=15; 3 samples with 5 measurements each) and stored at -20°C until further use.

Table A1: DNA concentration and quality measured at absorbance 260 by NanoDrop for DNA extracted using different beads including baked sand, zirconia and the beads that came with DNeasy PowerSoil kit

Beads used	Spore weight (mg)			Concentration (ng / µL)			A260/280[a]			A260/230[b]		
	Ptr	*Fg*	*Pst*	*Ptr*	*Fg*	*Pst*	*Ptr*	*Fg*	*Pst*	*Ptr*	*Fg*	*Pst*
Baked sand	10	-	-	37.2	-	-	1.8	-	-	0.3	-	-
Zirconia	10	2	10	25.5	12.9	5.1	1.7	1.8	2.2	2.1	0.5	0.04
DNeasy PowerSoil	10	10	10	18.6	48.4	7.0	1.8	1.8	1.8	1.4	2.0	1.2

a – an absorbance ratio for A260/280 between 1.8 and 2 indicates the purity of DNA with minimal protein contamination.

b - an absorbance ratio for A260/230 between 2 and 2.2 indicates a relatively pure DNA sample with minimal contamination from unwanted organic contaminants.

From the above table, it is evident that the beads that come with DNeasy PowerSoil kit were giving better quality and quantity of DNA for all three spores. Baked sand was only tested with *Ptr* spores and sand was efficient in grinding spores as it produced the highest DNA quantity among the three beads used, however the quality of the DNA was poor. Zirconia beads yielded better quantity and quality of DNA with *Ptr* spores which was not true with *Fg* and *Pst* spores as the concentration and A260/230 ratio was very low compared to the beads that came with the kit. Hence, the beads from DNeasy PowerSoil kit was selected to use consistently for all three spores in this research.

Table A2: Primer sets for qPCR assays to detect the target spores using qPCR method

Targets and gene of interest	Primer pairs	Sequences (5'-3')	Size (bp)
Ptr Tox A gene	Tox A1	Fwd : GTCATGCGTTCT ATCCTC	294
	Tox A2	Rev : CCTATAGCACCA GGTCGTCC	
Fg Elongation factor 1-α gene	Fgram379	Fwd : CCATTCCCTGG GCGCT	95
	Fgram411	Rev : CAGGTGGTTAG TGACTGG	90
Pst B-tubulin gene	PSBTQ	Fwd : CAATCACCGTCC CAGAGTTGACATC	151
	PSBTQ	Rev : ACGGACAGCAT GTTCTCTTCGACT	

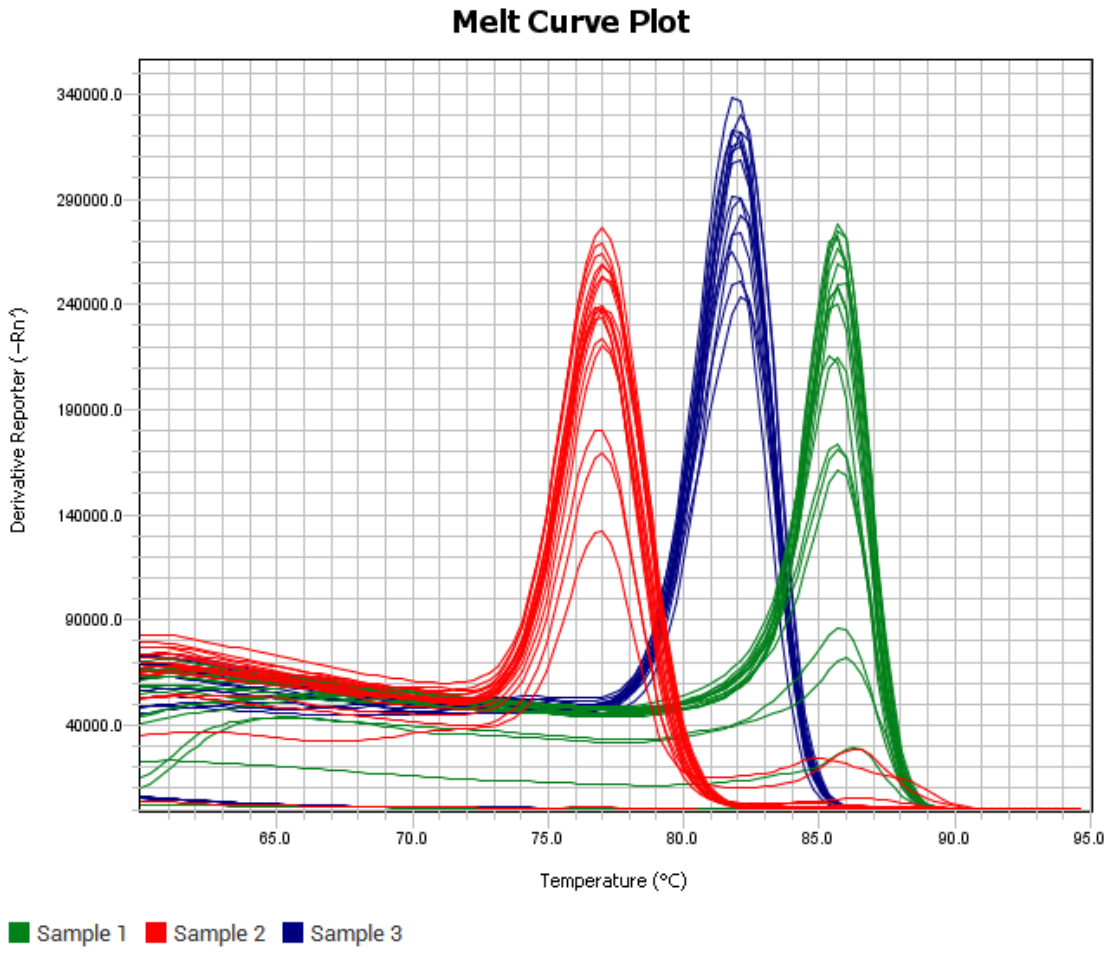

Figure A1: Melt curve analysis of qPCR detecting *Ptr*, *Fg* and *Pst* spores. The single peak observed for each amplicon is typically representing the specificity of the primers. Sample 1, 2 and 3 represents *Ptr*, *Fg* and *Pst* spores respectively.